

SEMMELWEIS EGYETEM
DOKTORI ISKOLA

Ph.D. értekezések

3421.

WÜRSCHING TAMÁS

Gyermekkori betegségek klinikuma, élettana és prevenciója
című program

Programvezető: Dr. Szabó Attila, egyetemi tanár
Témavezetők: Dr. Nagy Krisztián, egyetemi docens
Dr. Németh Zsolt, egyetemi tanár

THE USE OF AUTOLOGOUS TOOTH BONE GRAFT IN ALVEOLAR CLEFT RECONSTRUCTION

PhD thesis

Tamás Würsching

Semmelweis University Doctoral School
Károly Rácz Division



Supervisors: Krisztián Nagy MD, DMD, PhD
Zsolt Németh MD, PhD

Official reviewers: László Seres, MD, PhD
Dávid Lendvai, MD, DMD, PhD

Head of the Complex Examination Committee: Gábor Varga, DsC.

Members of the Complex Examination Committee:

Tamás Vereb, MD, DMD, PhD

Anita Gáborján, MD, PhD

Budapest
2026

Table of Contents

List of abbreviations	5
1. Introduction	7
1.1 Scientific background	7
1.2. Timing of alveolar bone grafting.....	8
1.2.1 Timing of secondary alveolar bone grafting and orthodontic considerations.....	9
1.3. Flap design.....	10
1.4. Iliac crest bone graft (ICBG)	10
1.5. Alternative donor sites and biomaterials.....	11
1.6. Autologous tooth bone (ATB)	13
1.7. The role of virtual surgical planning.....	14
1.8. Assessment of surgical outcomes	15
2. Objectives	17
3. Methods	19
3.1 Study design and ethical approval	19
3.2 Patient selection and characteristics.....	19
3.3 Preoperative imaging and 3D virtual planning	20
3.4 Surgical protocols	22
3.4.1. Preparation of the ATB graft and preparation of the recipient area.....	22
3.4.2. Harvesting the iliac crest bone graft.....	28
3.5 Postoperative care	28
3.6.1 CBCT subtraction method.....	29
3.6.2 CBCT-based qualitative scoring (<i>Stasiak</i>)	30
3.7 Statistical analysis.....	32
4. Results	34
4.1 Study cohorts	34
4.2 Clinical and radiological outcomes after 3 months follow-up (pilot study).....	36
4.2.1 Soft-tissue healing and local events	36
4.2.2 Early volumetric hard-tissue gain	36

4.2.3 Morphometric accuracy and shape agreement.....	36
4.3. Long-term outcomes based on CBCT evaluation (cohort study)	38
4.3.1. Descriptive statistics.....	38
4.3.2. Radiographical assessment.....	40
4.3.3 Statistical analysis	42
5. Discussion.....	44
6. Conclusions	49
7. Summary.....	51
8. New statements of the thesis	52
9. References	53
10. Bibliography of the candidate’s publications	64
11. Acknowledgements	66

List of abbreviations

ABG	alveolar bone grafting
ASIS	anterior superior iliac spine
ATB	autologous tooth bone
β -TCP	beta-tricalcium phosphate
CBCT	cone-beam computed tomography
CEJ	cemento-enamel junction
CLP	cleft lip and palate
CT	computed tomography
DFDBA	demineralized freeze-dried bone allograft
DSC	<i>Dice</i> similarity coefficient
FDBA	freeze-dried bone allograft
FGF	fibroblast growth factor
GMP	good manufacturing practice
GPP	gingivoperiosteoplasty
HA	hydroxyapatite
HD	<i>Hausdorff</i> distance
HU	<i>Hounsfield</i> unit
IAN	inferior alveolar nerve

ICBG	iliac crest bone graft
LFCN	lateral femoral cutaneous nerve
L-PRF	leukocyte-platelet rich fibrin
PABG	primary alveolar bone grafting
PDGF	platelet derived growth factor
PLGA	poly (lactic-co-glycolic acid)
PRF	platelet-rich fibrin
PRP	platelet-rich plasma
rhBMP-2	recombinant human bone morphogenic protein 2
SABG	secondary alveolar bone grafting
SLA	stereolithography
STL	standard tessellation language
TABG	tertiary alveolar bone grafting
UCLP	unilateral cleft lip and palate
VEGF	vascular endothelial growth factor
VSP	virtual surgical planning

1. Introduction

1.1 Scientific background

Cleft lip and palate (CLP) are among the most frequent congenital malformations overall with an estimated worldwide incidence of around 1.5-1.7 per 1000 live births, whereas Hungarian data show a cleft prevalence of 2.02/1000 per live births (1). The aetiology of CLP is multifactorial, with both genetic and environmental contributions (2). Maternal age, nutritional deficiencies (e.g.: folic acid), smoking or alcohol abuse during pregnancy, maternal hyperthermia, and certain viral infections are all supposed to affect craniofacial development. In approximately 75% of CLP cases the alveolar ridge is involved, leading to an alveolar cleft (3). The main characteristics of this are:

- Discontinuity of the maxilla
- Collapse of the dental arch segments
- Developmental and growth disturbances of adjacent teeth
- Oro-nasal communication
- Disturbances in nasal morphology.

These anomalies lead to compromised facial aesthetics, difficulties of masticatory function, breastfeeding, swallowing and speech, and overall worse psychosocial well-being. The reconstruction of the alveolar cleft is a crucial step in the treatment of patients with cleft lip and palate, with alveolar bone grafting (ABG) usually being the last primary surgical intervention after cheiloplasty and palatoplasty. The main goals are to stabilize the maxillary dental arch, obliterate the persistent oronasal fistulae, enhance facial symmetry, provide bone for tooth eruption, or dental implant placement, and enhance support of the nasal base (4).

1.2. Timing of alveolar bone grafting

The history of alveolar bone grafting reflects the changes in our understanding of craniofacial growth and function (5). Different approaches are usually categorized based upon the timing of the surgery:

- Primary alveolar bone grafting (PABG): performed before the age of 2, after lip repair but prior to the repair of the palate.
- Secondary alveolar bone grafting (SABG): performed after the age of 2, in patients with mixed dentition (6).
- Tertiary alveolar bone grafting (TABG): performed in patients with permanent dentition.

Early attempts at PABG, performed in infancy, sought to prevent secondary defects, and reduce the number of operations, but were later shown to impair midfacial growth due to premature ossification and scar tissue formation. Gingivoperiosteoplasty (GPP) was proposed as a graftless solution that relied on periosteal induction of bone formation; however, systematic reviews showed inconsistent results, with insufficient bone bridge formation in many patients (7-9). Secondary ABG was introduced in 1972 by *Boyne and Sands* (10), and became the gold standard after landmark studies demonstrated that grafting during the mixed dentition phase, before eruption of the permanent canine, provided optimal arch stability and allowed the physiological eruption of teeth adjacent to the cleft (11). Several studies have also confirmed that this approach does not interfere with the growth and development of the maxilla (12). TABG is generally reserved for late adolescents or adults, usually as a resort for patients who failed to present on time or as an attempt to correct failed grafts or to prepare for prosthetic rehabilitation. While functional rehabilitation (e.g., implant placement) might be feasible, volumetric maintenance of the graft is generally inferior, resorption rates are higher, and orthodontic movements are more limited. TABG is also associated with an increased risk of dehiscence and need for regrafting in wide defects (13).

1.2.1 Timing of secondary alveolar bone grafting and orthodontic considerations

The exact timing of SABG is based on dental development and maxillary growth (14). Though it is always done during the mixed dentition phase, there are two distinct approaches: it is either done at an earlier (4-7 years) or at a later age (8-12 years) (15, 16).

The early SABG approach aims to perform alveolar reconstruction prior to the eruption of the lateral incisor. Advocates of this method argue for improved guidance of erupting incisors and earlier closure of oronasal fistulae (17). Reported advantages include better residual bone volume outcomes at the cleft site; concerns include greater technical difficulty in small alveoli and a possibility of restriction of maxillary growth (18).

Most centres prefer grafting when the root of the cleft-side canine is one-half to two-thirds of its expected final length, usually between the age of 8-12. This approach is associated with the highest rates of successful bone bridging, canine eruption, and long-term stability. Grafting shortly before eruption of the permanent canine allows the canine to erupt through the graft, stimulating remodelling and consolidation of the bone bridge (19-21).

Orthodontic treatment of these patients is often necessary and is usually performed preoperatively. Expansion of the collapsed maxillary segments and alignment of anterior teeth are necessary to open the alveolar cleft site and to improve access. Extraction of any supernumerary or retained teeth around the cleft can be performed prior to or during the same surgery (22).

In bilateral cases stabilization and proper positioning of the premaxilla is critical. Strategies include one-stage bilateral grafting with premaxillary osteotomy and fixation when the premaxilla is protrusive/mobile, these cases, however, carry higher rates of wound breakdown and regrafting. Moreover, the preparation of extended flaps could compromise the vascular supply of the premaxilla and lead to severe complications (23). A staged approach with closure of oro-nasal fistulae and reconstruction of the nasal floor as a first step, followed by alveolar bone grafting in a second intervention might lead to a more predictable outcome (24).

1.3. Flap design

Successful SABG depends on a supple, well-vascularized mucosa capable of tension-free closure. Active infections or poor oral hygiene should be treated before grafting to lower failure risk. In terms of local flap design for alveolar cleft closure, the preferred method is usually the four-flap technique, as described by *Nordin and Abyholm* (25, 26), which provides an ideal soft-tissue closure above the graft. However, in cases of suture loosening due to flap tension, secondary wound healing might occur, and the consequent exposure might lead to the loss of the graft. This classic flap design does not address the width and thickness of keratinized gingiva of the teeth adjacent to the alveolar cleft, where consequent periodontal impairment may develop, resulting in eventual tooth loss.

1.4. Iliac crest bone graft (ICBG)

For decades, autologous bone harvested from the anterior iliac crest has been the gold standard graft for SABG. This donor site provides:

- Abundant corticocancellous bone
- High concentration of osteogenic cells
- Osteoinductive, osteoconductive and osteogenetic properties
- Favourable remodelling capacity in the recipient site

Donor site morbidity however remains a major drawback (27, 28). Possible complications include pain, gait disturbance, fracture of the anterior superior iliac spine (ASIS), nerve injury and paresthesia, especially of the lateral femoral cutaneous nerve (LFCN), hematoma or seroma formation, superficial or deep infection, and aesthetic concerns from scars (29). Meta-analyses and systematic reviews report complication rates between 10–30%, with long-term pain and functional limitation in a subset of patients. Hospitalization time and recovery are also prolonged, raising concerns, especially in children (30). These disadvantages led to the investigation for alternative donor sites and graft types (31, 32).

1.5. Alternative donor sites and biomaterials

Alternatives to the iliac crest aim to reduce donor site morbidity while achieving comparable results to this type of graft (33). These include autologous grafts from various extra- and intraoral donor sites, allografts, xenografts and certain supplementary materials to be used in combination with the grafts, such as platelet rich plasma (PRP), fibrin sealant, leukocyte-platelet rich fibrin (L-PRF) derivatives, etc.

A. Extraoral donor sites:

- a. Calvarium (split-thickness). Mainly cortical plates with lower tendency for resorption. Pros: large, flat grafts; scar is hidden in the hairline. Cons: chance of neurosurgical complications; longer operation time; less osteogenic than cancellous iliac bone; unsuitable in very young children.
- b. Proximal tibia. Cancellous bone harvested via small incision. Pros: reasonable amount; lower risk of gait disturbance than with iliac crest; low visible scarring. Cons: risk of tibial plateau injury; postoperative discomfort; not ideal for pediatric use.
- c. Rib. Curved corticocancellous segments. Pros: structural support. Cons: chest wall pain; risk of pneumothorax; unpredictable remodelling; it is rarely the first choice for SABG.

B. Intraoral donor sites:

- a. Mandibular symphysis (chin): Supplies cortico-cancellous blocks/chips. Pros: proximity to recipient site; no visible extraoral scar; short harvest time. Cons: limited volume; risk to lower incisor roots and mental nerve; chance of temporary chin hypoesthesia; potential chin contour change. Best suited for unilateral narrow-to-moderate width clefts, often as a composite graft combined with particulate xenografts to increase volume (34).
- b. Mandibular ramus / coronoid process: Dense cortical bone to be used as a block or as particulate chips after processing. Pros: minimal aesthetic impact; good bone

quality. Cons: limited cancellous component; risk of trismus or transient inferior alveolar nerve (IAN) paresthesia.

- c. Maxillary tuberosity / zygomatic buttress / palatal tori. Provide small particulate volumes for minor defects or in combination with other grafts. Pros: same surgical field; low morbidity. Cons: very limited quantity; variable quality.

All intraoral bone grafts have the advantage of having the same embryologic origin as the maxilla, meaning these grafts contain intramembranous bone. This tends to resorb less and maintain volume better than endochondral bone (e.g.: the iliac crest) in craniofacial sites.

C. Allografts (FDBA/DFDBA) are processed human bone in particulate or block form, usually coming from femoral heads of living donors (35, 36). They offer osteoconductive and osteoinductive properties with no donor site morbidity (37). Their use in alveolar cleft reconstruction is not common, but a study by *Chauvel-Picard et al.* (38) showed that hard-tissue gain after one year was 58.5%

D. Xenografts (e.g., deproteinized bovine bone mineral) are highly osteoconductive with very slow resorption. They are good for space maintenance and act as a scaffold for creeping substitution. In some centres they are commonly used in combination with autografts (39, 40). However, the persistence of particles and limited remodelling capacity generally render these inadequate as monotherapy in cleft patients.

E. Alloplastic / synthetic materials, such as β -TCP, HA/ β -TCP, bioactive glass (41, 42), calcium phosphate cements are purely osteoconductive. Pros include unlimited supply, customizable granule size and predictable resorption profiles (43). However, they show inferior integration as standalone graft, and are best used as composites with autografts or PRF.

F. Bone morphogenic proteins (rhBMP-2) are potent osteoinductive factors delivered on an absorbable collagen sponge. They yield outcomes close to ICBG bone fill in selected cases while avoiding a donor site (44, 45). However, their use is considered off-label in children in

many jurisdictions, moreover they are linked to dose-dependent oedema, airway swelling, and ectopic bone formation (46, 47). Their cost is also higher compared to other grafts.

G. Platelet rich plasma/fibrin (PRP/PRF) are autologous platelet concentrates. PRF supports tissue repair initiation through containment of growth factors, cytokines and adhesion proteins that have a role in the haemostatic cascade, connective tissue synthesis, and angiogenesis (48, 49). PRF also improves the natural healing potential of hard and soft-tissues by containing growth factors, such as VEGF, FGF, PDGF, and modulating pain and inflammation. There is however inconsistent evidence for added bone volume as standalone graft, they are best used as adjuncts, combined with other types of grafts, particularly with alloplastics or xenografts which only have osteoconductive properties (50).

H. Tissue-engineering strategies such as collagen/PLGA scaffolds, decellularized matrices (51, 52), and stem-cell-based constructs show strong preclinical performance (53, 54). Clinical use is limited by regulatory hurdles, cost, and need for standardized, GMP-compliant workflows. Early clinical feasibility studies suggest potential as adjuncts, not replacements.

1.6. Autologous tooth bone (ATB)

Auto-tooth bone is an autologous graft material, originally developed in Korea by *Kim et al.* in the early 2010s, which is derived from extracted teeth (55, 56). The idea is to process extracted teeth into particulate or block grafts through chemical and mechanical preparation (57). Unlike synthetic grafting materials, ATB possesses both osteoconductive and osteoinductive properties, promoting rapid new bone formation and remodelling. This material is composed of an incompletely demineralized dentin matrix, which contains type I collagen, similarly to alveolar bone, as well as BMPs and calcium phosphate, all of which are key components of bone regeneration. The mineral components of ATB consist of four stages (types) of calcium phosphate: hydroxyapatite, tricalcium phosphate, octacalcium phosphate, and amorphous calcium phosphate. When using ATB for guided bone regeneration, *Kim et al.* found that after 3 months, most of the graft underwent resorption, and excellent bone healing was observed, which occurred as a result of osteoinduction and

osteoconduction. Regarding the histomorphometric analysis of the samples collected during the 3–6-month healing period, new bone formation was detected in 46–87% of the area of interest, and excellent bony remodelling was achieved. ATB has been successfully applied so far in periodontal regenerative surgery (58), alveolar ridge preservation (59), preprosthetic surgery, and implantology. There are also case reports presenting successful outcomes in alveolar cleft reconstruction, *Jeong et al.* (60) were able to place a 3 mm-wide implant with 45 Ncm insertion torque 3.5 months after ABG using ATB (61).

1.7. The role of virtual surgical planning

Virtual surgical planning (VSP) has become a valuable auxiliary technique in the management of craniofacial malformations and cleft surgery, particularly so in alveolar bone grafting (62). These techniques utilize preoperative three-dimensional (3D) imaging, most commonly cone-beam computed tomography (CBCT), to generate accurate virtual models of the maxillofacial area. These models allow the surgeon to assess the morphology of the alveolar cleft, the number and position of adjacent teeth, and the relationship with critical structures such as the nasal floor and maxillary sinus (63).

One of the main advantages of VSP is the ability to visualize the shape and quantify the volume of the alveolar defect, which helps to estimate the required graft material more precisely and aids in the selection of an appropriate donor site. Virtual simulations also enable the surgeon to plan the ideal size and contour of the graft, with consideration of future orthodontic tooth movement or implant placement (64-66). In complex cases, patient-specific surgical guides or 3D-printed anatomical models may be fabricated, allowing more precise intraoperative execution of the planned procedure (67, 68).

During the postoperative phase, the virtual surgical plan also gives the opportunity to evaluate outcomes better. Pre- and postoperative 3D datasets can be compared to assess bone fill, graft resorption, and integration with surrounding bone.

Despite the benefits, VSP in alveolar cleft repair has certain limitations. The need for advanced imaging equipment, specialized surgical planning software, and medical-grade 3D printers may increase costs (69). Furthermore, the use of CBCT comes with radiation exposure, although this is generally justified in the context of cleft care where repeat radiographic assessments are indicated. In summary, VSP can improve the precision and predictability of alveolar cleft reconstruction by helping preoperative assessment, enhancing intraoperative accuracy, and standardizing the evaluation of outcomes.

1.8. Assessment of surgical outcomes

Alveolar bone grafting is considered successful when it achieves sufficient bone fill in the alveolar cleft. However, the goal of grafting is not only radiographic bone fill, but there are also clinical and functional considerations: eruption of adjacent teeth, orthodontic alignment, lack of residual fistulae, prosthetic feasibility, and long-term stability (70).

The proper assessment of surgical outcomes remains challenging. A postoperative evaluation is crucial not only to measure the success of the procedure, but also to enable the early detection of graft resorption or displacement, which are among the most frequent complications of alveolar bone grafting. The earliest assessment methods, such as the use of *Bergland and Chelsea* (71, 72) scales, relied on a two-dimensional approach, using intraoral X-rays. Over time, with the emergence of computed tomography (CT) and especially cone-beam computed tomography (CBCT) technologies, several 3D evaluation methods have been developed to assess the outcomes of ABG (63, 73). While 2D methods are limited by structural overlaps and cannot provide volumetric data, and tend to overestimate graft volume, 3D techniques using CT overcome these limitations (74, 75). Moreover, CBCT is often preferred over conventional CT for evaluating bone grafts due to its lower radiation exposure and its ability to accurately estimate the graft volume. Three-dimensional radiological imaging helps assess the presence and spatial location of the bone graft (76). It allows the size and location of graft resorption to be precisely specified. It can also help to evaluate the process of teeth eruption in the grafted area (77). CBCT has certain limitations

in comparison with CT examination. Firstly, the *Hounsfield* unit (HU) scale cannot offer a credible assessment of bone quality. Another drawback to CBCT is a documented underestimation of bone volume.

2. Objectives

Despite its status as the gold standard in alveolar cleft reconstruction ICBG is associated with significant donor site morbidity and high resorption rates. ATB offers an autologous and biologically active alternative grafting material with osteoconductive and osteoinductive properties, which also eliminates the need for an extraoral donor site.

This thesis evaluates the use of ATB and ICBG in alveolar bone grafting of patients with cleft lip and palate. For precise comparison of the outcomes modern CBCT-based assessment methods, such as volumetric subtraction analysis and the *Stasiak* rank scale are being implemented. Both short- and long-term radiological data are presented and interpreted to support the findings of the research, and to contribute to the international evidence base guiding future clinical protocols.

Through this research, the aim is to reduce patient morbidity, improve clinical outcomes, and advance the field of cleft care by integrating surgical innovation with state-of-the-art radiological evaluation.

The objectives of this doctoral thesis are grounded in the findings and methodology of two key studies: the retrospective pilot study by *Molnár et al.*(78), and the retrospective cohort study by *Würsching et al.*(79). These articles provide the scientific foundation for defining the specific research aims of this work.

Primary objectives:

- The evaluation of short-term volumetric hard-tissue gain after using ATB for SABG in patients with UCLP by 3D subtraction analysis based on preoperative CBCT and 3 months postoperative control images.
- The evaluation of long-term volumetric stability and resorption patterns of ATB compared to ICBG in secondary alveolar bone grafting of patients with unilateral cleft lip and palate, using standardized CBCT-based analysis.

Secondary objectives:

- To validate the efficacy of the surgical procedure and volumetric stability of the graft, by calculating the ratio between the actual volumetric hard-tissue gain and the planned hard-tissue volume.
- Assessment of the similarity between the planned and actual hard-tissue morphologies by calculating the *Dice Similarity Coefficient* (DSC) and *Hausdorff Distance* (HD).
- Assessment of the success of permanent canine eruption through ATB compared to ICBG.
- To evaluate the prevalence of short- and long-term surgical complications in each group.
- To assess the relationship between initial defect volume and outcome scores.
- To evaluate intra- and interrater reproducibility of the *Stasiak* scale.

Hypothesis:

- Volumetric analysis and clinical outcomes show that ATB can be integrated into SABG protocols with comparable short-term outcomes to ICBG.
- ATB demonstrates volumetric stability and functional outcomes equivalent to ICBG over long-term follow-up, while minimizing donor site morbidity.

3. Methods

3.1 Study design and ethical approval

This thesis integrates the outcomes of two complementary clinical studies: a retrospective pilot study and a retrospective longitudinal cohort study. Both studies were approved by Semmelweis University's Regional and Institutional Committee of Science and Research Ethics (Approval Number: SE RKEB 251/2020). The study protocol was submitted and approved by the U.S. National Library of Medicine (www.clinicaltrials.gov; trial registration number: NCT05971914). The research plan was compiled following the legislation in force and the Declaration of Helsinki from the World Medical Association (reference number: 23/2002. V.9.). Surgical interventions were undertaken with the understanding and written consent of each subject's caregiver.

3.2 Patient selection and characteristics

All the enrolled patients for both studies were being treated for cleft lip and palate at the Centre of Facial Reconstruction at the Pediatric Center of Semmelweis University, Budapest.

3.2.1. For the pilot study of *Molnár et al.*, all the patients underwent SABG surgery between August of 2021 and April of 2022. Only patients exhibiting a complete unilateral cleft lip and palate (UCLP) were recruited for this study. The exclusion criteria were:

- a) major relevant general medical conditions or syndromic cases,
- b) systemic use of steroids,
- c) current or previous intravenous bisphosphonate treatment,
- d) acute infection at the operation site,
- e) any previous attempts at alveolar bone grafting.

In every case the development of the cleft-side canine was considered during planning of the surgery, as was the need for orthodontic treatment. All the patients included in the study required orthodontic maxillary expansion. The development of the canine was followed using periapical X-rays. Only once the canine's root development was between one-third and two-thirds of its expected final length, was the decision made to proceed with surgery. At this point CBCT scans were taken for surgical planning. Each patient was required to have presented at least three deciduous teeth, which were scheduled for extraction, as in the pilot study every patient underwent SABG using autologous tooth bone graft. All enrolled patients were examined by two independent dentists to assure that tooth removal was in accordance with the patients' age and orthodontic planning.

3.2.2. For the cohort study by *Würsching et al.* patients who had undergone secondary alveolar bone grafting between 2020 and 2023 were recruited. Inclusion criteria were complete UCLP without other congenital deformities, ABG surgery using either an iliac crest cancellous bone graft or ATB from deciduous or supernumerary teeth, and CBCT imaging at least one year after grafting.

The exclusion criteria were:

- a) bilateral clefts,
- b) any previous attempt at bone grafting,
- c) the use of any other type of grafting material (e.g., xenografts, other donor site),
- d) and a lack of long-term follow-up CBCT.

The STROBE checklist was implemented during the preparation of this manuscript.

3.3 Preoperative imaging and 3D virtual planning

For precise assessment of the alveolar cleft anatomy, and to measure the required volume of the graft, the regular preoperative work-up of these patients always included a CBCT scan.

These scans were acquired using a NewTom VGi evo® device with a 12 cm × 8 cm field of view, and a 200 µm voxel size (NewTom, Cefla S.C., Imola, Italy). CBCT data were also acquired at the 3-month follow-up for the pilot study, and at least one year postoperatively for the cohort study. Digital imaging and communications in medicine (DICOM) datasets were imported into the 3D Slicer open-source image-processing software (www.slicer.org) Baseline and follow-up CBCT scans were segmented utilizing a semi-automatic segmentation method in the ‘Segment Editor’ module of 3D Slicer (80, 81). Separate binary label maps were generated for the bone of the maxilla. The maxilla was segmented utilizing the region-growing tool ‘Grow from seeds’, and thereafter the ‘Watershed’ tool was used to segment all the teeth separately (82). The software automatically generated 3D models of binary label maps, with real-time rendering. (Figure 1.)

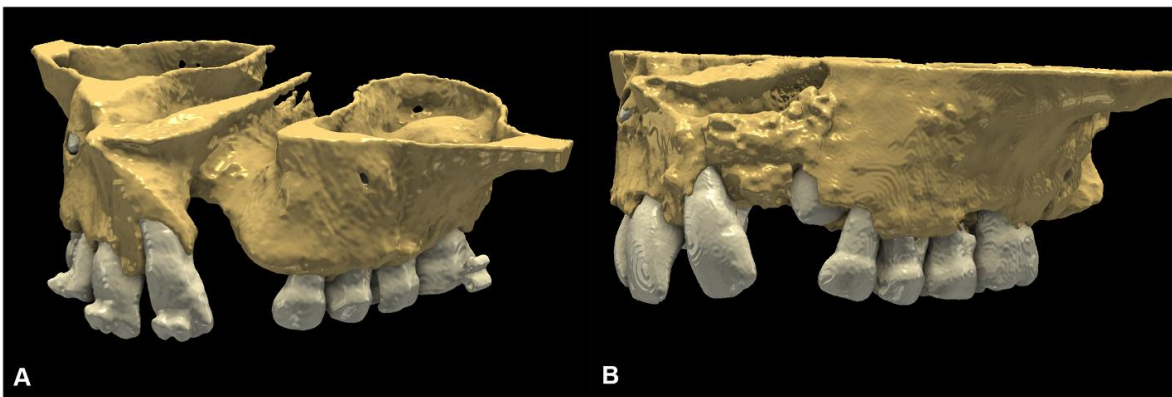


Fig. 1. Segmented 3D models of CBCT datasets: (A) virtual model of baseline hard-tissue conditions; (B) virtual model of 3-month follow-up hard-tissue conditions.

Based on the extent and morphology of the cleft the desired shape of the nasoalveolar graft was also designed in 3D Slicer. Since every case was unilateral, the non-cleft side anatomy was used as a reference during graft planning. The upper border of the defect was taken as the lowest part of the piriform aperture on the non-affected side, while the lower border was taken as the cemento-enamel junction (CEJ) of the neighbouring teeth. The buccal and palatal borders were determined by a line connecting the most buccal and palatal points of the alveolar process, next to the defect. This also gave us the opportunity to determine the exact volume of the graft in cm³. This facilitated preoperative planning because the maximum

amount of material the ATB machine can produce is approximately 3 cm³. The achievable volume of the ATB could be predicted based on the volume of the deciduous teeth, which was a limiting factor, since in case the number and condition of removable deciduous teeth was not sufficient the iliac crest graft had to be used.

After planning, the model was exported as a standard tessellation language (STL) file. As the final step, a grafting template was constructed using an open-source computer-aided design (CAD) software (Blender®; Blender Foundation, Amsterdam, The Netherlands), as described by Fábíán et al. (67, 69) (Figure 2.) The designed parts were manufactured with a stereolithography (SLA) 3D printer (Phrozen Shuffle XL; Phrozen, Hsinchu City, Taiwan) using class I biocompatible, surgical-grade resin (Dental SG; NextDent BV, Soesterberg, The Netherlands). These 3D printed models enabled intraoperative visualization of defect dimensions and gave guidance for graft shaping. This ensured optimal defect filling, minimized graft waste, and standardized intraoperative workflows.

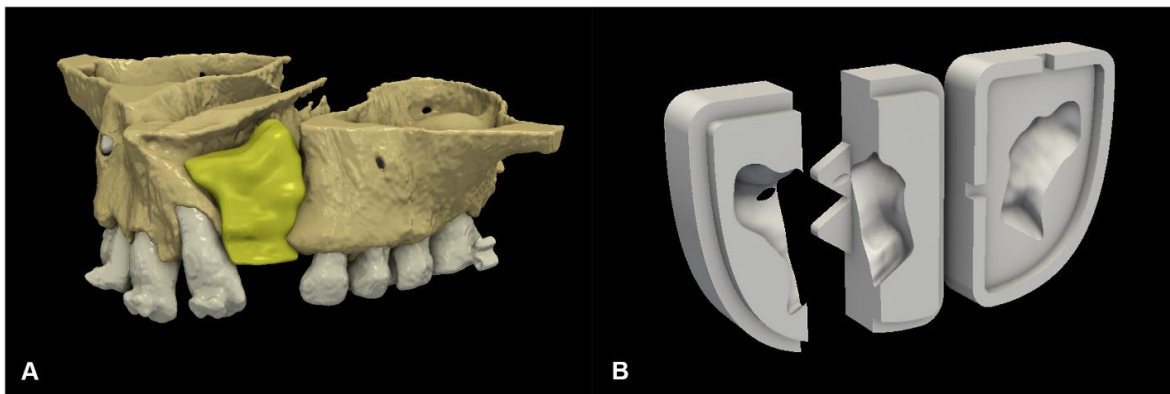


Fig. 2. Preoperative virtual planning: (A) digital 3D plan of cleft reconstruction; (B) CAD-modelled grafting template.

3.4 Surgical protocols

3.4.1. Preparation of the ATB graft and preparation of the recipient area

Teeth were extracted under general anaesthesia with the gentle application of forceps and elevators. Extracted teeth were prepared immediately after removal, according to the

Bonmaker® protocol (Korea DentalSolution Co Ltd, Busan, Korea) (Figure 3.) The outer surface of the teeth was debrided with diamond-coated burs (55, 56). Following the removal of pulp tissue, carious lesions and restorations, the crowns and roots were both ground in the Bonmaker® tooth grinder. After grinding, the tooth particles (particle size: 425–1500 µm) underwent disinfection and preparation via proprietary A, B, and C liquids inside the Bonmaker® device. Between patients, the equipment underwent a regular disinfection cycle, according to the manufacturer's instructions.

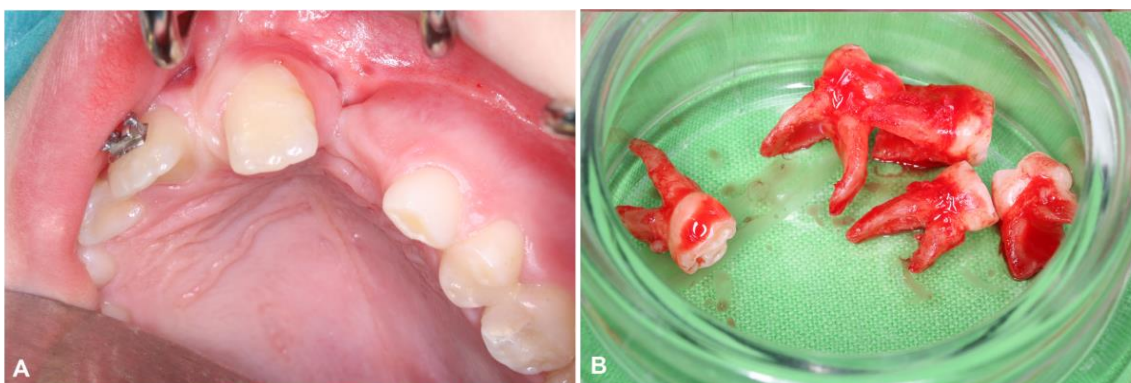


Fig. 3. Baseline clinical situation and tooth extraction: (A) baseline clinical situation; (B) extracted deciduous teeth.

During the preparation and disinfection procedure (which usually took 30–35 minutes), flap preparation and exploration of the alveolar cleft and oronasal fistula were carried out. Articaine hydrochloride 4% with 0.0001% epinephrine (Ultracain DS Forte; Sanofi-Aventis, Paris, France) was used for local anaesthesia. A full-thickness incision was made starting at the ipsilateral maxillary tuberosity, continued in a continuous intrasulcular incision along all teeth located distally from the oronasal fistula, with a no. 15 blade (Aesculap; Braun AG, Tuttlingen, Germany). At the level of the cleft and the oronasal fistula (located in the lateral incisor position), the incision was continued along the alveolar crest in full-thickness, followed by a split-thickness incision at the mucogingival junction of the adjacent central incisor, and continued vertically in the midline labial frenulum. Subsequently, the area of keratinized gingiva around teeth located distally from the cleft was elevated in full thickness with blunt dissection. Flap elevation was continued by sharp dissection apically from the

mucogingival junction of the distal teeth, as well as at the loose mucosa over the central incisor, where the keratinized gingiva was left untouched. The periosteal layer of the complete hemimaxilla was then exposed, followed by excision of the epithelial down growth in the oronasal fistula, which was closed with resorbable monofilament sutures (Chirmax Monolac 5/0) by approximating adjacent scar tissue margins. Scar tissue in the cleft area was outlined by mesial, distal, and palatal incisions to allow for nasal repositioning, exposing the bony cleft and creating a secluded space for graft insertion (Figures 4. and 5).

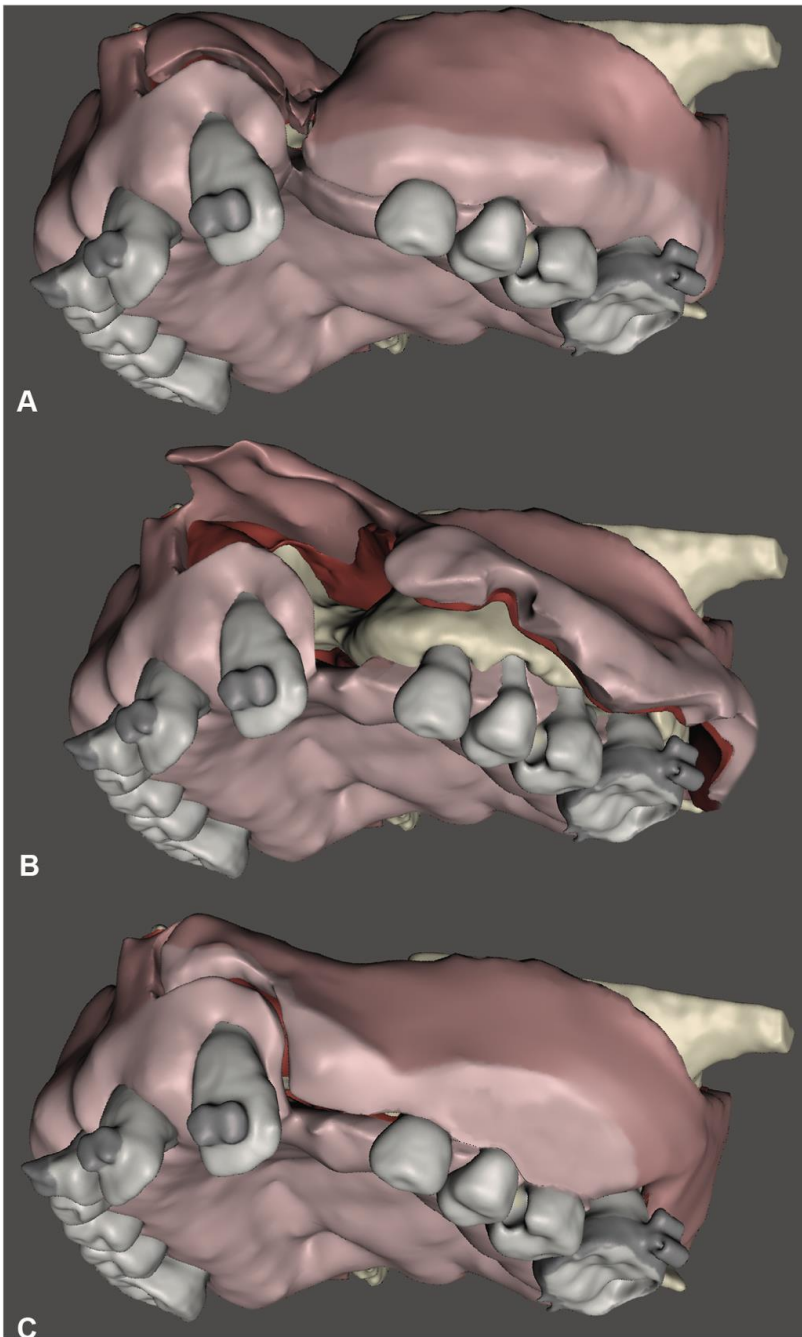


Fig. 4. Schematic presentation of the split-thickness papilla curtain flap: (A) initial incision (light pink: keratinized mucosa, dark pink: mobile mucosa); (B) flap elevation (red: periosteum); (C) mesially shifted flap closure.

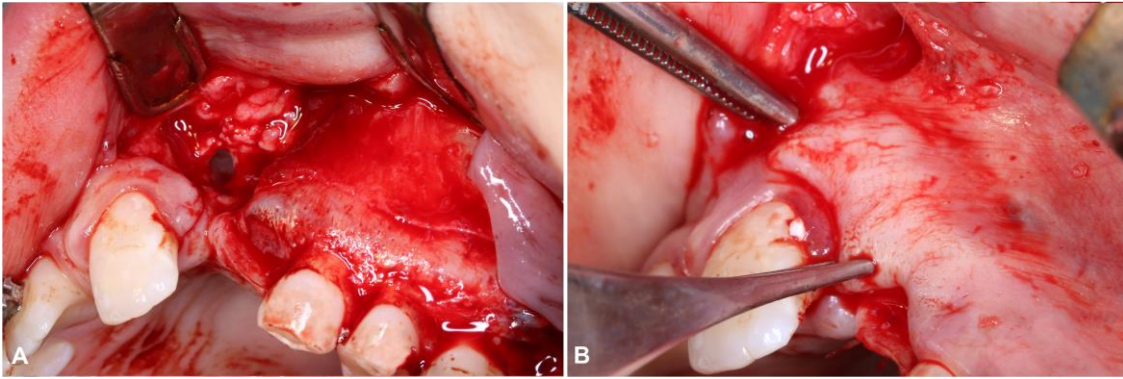


Fig. 5. Intraoperative situation: (A) surgical access of the UCLP; (B) tension-free mesial flap advancement.

Ready-to-use ATB was mixed with fibrin sealant (Tisseel®; Baxter, Glenview, Illinois, USA) in the digitally planned and 3D-printed grafting templates to obtain a sticky ATB graft that matched the shape and extent of the bony defect (83). The sticky ATB graft was then inserted in the alveolar defect (Fig. 6). Following cleft augmentation, the split-thickness papilla curtain flap was repositioned by shifting all buccal surgical papillae mesially to the adjacent or the second-adjacent interproximal space, depending on the horizontal extent of the cleft. Next, the papilla in the close vicinity of the oronasal fistula was relocated to the level of the mesial vertical incision in the midline frenulum (Fig. 7).

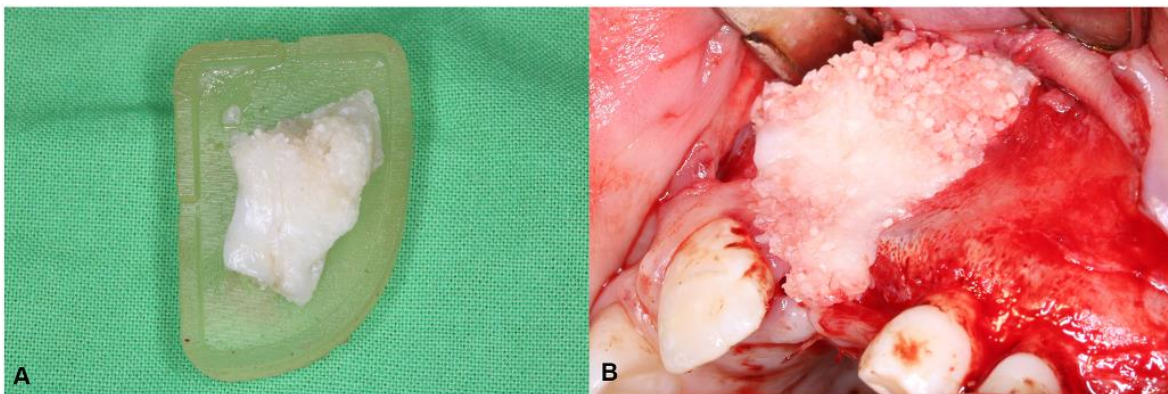


Fig. 6. Hard-tissue reconstruction of the UCLP: (A) the mixture of fibrin sealant and ATB particles was shaped by the 3D-printed grafting template to prepare the sticky ATB graft; (B) reconstruction of the UCLP with the sticky ATB graft.

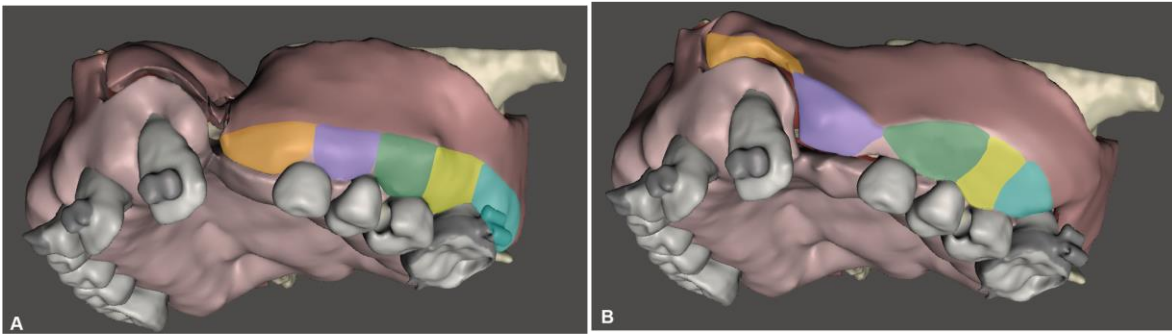


Fig. 7. Schematic demonstration of the mesial papilla shift: (A) preoperative state (the first interdental papilla is located distally to the alveolar cleft, marked in purple); (B) Postoperative state (the interdental papilla, marked in purple, was shifted mesially to cover the area of the alveolar cleft).

As a result, healthy continuous keratinized gingiva was shifted over the cleft to cover the grafted area and to ensure simultaneous reconstruction of the distorted vestibulum and lacking keratinized tissues. To stabilize the tension free split-thickness papilla curtain flap, suturing was carried out with resorbable monofilament sutures (Chirmax Monolac 5/0), utilizing circumferential double sling sutures and single interrupted mucosal sutures (Figure 8A).

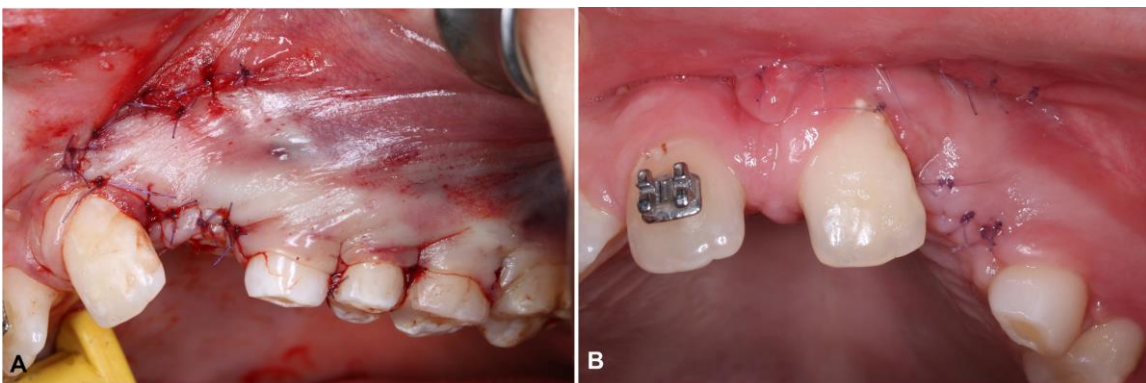


Fig. 8. Wound closure and postoperative control: (A) wound closure with primary intention; (B) 2-week postoperative control.

3.4.2. Harvesting the iliac crest bone graft

In cases where the number of extractable teeth was deemed insufficient for the preparation of ATB, cancellous bone from the iliac crest was used instead. In these cases, a two-team approach was chosen to reduce the operation time. The skin was draped and prepared, leaving the anterior superior iliac spine (ASIS) and the anterior iliac crest exposed. Before incision, local anaesthetic was administered (2% Lidocaine with 0.01% Epinephrine). The skin incision was approximately 2 cm long and respected the patient's relaxed skin tension lines. During the early adolescent age, when secondary alveolar bone grafting is performed, the iliac crest is usually still covered by a layer of cartilage, which was incised in a rectangular shape. This piece was elevated medially, hinged on the inner edge of the iliac crest. Curettes were used to harvest cancellous bone chips. These were inserted into the 3D-printed mold and were mixed with Tisseel fibrin glue, as described above, to give the graft better morphological stability. After the setting of the fibrin glue, the graft was removed from the mold, preserving the shape designed preoperatively, and was ready to be transferred to the cleft site. A collagen sponge was inserted into the donor area to promote hemostasis. The retracted cartilage was repositioned, and the wound was closed in layers. No drains were used.

3.5 Postoperative care

Postoperative systemic antibiotic therapy (875/125 mg amoxicillin/clavulanic acid twice a day, or 300 mg clindamycin four times a day in cases of penicillin allergy) was prescribed. Patients were advised to clean the area gently with an ultra-soft toothbrush and rinse with a 0.2% chlorhexidine-digluconate mouthwash for two weeks after surgery. Sutures usually resorbed 3–4 weeks after surgery (Figure 8B.). Clinical follow-up intervals included early inspection (7–10 days), intermediate controls (3 and 6 months), and extended follow-up (1 year and beyond, yearly controls up to 3–5 years). Clinical assessments included soft-tissue healing, eruption of adjacent teeth, and complications such as infection, dehiscence, or graft loss.

3.6 Radiological assessment and outcome measures

3.6.1 CBCT subtraction method

Following the segmentation of both preoperative and 3-month follow-up CBCT scans, spatial registration was carried out to validate volumetric and morphological hard-tissue changes. Registration of DICOM datasets was performed using the ‘General Registration (Elastix)’ module, which is an automatic intensity-based medical image registration algorithm (84). After spatial registration, the preoperative 3D model of the maxilla was subtracted from the postoperative 3D model (80, 81, 85). Subsequently, the hard-tissue difference between the two time points could be visualized and evaluated in 3D. The volumes of the newly formed hard-tissues were calculated and compared with the preoperatively planned volumes. The primary outcome of this investigation was the evaluation of volumetric hard-tissue gain by 3D subtraction analysis. The secondary outcomes of the study were:

- Validation of the efficacy of the surgical procedure and volumetric stability of the graft, by calculating the ratio between the actual volumetric hard-tissue gain and the planned hard-tissue volume
- Assessment of the similarity between the planned and actual hard-tissue morphologies by calculating the *Dice Similarity Coefficient* (DSC) and *Hausdorff Distance* (HD).

DSC is a spatial overlap index and a reproducibility validation metric. The value of DSC ranges from 0, indicating no spatial overlap between two sets of binary segmentation results, to 1, indicating complete overlap (69, 86). HD is the longest distance from a point in one of the two models to its closest point in the other model, meaning that the lower the HD value the more the two models overlap. To calculate DSC and HD the Slicer RT extension of 3D Slicer was used.

3.6.2 CBCT-based qualitative scoring (*Stasiak*)

In the second study assessment of the surgical outcomes was performed following the protocol described by *Stasiak et al.*, namely using a CBCT-based qualitative scoring system that relies on the presence and the relative dimensions of the bony bridge between the medial and lateral side of the alveolar cleft in four different vertical positions along the central incisor. This method was chosen instead of the volumetric subtraction analysis, because of the longer follow-up time. Years after the SABG surgery the initial anatomical circumstances in the vicinity of the alveolar cleft are prone to change. The reasons behind this are further growth of the maxilla, eruption of teeth into the graft and changes of tooth positions due to orthodontic movements. These changes render the use of the subtraction analysis unreliable.

The evaluation began by reorienting the images along the long axes of the central incisors on each respective side. The cemento-enamel junction (CEJ) served as the reference point for determining four measurement levels: 3 mm, 5 mm, 7 mm, and 9 mm. The CEJ was defined as the most apical point of the enamel in the midsagittal section of the incisor. The next step involved examining the presence or absence of a bone bridge through the continuous analysis of the region. Next, the alveolar bone was ranked at the designated levels by identifying the narrowest points between the central incisors and canines, using a horizontal scale, as follows:

- 0 = No alveolar bone bridge;
- 1 = The thickness of the alveolar bone bridge $< \frac{1}{2}$ of the labiolingual width of the central incisor's root;
- 2 = The thickness of the alveolar bone bridge $\geq \frac{1}{2}$ of the labiolingual width of the central incisor's root and less than the labiolingual width of the central incisor's root;
- 3 = The thickness of the alveolar bone bridge is at least the labiolingual width of the central incisor's root. (Figure 9.)





Score	CBCT cross-sectional image (left side is on the left side)	Description
0		No alveolar bone bridge.
1		Thickness of the alveolar bone bridge < 1/2 of the labiolingual width of central incisor's root.
2		Thickness of the alveolar bone bridge ≥ 1/2 of the labiolingual width of central incisor's root and less than the labiolingual width of central incisor's root.
3		Thickness of the alveolar bone bridge amounts to at least the labiolingual width of central incisor's root.

Fig. 9. Horizontal scale for bone fill assessment, as described by *Stasiak et al.* (87-89)

To assess the overall bone quality, the rank scores for each level were summed up for each side. The total score was interpreted using an interval scale, as follows:

- 0 = Failure;
- 1–4 = Poor outcome;
- 5–8 = Moderate outcome;
- 9–12 = Good outcome.

A score of 0 was assigned when no bone bridge was present. In cases where a narrow bone bridge existed but fell between or above the designated measurement levels (3, 5, 7, or 9 mm), a modified evaluation was applied. This involved conducting scoring at the actual bone bridge level and attributing the score to the nearest standard level. Additionally, for cases with severe root resorption of the central incisors, classification using the horizontal scale was still performed at the 9 mm level. However, the assessment was adjusted by comparing the root width, measured 0.5 mm below the apex, to provide a more accurate evaluation.

3.7 Statistical analysis

For *Molnár et al.*'s pilot study the primary focus was to determine the amount of hard-tissue change rather than determining absolute baseline and follow-up values. Therefore, only descriptive statistics were used. Data were expressed as mean value \pm standard deviation.

For *Würsching et al.*'s cohort study the *Kappa* correlation coefficient with linear weights was used for the intra-rater and inter-rater reproducibility measurements of the *Stasiak* score system. To test the normality of the acquired data, the *Shapiro–Wilk* test was used. The non-parametric *Wilcoxon* signed-rank test was used for a comparison of the cleft-side and non-cleft-side bone volume. The non-parametric *Mann–Whitney U* test was used to compare the *Stasiak* score and the patient's age at the time of surgery of the iliac crest group and the ATB group. *Student's t*-test was used to compare the initial defect volume of the two groups. As a prerequisite to the *Student's t*-test the *Shapiro–Wilk* test was used to confirm that the volume

data were normally distributed in both groups, and *Levene's* test was used to show the homogeneity of the variances. The correlation between the bone defect volume and the outcome score was analyzed separately for the iliac crest and ATB groups, using *Spearman's* rank correlation. Statistical significance was set at $p < 0.05$. The data were collected in Microsoft Excel (Microsoft, Washington, CA, USA). Statistical analyses were performed using SPSS version 30.0. (IBM Corporation, Redmond, WA, USA).

4. Results

4.1 Study cohorts

Pilot study: Seven consecutive SABG cases reconstructed with particulate ATB graft using a split-thickness papilla curtain flap were recruited for the pilot study. All cases exhibited UCLP requiring secondary alveolar reconstruction during mixed dentition. Five patients were male, two were female. The patients were aged 9–11 years, with a mean age of 10.43 ± 0.79 years. Two defects were located on the right side and five on the left. In total, 35 deciduous teeth and two supernumerary teeth were extracted and utilized for preparation of the ATB graft. In every case, the patient’s own teeth provided enough material for proper reconstruction of the alveolar defect, using an average of 4.75 ± 2.49 teeth per patient. Patient demographic data are shown in Table 1. Orthodontic preparation was completed prior to surgery according to the centre’s protocol. No patients were lost to follow-up within the early assessment window.

Table 1. Patient demographic and surgical data.

Patient	Age	Sex	No. of extracted teeth	Surgical area location
1	11	M	4	Right side
2	10	M	5	Right side
3	11	M	10	Left side
4	11	F	4	Left side
5	10	M	4	Left side
6	9	M	5	Left side
7	11	F	5	Left side
Mean \pm st. deviation	10.43 ± 0.79	n/a	5.29 ± 2.14	n/a

Retrospective cohort study: During the examination period, a total of 42 ABG surgeries were performed in our department. In 12 cases, the defect was bilateral; in 30 cases, the defect was unilateral. In 14 cases, an ATB graft was used; in 25 cases, the donor site was the iliac crest; in three cases, the donor site was the chin. Long-term CBCT data was available for 39 patients; three patients were lost to follow-up. Twenty-one participants exhibiting UCLP were found to be eligible and were enrolled in the current study (Figure 10.). Thirteen patients were male, eight were female. Their age at the time of surgery was between 8 and 14 years; the mean age was 10.4 ± 1.7 years. Sixteen defects were located on the left side and five on the right side. In eleven cases, the donor site for the graft was the iliac crest. In the other 10 cases, a total of 53 deciduous teeth and 4 supernumerary teeth were extracted and utilized for the preparation of the ATB graft. In these cases, the patient's own teeth provided enough material for the proper reconstruction of the alveolar defect, using an average of 5.3 ± 2.26 teeth per patient. The mean follow-up time was 30 ± 13.1 months.

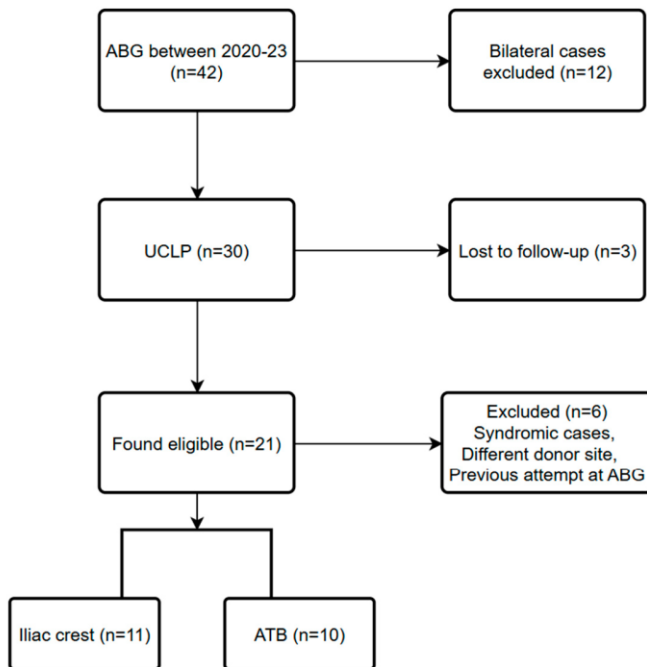


Fig. 10. STROBE flowchart.

4.2 Clinical and radiological outcomes after 3 months follow-up (pilot study)

4.2.1 Soft-tissue healing and local events

Clinical follow-up focused on soft-tissue integrity over the graft, control of oedema, oral hygiene, and the presence of minor dehiscence, or any adverse events. All patients were able to leave the hospital on the first postoperative day without any major complaints and could return to normal daily activity shortly after surgery. Initial wound healing was uneventful in all the seven cases. No unexpected adverse patterns were described within the early window. The quality of keratinized tissues was favourable, fully eliminating any muscle pull or vestibular distortions over the cleft. During the follow-up period, eruption of the cleft-side canine was observed in one patient.

4.2.2 Early volumetric hard-tissue gain

Planned graft volumes averaged $1.14 \text{ cm}^3 \pm 0.36 \text{ cm}^3$, whereas hard-tissue gain, as measured on the 3-months follow-up CBCT scans, averaged $0.65 \text{ cm}^3 \pm 0.26 \text{ cm}^3$ (Figure 11.). The primary outcome data are summarized in Table 2.

4.2.3 Morphometric accuracy and shape agreement

The ratio between actual and planned graft volume ranged between 34.17% and 108.21%, resulting in an average ratio of $59.92\% \pm 24.35\%$. (Table 3.) Agreement between planned and realized 3D contours yielded a mean **DSC** of 0.43 ± 0.20 and a **HD** of $1.83 \pm 0.77 \text{ mm}$, reflecting only partial overlap of the reconstructed alveolar volume with the intended design at 3 months follow-up (Figure 12.) Surface deviation maps highlighted systematic positive deviations (overfill bulges) on the buccal side, and negative deviations (underfill) at the nasal floor and the palatal aspect of the defect.

Table 2. Planned and achieved volumetric hard-tissue gain.

Patient	Planned hard tissue gain (cm ³)	Hard tissue gain at 3-month follow-up (cm ³)
1	0.82	0.48
2	1.65	1.15
3	1.03	0.35
4	0.61	0.66
5	1.44	0.7
6	1.26	0.75
7	1.17	0.49
Mean ± st. deviation	1.14 ± 0.36	0.65 ± 0.26

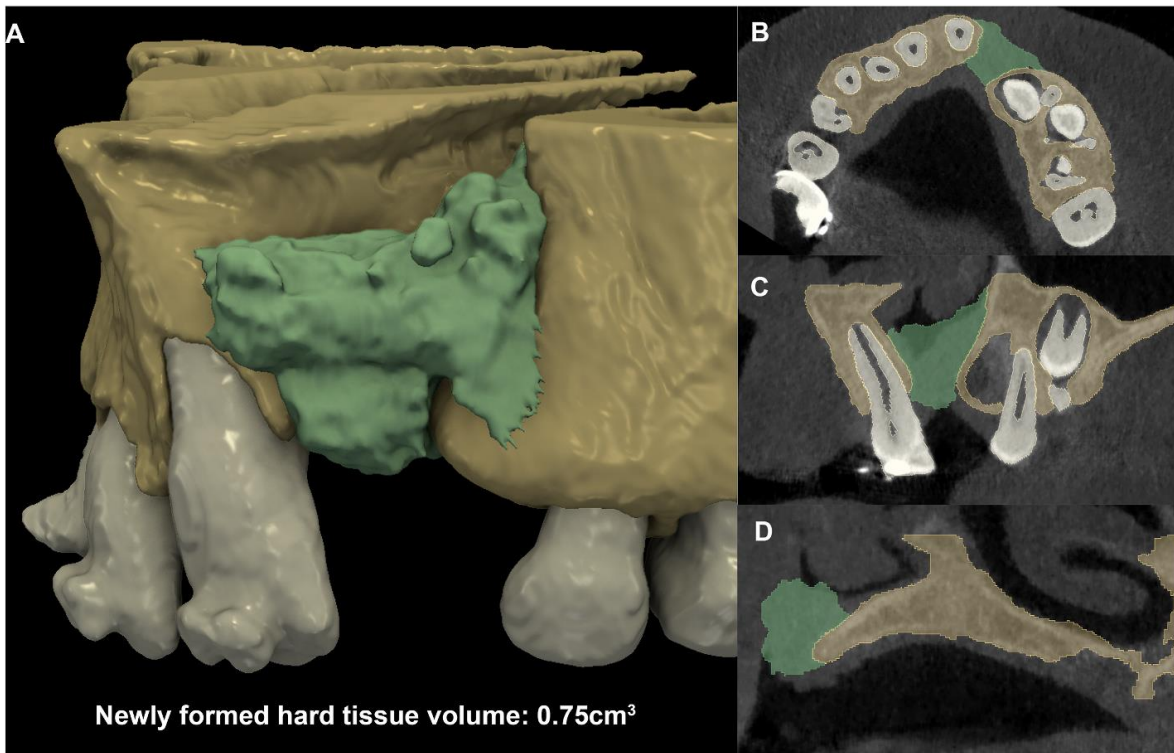


Fig. 11. Volumetric evaluation of the newly formed hard-tissues: (A) 3D view; (B) axial view; (C) coronal view; (D) sagittal view.

Table 3. Volumetric and morphological stability of the graft.

Patient	Achieved volume/ planned volume ratio (%)	Dice similarity coefficient (DSC)	Hausdorff distance (HD) average (mm)
1	58.36	0.65	0.97
2	69.27	0.57	1.56
3	34.17	0.25	2.31
4	108.21	0.41	1.91
5	48.40	0.14	3.24
6	59.55	0.65	1.10
7	41.49	0.36	1.70
Mean \pm st. deviation	59.92 \pm 24.35	0.43 \pm 0.2	1.83 \pm 0.77

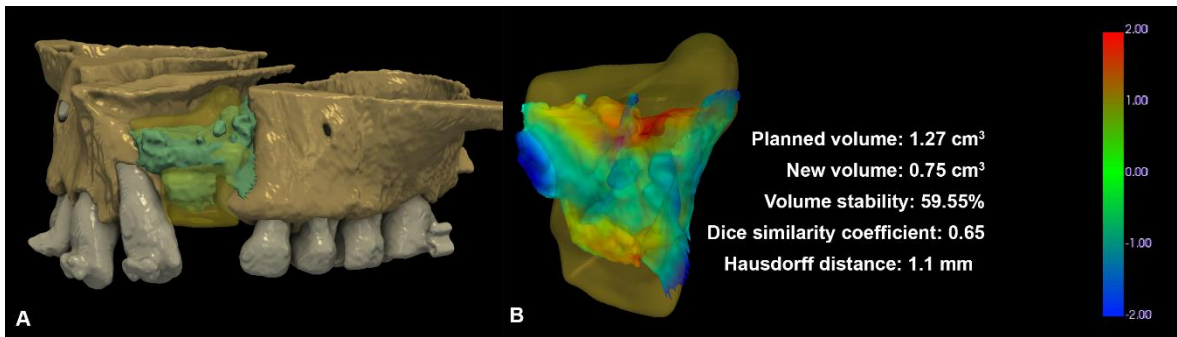


Fig. 12. Relationship between planned outcome and actual outcome:(A) 3D virtual model of planned and actual outcome (planned in transparent yellow, actual in green); (B) colormap model visualizing the morphological differences between the newly formed hard-tissues and the morphology of the planned outcome.

4.3. Long-term outcomes based on CBCT evaluation (cohort study)

4.3.1. Descriptive statistics

The mean volume of the initial defect in the iliac crest group was 0.927 cm³ (SD = 0.316 cm³) and, in the ATB group, it was 1.176 cm³ (SD = 0.449 cm³). The mean age at the time of surgery in the iliac crest group was 10.9 years (SD = 2.1 years) and, in the ATB group, it was 9.9 years (SD = 1.2 years). There was no obvious difference between the occurrence of

early (dehiscence) or late (fistula) complications. In one patient, a severe periodontal defect also developed on the distal surface of tooth 21, which led to extraction. In the ATB group, canine eruption did not happen in two cases during the observed period, whereas no such problems were observed in the other group (Tables 4. And 5.).

Table 4. Descriptive statistics of the iliac crest group.

Iliac crest	Vdefect (cm3)	Dehiscence	Fistula	Canine	Stasiak score	Age at surgery (years)	Follow-up (months)
Patient 1.	1.085	no	no	erupted	11	9	58
Patient 2.	1.492	yes	fistula	erupted	9	14	24
Patient 3.	0.973	no	no	erupted	0	14	41
Patient 4.	0.578	no	no	erupted	9	12	36
Patient 5.	0.504	yes	no	erupted	11	13	14
Patient 6.	0.916	no	no	erupted	0	10	49
Patient 7.	0.973	no	no	erupted	9	8	18
Patient 8.	0.788	no	fistula	erupted	6	10	24
Patient 9.	0.512	no	no	erupted	8	9	52
Patient 10.	1.295	no	no	erupted	0	10	12
Patient 11.	1.079	yes	no	erupted	1	11	56

Table 5. Descriptive statistics of the ATB group.

ATB	Vdefect (cm3)	Dehiscence	Fistula	Canine	Stasiak score	Age at surgery (years)	Follow-up (months)
Patient 12.	1.994	no	no	not erupted	0	10	28
Patient 13.	0.819	no	no	erupted	9	9	25
Patient 14.	1.653	yes	no	erupted	10	8	20
Patient 15.	1.03	no	no	erupted	7	11	20
Patient 16.	1.226	yes	21 def.	erupted	2	11	26
Patient 17.	0.609	no	no	erupted	11	11	28
Patient 18.	1.438	no	no	not erupted	3	8	29
Patient 19.	1.256	no	no	erupted	11	10	25
Patient 20.	1.169	no	fistula	erupted	2	11	25
Patient 21.	0.565	no	no	erupted	9	10	23

4.3.2. Radiographical assessment

The measurements on both the cleft and non-cleft sides were performed three times by two observers in all the patients, and during each instance, all the 168 sites were measured. The first observer performed the measurements twice during a 4-week period, and the second observer performed the measurements only once. Finally, a consensus reading was performed by both observers.

On the cleft side of the iliac crest group, fifteen sites were classified as 0, four sites as 1, ten sites as 2, and thirteen sites as 3. On the cleft side of the ATB group, twelve sites were

classified as 0, five sites as 1, ten sites as 2, and thirteen sites as 3. On the control side, no 0 or 1 scores were obtained. There were six sites classified as 2 and seventy-eight sites as 3.

The surgical outcome showed a high level of variability. The mean total score on the cleft side in the **iliac crest** group was **5.8 (SD: ± 4.6)**; in the **ATB** group, the mean total score on the cleft side was **6.4 (SD: ± 4.2)**. (Figure 13.). On the non-cleft side, the mean total score was 11.7 (SD: ± 0.5). In the **iliac crest** group, the results showed 27% failure, 9% poor, **18% moderate**, and **46% good** results of the surgical procedure. In the **ATB** group, the results were 10% failure, 30% poor, **10% moderate**, and **50% good**. The alveolar bone was classified as good in all the patients on the non-cleft side.

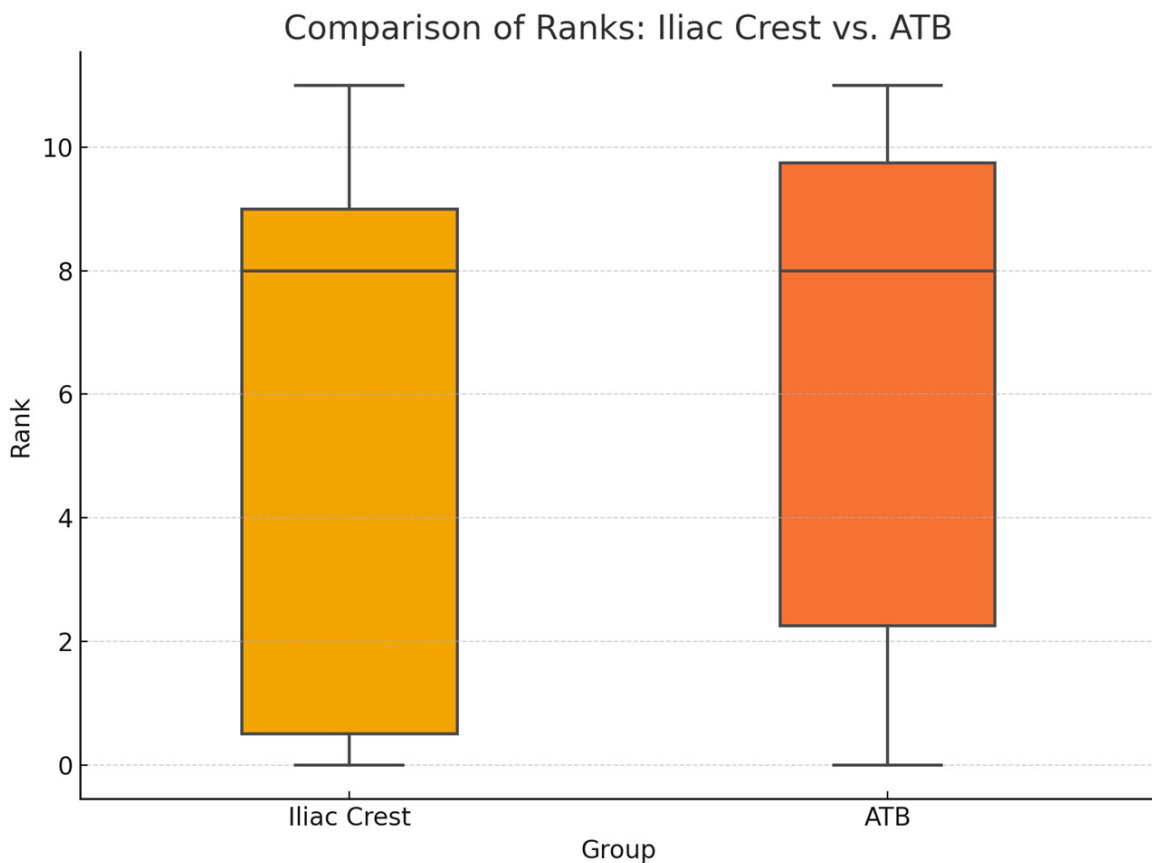


Figure 13. Comparison of the mean of the rank scores on the cleft side

4.3.3 Statistical analysis

Regarding all the statistical measurements, a 95% confidence interval was adopted. The *Wilcoxon* signed-rank test showed statistically significant (ATB: $p = 0.002$, iliac crest: $p = 0.005$) differences between the cleft- and non-cleft-side measurements, which was independent of the type of graft being used. The linearly weighted *Kappa* coefficient result was 0.85 for intra-rater and 0.82 for inter-rater reproducibility. These results showed the excellent reproducibility of the method published by *Stasiak et al.*

The *Mann–Whitney U* test showed **no significant** differences between either the ***Stasiak* scores** ($U = 47.5$, $p = 0.617$) or the **age** at the time of surgery ($U = 67.5$, $p = 0.388$) of the two groups. A comparison of the defect volumes between the two groups was performed using an independent sample *Student's* t-test. Prior to the analysis, the assumptions for parametric testing were evaluated: *Shapiro–Wilk* tests confirmed that the volume data were normally distributed in both the iliac crest ($p = 0.61$) and ATB ($p = 0.86$) groups, and *Levene's* indicated the homogeneity of the variances ($p = 0.36$). The *Student's* t-test revealed **no statistically significant** difference in the mean **defect volume** between the iliac crest group and the ATB group ($t(df) = -1.48$, $p = 0.155$).

The correlation between the initial bone defect volume and the outcome *Stasiak* score was analysed separately for the iliac crest and ATB groups, using *Spearman's* rank correlation. In the **iliac crest** group, a **weak negative** correlation was observed ($\rho = -0.19$, $p = 0.58$), while the **ATB** group showed a **moderate negative** correlation ($\rho = -0.36$, $p = 0.31$). However, neither correlation reached statistical significance ($p > 0.05$). Scatter plots with trendlines are used to illustrate the inverse relationship between the defect volume and outcome score in both groups. (Figure 14).

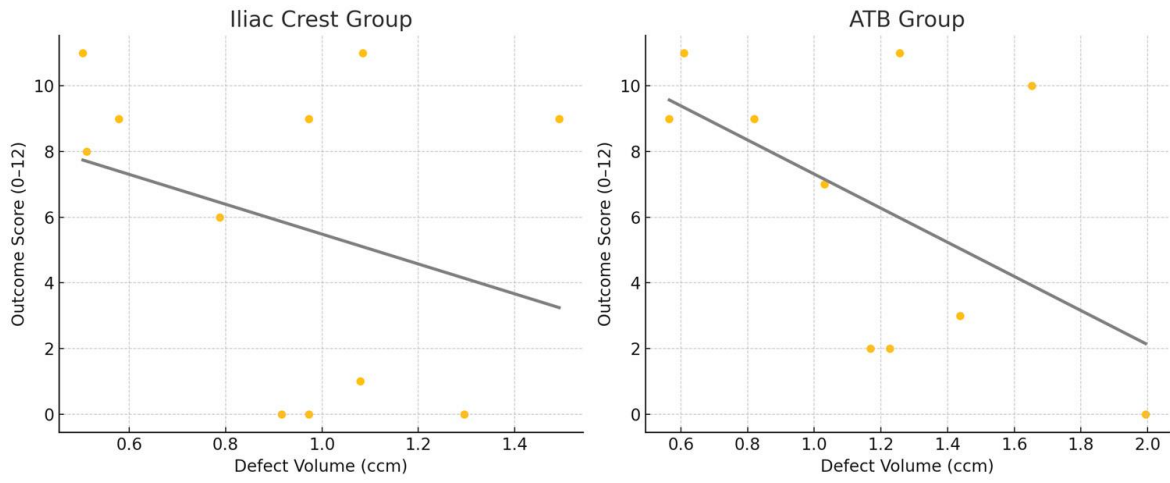


Figure 14. Correlation between initial defect size and outcome score.

5. Discussion

This thesis integrates two complementary datasets: an early pilot series employing CBCT subtraction analysis after autologous tooth bone-based SABG, and a comparative cohort assessing long-term morphology with a CBCT rank scale in ATB versus iliac crest bone graft.

In the first study the efficacy of a 3D-planned ATB graft in conjunction with a split-thickness papilla curtain flap was evaluated for secondary alveolar bone grafting of patients exhibiting UCLP. Autologous tooth bone grafts can effectively restore damaged alveolar bone using autologous tissue and offer solutions to several challenges associated with other grafting materials, such as insufficient osteoconduction, a lack of osteoinduction, sterilization concerns, and the risk of disease transmission. This type of graft is commonly used in preprosthetic and periodontal regenerative surgery.

Although there have been previous case reports describing the use of ATB during SABG (60, 90, 91) these were single case reports. To the best of our knowledge, this was the first study to report clinical and 3D-radiographic data demonstrating favourable defect fill in alveolar clefts, utilizing ATB in a series of patients. Although graft resorption was observed, the amount lost was in line with what can be expected from the use of iliac crest, according to the literature (92). The average volume of the remaining graft at the 3-month follow-up was well above 50% when compared with the planned graft volume. In one case, the actual graft volume even exceeded the planned volume by 8%, thereby suggesting that ATB graft could have an advantageous effect on bone regeneration. The relatively low average DSC value (0.43 ± 0.2) and the high HD ($1.83 \text{ mm} \pm 0.77 \text{ mm}$) indicated a low correlation between the preoperatively planned graft shape and the actual graft shape at 3-months follow-up. This phenomenon could be observed regardless of graft volume stability, and even cases with high graft stability showed a moderate morphological similarity to the planned graft shape. According to the 3D reconstructed images, this was due to buccal displacement of the graft during healing. In most cases, sufficient palatal fill could not be achieved, and the ATB graft did not reach the nasal base. This was most probably due to the pressure applied on the graft

by the nasal and palatal flaps. This suggests a need for further modifications to the flap design on the palatal aspect, or perhaps use of a rigid barrier on the palatal/nasal aspect in conjunction with the graft. A similar approach was adopted by *Ishii et al.* (93) who positioned a rigid cortex bone plate on the palatal aspect to compensate for the pressure applied by the nasal/palatal flaps, and to maintain a safe, secluded space. Limitations of the current study included the relatively low sample size, due to the pilot nature of the examination, and the lack of histological information on graft integration. Although histological evaluations have been performed previously (94) , only tissue integration of the ATB particles could be assessed in this current study. With the aid of 3D technology, quantitative radiographic evaluation was possible; however, the inability to perform qualitative, histological evaluation was a significant limitation.

The Bonmaker® device is suitable for preparing extracted teeth and obtaining ATB particulate grafting material. As confirmed by previous radiographic and histological studies (94, 95) ATB powder may act as a resorbable scaffold and a space-maintaining device to facilitate the healing of alveolar cleft defects. After the preparation of the ATB powder and its mixture with fibrin sealant, a sticky ATB graft was acquired with excellent intraoperative handling properties. The time required for the harvesting of a hip graft is comparable to ATB preparation. Nevertheless, the ATB protocol has two benefits: (i) approximately half of the duration - 20 min - is fully automatic, executed by the Bonmaker® device, which does not require user interaction, thus allowing medical personnel to undertake other activities during the surgery; and (ii) ATB preparation is straightforward — it does not require a highly qualified physician, with nurses fully capable of handling the graft preparation. The estimated costs for the presented surgical approach were as follows: 3D printing 5 EUR, Bonreagent 35 EUR, fibrin glue 100 EUR. The use of these auxiliary techniques increased the costs for the operation itself, although these expenses were not considered to be exceptionally high. On the other hand, avoidance of an extraoral donor site may reduce hospitalization time, as all patients in our study were discharged from hospital on the first postoperative day. This was in contrast with the study by *Brudnicki et al.* (30), who stated the mean length of hospitalization postoperatively was 2.9 days and varied from 1 to 8 days. Most patients were

discharged on the second (66 cases) or third day (102 cases) following the procedure. In higher-income countries, where the cost of hospital stay is more expensive, the use of these auxiliary techniques may lower the overall costs of the treatment, but exact calculations to support this statement were beyond the scope of our study. To ensure the compaction and tight fit of the grafting material inside the cleft, 3D preoperative planning was successfully utilized to manufacture a 3D-printed grafting template to shape the sticky ATB graft before insertion. Closure of the oronasal fistula was achieved in all cases.

Modifications of the original four-flap design, to improve certain aspects of the technique - for example, minimizing injury to the dental papillae and periodontium of the involved dentition, or increasing the amount of attached gingiva surrounding the canine - have been described previously (*L'opez-Cedrún et al.,(96)*). Most of these modifications continue to use a full thickness mucoperiosteal flap, and the suture line remains directly above the graft. The novel split-thickness papilla curtain flap aims to ensure the following: (a) tension-free wound closure without compromising flap circulation, via vertical or horizontal releasing incisions; (b) that a sufficient amount of keratinized gingiva is rotated mesially to surround the tooth on the mesial side of the cleft (usually the lateral or mesial incisor). It also has the benefit of shifting the suture line from directly above the grafted area to a more mesial position, where the sutures will rest on the well vascularized periosteal surface of the premaxilla. The nasal and palatal mucosa on the mesial side of the cleft is still elevated in full thickness, as previously described and now widely applied. The presented flap design resulted in primary-intention wound healing in 100% of the cases, with minimal pain and oedema, as well as excellent, inflammation-free, early wound healing. These pilot results indicated the applicability of the split-thickness papilla curtain flap, and in our experience, this modification showed superior results compared with the traditional mucoperiosteal flap approach. Nevertheless, this needs to be further investigated in future comparative clinical studies. The application of ATB as an autogenous grafting material provides a cost- and time-effective alternative for patients. Its application with the split-thickness papilla curtain flap proved to be an effective surgical approach with a low duration, while providing favourable hard and soft-tissue conditions. This report introduces the early results of a pilot study

regarding the use of ATB in alveolar cleft reconstruction, combined with a split-thickness papilla curtain flap. Although the results were favourable, the study had its limitations - namely the short follow-up period and relatively small sample size.

In the second study, the long-term outcomes of using ATB for alveolar bone grafting in patients with a unilateral cleft lip and palate were compared to the results achieved by using the iliac crest as a donor site. There was no randomization during allocation of patients to the study and the control groups, ATB was the preferred method in the cases where the number of deciduous teeth was adequate. For the rest of the patients, the donor site was the iliac crest, in which a two-team approach was adopted to optimize the surgical time. To achieve the proper amount of graft material according to the preoperative planning, an average of 5.3 ± 2.26 teeth per patient were used. As the early loss of deciduous teeth can lead to complications during eruption of the patients' permanent teeth, our aim was to avoid unnecessary and early extractions. This means, however, that the roots of these teeth were usually partially or completely resorbed, leading to less graft volume per extracted tooth. This also means that the amount of graft that can be prepared using this method is usually only sufficient for small to medium sized unilateral clefts, so no bilateral cases were treated this way, and they were excluded from this study.

Alveolar bone grafting is considered successful when it achieves sufficient bone filling in the alveolar cleft. The eruption of adjacent teeth, particularly the canine, through the grafted bone is also a critical indicator of treatment success (97). Additionally, the lack of oronasal fistulae, healthy periodontal tissues around teeth adjacent to the graft site, and the maintenance of alveolar bone stability and continuity over time are also essential criteria. A recent meta-analysis by *Jahanbin et al.* showed that the total percentage of bone filling after 1 year, according to CBCT, was about 63.38% (70). Due to the limited sample size in this study, it is not possible to conclude whether there is a significant difference between the rate of early or late complications between the two groups. However, the fact that canine eruption in the iliac crest group happened in every case and, in the ATB group, there were two cases out of ten where it did not, needs to be addressed. This must be followed on a longer-term basis and regarding a larger sample size, as the failure of the canines to spontaneously erupt leads to

further surgical interventions, which is a factor that must be considered when choosing ATB as a potential graft material.

CBCT is increasingly used to evaluate the results of ABG, due to its ability to provide detailed 3D imaging with lower radiation than conventional CT, replacing conventional methods based on 2D X-rays. While several CBCT-based methods exist, none have achieved universal recognition (63, 98, 99). Volumetric assessments quantify bone fill, but lack spatial specificity, limiting their value regarding clinical decision making. Grading scales using 2D measurements at vertical levels, such as those by *Soumalainen and Liu* (76, 100), offer partial localization, but are affected by the dental eruption status and have limited generalizability. Assessment approaches are generally classified as continuous (e.g., bone volume or resorption rates) or categorical (e.g., bone height/width). Continuous methods, while quantitative, lack standardized clinical thresholds and fail to identify critical bone deficits impacting orthodontic outcomes. *Stasiak et al.* introduced a more advanced, clinically applicable method that divides the cleft into defined zones, enabling the precise localization of bone presence and resorption (87-89). It uniquely considers the impact of bone loss on adjacent teeth and considers root resorption. This spatially detailed approach supports more informed decisions about regrafting and orthodontic planning, representing a major improvement to CBCT-based ABG evaluations. This method was implemented in the current study, and proved to be reliable and reproducible, with excellent rates of intra- and inter-rater reliability. The results show that there are no significant differences between the outcomes of the two groups based on the *Stasiak* scale and, in both groups, at least 60% of the cases fell into the moderate or good category, meaning no regrafting was deemed necessary. In terms of the other cases, approximately 40% of the cases where the outcome fell into the poor or the failure category, regrafting or prosthetic rehabilitation needed to be considered on an individual basis.

6. Conclusions

Synthesizing the early pilot data after 3 months follow-up and the evidence supported by the longer-term cohort study, autogenous tooth bone (ATB) emerges as a feasible and promising alternative to iliac crest cancellous bone for secondary alveolar bone grafting of patients with cleft lip and palate, particularly in unilateral defects during the mixed dentition.

Short-term integration dynamics from the pilot series show that at 3 months, mean hard-tissue gain after ATB grafting was approximately 60% of the planned volume, indicating substantial, early mineralized fill within the defect. Notably one case slightly exceeded planned volume, consistent with active bone regeneration and favourable scaffold behaviour. Soft-tissue healing was uneventful in all seven cases, with primary closure and improved keratinized tissue coverage—outcomes attributable in part to the split-thickness papilla curtain flap, which relocates healthy gingiva over the graft while moving the suture line off the grafted zone.

However, the morphological assessment of the pilot data showed that despite satisfactory volumetric gains, the “shape fidelity” of the healed graft to the preoperative plan was modest, with a tendency toward buccal displacement and insufficient palatal and nasal fill which most likely could be attributed to pressure by the palatal and nasal flaps. This suggests that technical modifications, e.g., the use of rigid palatal/nasal barrier membranes or cortical plates may further optimize 3D architecture where it matters for orthodontic eruption paths and nasal base support.

The cohort study documented no statistically significant difference in cleft-side bone quantity between ATB and iliac crest groups, while differences between cleft and non-cleft sides persisted, with both groups remaining inferior to the contralateral healthy side independently of graft type. The evaluation method demonstrated excellent intra- and inter-rater reliability, strengthening the validity of these comparisons. Clinically, at least 60% of cases in both groups achieved moderate-to-good *Stasiak* categories - thresholds generally consistent with avoiding regrafting and supporting continued orthodontic care - whereas the remainder required individualized consideration for regrafting or prosthetic planning. Together, these

findings position ATB as a clinically acceptable option for long-term alveolar reconstruction outcomes, not inferior to iliac crest, without exposing the child to an extraoral donor site.

There are, however, certain limitations to both studies. The long-term cohort remains modest (n = 21) with nonrandomized allocation between ATB and iliac crest. The small number of patients renders the statistical assessment of early and late complications (e.g.: lack of canine eruption) unreliable. The pilot series is also small (n = 7), descriptive, and lacks histological evaluation; while prior work supports ATB's osteoinductive/osteoconductive behaviour, tissue-level integration within cleft sites over time remains to be investigated more rigorously. The pilot's early shape drift also proves that "volume met" doesn't necessarily mean optimal architecture. Moreover, the cohort's primary endpoint only used a categorical scale, lacking a continuous, volume-based assessment of long-term integration of the graft. These constraints underline the need for larger, controlled, and methodologically harmonized studies.

As a conclusion, given comparable long-term radiographic outcomes to iliac crest in this cohort and favourable early healing profiles, ATB may be considered as a first-line option when sufficient tooth-derived graft volume is obtainable, and the surgical team is trained in the workflow.

7. Summary

The two studies this thesis is based upon examine autogenous tooth bone as a graft for secondary alveolar bone grafting in patients with unilateral cleft lip and palate.

The first pilot study details the operative concept on a small cohort of seven patients: extracted deciduous and supernumerary teeth were processed into particulate ATB graft. Mixing it with fibrin sealant inside a 3D-printed mold based on virtual surgical planning yielded a “sticky” block that improved handling and fit. Soft-tissue closure employed the split-thickness papilla curtain flap, which shifts keratinized gingiva over the graft and moves the suture line away from the grafted zone. Patients were discharged on the first postoperative day, and early healing was uneventful with favourable soft-tissue conditions. Three-month radiographic outcomes based on CBCT subtraction analysis showed that planned graft volume averaged $1.14 \pm 0.36 \text{ cm}^3$ and measured hard-tissue gain averaged $0.65 \pm 0.26 \text{ cm}^3$ ($\approx 60\%$ realization). Morphological similarity between planned and achieved grafts was moderate (mean DSC: 0.43 ± 0.20 ; mean HD: $1.83 \pm 0.77 \text{ mm}$), with a consistent trend toward buccal displacement and insufficient palatal/nasal fill.

The second, retrospective cohort study by *Würsching et al.*, included 21 patients exhibiting UCLP treated with either ICBG (n=11) or ATB (n=10). Outcomes were assessed on long-term CBCT (mean follow-up was 30 ± 13 months) using the grading system published by *Stasiak et al.* Key findings were, that bone on the cleft side remained significantly less than the contralateral non-cleft side in both groups (ATB $p=0.002$; iliac crest $p=0.005$), yet there was no significant difference between the two groups on the cleft side (*Mann–Whitney* $U=47.5$, $p=0.617$). At least 60% of cases in each group achieved moderate or good outcomes on *Stasiak* grading. On average, approximately 5 teeth provided sufficient ATB volume for unilateral defects. To sum up, the data support that ATB is a feasible alternative to iliac crest for unilateral alveolar cleft reconstruction, delivering short- and long-term CBCT outcomes comparable to iliac crest, while avoiding donor-site morbidity, although neither material fully restores the cleft to the contralateral healthy side.

8. New statements of the thesis

1. A digitally planned ATB graft using deciduous and supernumerary teeth, combined with fibrin sealant produced substantial early hard-tissue fill of the alveolar cleft in patients with UCLP. Volumetric stability however didn't necessarily mean reliability in graft morphology
2. The split-thickness papilla curtain flap is a practical modification to the *Nordin-Abyholm* 4-flap technique, that relocates keratinized mucosa over the graft and achieves uneventful early healing.
3. Autogenous tooth bone yields long-term radiographic and clinical outcomes comparable to iliac crest for unilateral alveolar cleft grafting.
4. Initial defect size showed no significant correlation with categorical outcome regardless of the type of graft.
5. ATB enables unilateral alveolar cleft reconstruction without extraoral donor morbidity and can be proposed as a patient-friendly first-line option in select cases.

9. References

1. Acs L, Nemes B, Nagy K, Acs M, Banhidy F, Rozsa N. Maternal factors in the origin of cleft lip/cleft palate: A population-based case-control study. *Orthod Craniofac Res.* 2024;27 Suppl 1:6-13.
2. Leslie EJ, Marazita ML. Genetics of cleft lip and cleft palate. *Am J Med Genet C Semin Med Genet.* 2013;163c(4):246-58.
3. Allori AC, Mulliken JB, Meara JG, Shusterman S, Marcus JR. Classification of Cleft Lip/Palate: Then and Now. *Cleft Palate Craniofac J.* 2017;54(2):175-88.
4. Slator R, Perisanidou LI, Waylen A, Sandy J, Ness A, Wills AK. Range and timing of surgery, and surgical sequences used, in primary repair of complete unilateral cleft lip and palate: The Cleft Care UK study. *Orthod Craniofac Res.* 2020;23(2):166-73.
5. Kaura AS, Srinivasa DR, Kasten SJ. Optimal Timing of Alveolar Cleft Bone Grafting for Maxillary Clefts in the Cleft Palate Population. *J Craniofac Surg.* 2018;29(6):1551-7.
6. Cho-Lee GY, García-Díez EM, Nunes RA, Martí-Pagès C, Sieira-Gil R, Rivera-Baró A. Review of secondary alveolar cleft repair. *Ann Maxillofac Surg.* 2013;3(1):46-50.
7. Yamanishi T, Arimura Y, Kirikoshi S, Hara T, Nishio T, Seikai T, et al. Clinical outcomes of gingivoperiosteoplasty for unilateral cleft lip and palate performed in early childhood. *J Plast Reconstr Aesthet Surg.* 2024;97:268-74.
8. Pontell ME, Taylor JA. Discussion: The Effects of Gingivoperiosteoplasty and Cleft Palate Repair on Facial Growth. *Plast Reconstr Surg.* 2024;153(5):1120-1.
9. Balumuka D, Daly GE, Krakauer K, Burch S, Jedrzejewski B, Johnson A, et al. Gingivoperiosteoplasty in Children with Cleft Lip and Palate: The Need for Alveolar Bone Grafting. *Cleft Palate Craniofac J.* 2025;62(8):1395-401.
10. Boyne PJ, Sands NR. Secondary bone grafting of residual alveolar and palatal clefts. *Journal of oral surgery (American Dental Association : 1965).* 1972;30(2):87-92.
11. Boyne PJ, Sands NR. Combined orthodontic-surgical management of residual palato-alveolar cleft defects. *Am J Orthod.* 1976;70(1):20-37.

12. Guo J, Li C, Zhang Q, Wu G, Deacon SA, Chen J, et al. Secondary bone grafting for alveolar cleft in children with cleft lip or cleft lip and palate. *Cochrane Database Syst Rev*. 2011(6):Cd008050.
13. Dempf R, Teltzrow T, Kramer FJ, Hausamen JE. Alveolar bone grafting in patients with complete clefts: a comparative study between secondary and tertiary bone grafting. *Cleft Palate Craniofac J*. 2002;39(1):18-25.
14. Fahradyan A, Tsuha M, Wolfswinkel EM, Mitchell KS, Hammoudeh JA, Magee W, 3rd. Optimal Timing of Secondary Alveolar Bone Grafting: A Literature Review. *J Oral Maxillofac Surg*. 2019;77(4):843-9.
15. Brudnicki A, Regulski PA, Sawicka E, Fudalej PS. Alveolar Volume Following Different Timings of Secondary Bone Grafting in Patients with Unilateral Cleft Lip and Palate. A Pilot Study. *J Clin Med*. 2021;10(16).
16. Weissler EH, Paine KM, Ahmed MK, Taub PJ. Alveolar Bone Grafting and Cleft Lip and Palate: A Review. *Plast Reconstr Surg*. 2016;138(6):1287-95.
17. Doucet JC, Patel MH, Russell KA. Evaluation of Cleft Adjacent Canine Eruption in Patients With Alveolar Cleft Treated With Early Secondary Alveolar Bone Grafting. *Cleft Palate Craniofac J*. 2025:10556656251356211.
18. Yu X, Huang Y, Li W. Correlation between alveolar cleft morphology and the outcome of secondary alveolar bone grafting for unilateral cleft lip and palate. *BMC Oral Health*. 2022;22(1):251.
19. Garib D, Massaro C, Yatabe M, Janson G, Lauris JRP. Mesial and distal alveolar bone morphology in maxillary canines moved into the grafted alveolar cleft: Computed tomography evaluation. *Am J Orthod Dentofacial Orthop*. 2017;151(5):869-77.
20. Kim EN, Moss WD, Kunkel RP, Yamashiro DK, Gociman BR. Simultaneous Closure of the Cleft Alveolus and Hard Palate with Concomitant Bone Grafting. *Plast Reconstr Surg Glob Open*. 2022;10(2):e4099.
21. Kim J, Jeong W. Secondary bone grafting for alveolar clefts: surgical timing, graft materials, and evaluation methods. *Arch Craniofac Surg*. 2022;23(2):53-8.

22. Conville R, Zakaria NN, Woods M, Khoshkhounejad G. Does Tooth Removal at the Time of Secondary Alveolar Bone Grafting Influence the Outcome for Cleft Patients? *Cleft Palate Craniofac J*. 2025;10556656251346720.
23. Bittermann GKP, van Es RJJ, de Ruiter AP, Frank MH, Bittermann AJN, van der Molen ABM, et al. Incidence of complications in secondary alveolar bone grafting of bilateral clefts with premaxillary osteotomy: a retrospective cohort study. *Clin Oral Investig*. 2020;24(2):915-25.
24. Jing B, Yao M, Tsauo C, Luo X, Shi B, Zheng Q, et al. A 2-Stage Approach to Alveolar Cleft Repair with Combined Cortical and Cancellous Bone Grafting. *Plast Reconstr Surg*. 2025;156(2):257e-66e.
25. Nordin KE, Larson O, Nylén B, Eklund G. Early bone grafting in complete cleft lip and palate cases following maxillofacial orthopedics. I. The method and the skeletal development from seven to thirteen years of age. *Scand J Plast Reconstr Surg*. 1983;17(1):33-50.
26. Åbyholm FE, Olav B, and Semb G. Secondary Bone Grafting of Alveolar Clefts: A Surgical/Orthodontic Treatment Enabling a Non-prosthetic Rehabilitation in Cleft Lip and Palate Patients. *Scandinavian Journal of Plastic and Reconstructive Surgery*. 1981;15(2):127-40.
27. Rawashdeh MA, Telfah H. Secondary alveolar bone grafting: the dilemma of donor site selection and morbidity. *Br J Oral Maxillofac Surg*. 2008;46(8):665-70.
28. Eufinger H, Leppänen H. Iliac crest donor site morbidity following open and closed methods of bone harvest for alveolar cleft osteoplasty. *J Craniomaxillofac Surg*. 2000;28(1):31-8.
29. Dimitriou R, Mataliotakis GI, Angoules AG, Kanakaris NK, Giannoudis PV. Complications following autologous bone graft harvesting from the iliac crest and using the RIA: a systematic review. *Injury*. 2011;42 Suppl 2:S3-15.
30. Brudnicki A, Rachwalski M, Wiepszowski Ł, Sawicka E. Secondary alveolar bone grafting in cleft lip and palate: A comparative analysis of donor site morbidity in different age groups. *J Craniomaxillofac Surg*. 2019;47(1):165-9.

31. Wu C, Pan W, Feng C, Su Z, Duan Z, Zheng Q, et al. Grafting materials for alveolar cleft reconstruction: a systematic review and best-evidence synthesis. *Int J Oral Maxillofac Surg.* 2018;47(3):345-56.
32. Dissaux C, Ruffenach L, Bruant-Rodier C, George D, Bodin F, Remond Y. Cleft Alveolar Bone Graft Materials: Literature Review. *Cleft Palate Craniofac J.* 2022;59(3):336-46.
33. Putri IL, Fabian P, Wungu CDK. A meta-analysis of alveolar bone grafting using bone substitutes in cleft lip and palate patients. *Tzu Chi Med J.* 2024;36(1):53-8.
34. Rahpeyma A, Khajehahmadi S. Chin bone graft for maxillary alveolar cleft: indications and limitations. *J Craniofac Surg.* 2014;25(5):1650-2.
35. Francoise CA, Sescleifer AM, Okeke RI, Tyson CV, Plikaitis C. Efficacy of Demineralized Bone Matrix for Revision Alveolar Bone Grafting in Patients Previously Treated with Bone Morphogenetic Protein 2 (BMP-2). *The Cleft Palate Craniofacial Journal.* 2024;61(7):1179-85.
36. Blume O, Back M, Born T, Donkiewicz P. Reconstruction of a Unilateral Alveolar Cleft Using a Customized Allogenic Bone Block and Subsequent Dental Implant Placement in an Adult Patient. *J Oral Maxillofac Surg.* 2019;77(10):2127.e1-.e11.
37. Le BT, Woo I. Alveolar cleft repair in adults using guided bone regeneration with mineralized allograft for dental implant site development: a report of 2 cases. *J Oral Maxillofac Surg.* 2009;67(8):1716-22.
38. Chauvel-Picard J, Lambert C, Gaget D, Asselborn M, Lange E, Gleizal A. Osseous Outcomes of Cleft Alveolar Bone Grafting with Allograft and Platelet-Rich Fibrin: Preliminary Study with Radiological Outcome. *Cleft Palate Craniofac J.* 2025;62(9):1549-54.
39. Aly LAA, Hammouda N. Secondary closure of alveolar cleft with resorbable collagen membrane and a combination of intraoral autogenous bone graft and deproteinized anorganic bovine bone. *Annals of Maxillofacial Surgery.* 2016;6(2):165-71.
40. Ryu J, Hwang DS. Descriptive analysis of autologous and xenograft materials for secondary alveolar bone grafting in cleft lip and palate patients: a literature review. *Maxillofac Plast Reconstr Surg.* 2025;47(1):22.

41. Yuan KF, Lai QG, Qi C, Guo XH, Shi RJ, Xu X, et al. [Clinical study of bioglass for repairing alveolar cleft.]. *Shanghai Kou Qiang Yi Xue*. 2004;13(5):465-8.
42. Verdier E, Azzis O, Marchand M, Jeanne S, Lebullenger R, Gatibelza ME, et al. Secondary alveolar bone grafting of clefts using bioactive glass 45S5: Long-term dental and periodontal status. *Am J Orthod Dentofacial Orthop*. 2025;168(3):339-47.
43. Brezulier D, Chaigneau L, Jeanne S, Lebullenger R. The Challenge of 3D Bioprinting of Composite Natural Polymers PLA/Bioglass: Trends and Benefits in Cleft Palate Surgery. *Biomedicines*. 2021;9(11).
44. Alonso N, Tanikawa DYS, Freitas RdS, Canan L, Ozawa TO, Rocha DL. Evaluation of Maxillary Alveolar Reconstruction Using a Resorbable Collagen Sponge with Recombinant Human Bone Morphogenetic Protein-2 in Cleft Lip and Palate Patients. *Tissue Engineering Part C: Methods*. 2010;16(5):1183-9.
45. Makar KG, Buchman SR, Vercler CJ. Bone Morphogenetic Protein-2 and Demineralized Bone Matrix in Difficult Bony Reconstructions in Cleft Patients. *Plastic and Reconstructive Surgery – Global Open*. 2021;9(6):e3611.
46. Xiao W-l, Jia K-n, Yu G, Zhao N. Outcomes of bone morphogenetic protein-2 and iliac cancellous bone transplantation on alveolar cleft bone grafting: A meta-analysis. *Journal of Plastic, Reconstructive & Aesthetic Surgery*. 2020;73(6):1135-42.
47. Leal CR, de Carvalho RM, Ozawa TO, de Almeida AM, da Silva Dalben G, da Cunha Bastos JC, Jr., et al. Outcomes of Alveolar Graft With Rhbmp-2 in CLP: Influence of Cleft Type and Width, Canine Eruption, and Surgeon. *Cleft Palate Craniofac J*. 2019;56(3):383-9.
48. Behnia H, Khojasteh A, Soleimani M, Tehranchi A, Atashi A. Repair of alveolar cleft defect with mesenchymal stem cells and platelet derived growth factors: a preliminary report. *J Craniomaxillofac Surg*. 2012;40(1):2-7.
49. Li T, Wang YY, Liu C. The effectiveness of using platelet-rich concentrate with iliac bone graft in the repair of alveolar cleft: a meta-analysis of randomized controlled trials. *Int J Oral Maxillofac Surg*. 2023;52(10):1049-56.
50. Lavagen N, Nokovitch L, Algrin A, Dakpe S, Testelin S, Devauchelle B, et al. Efficiency of advanced-PRF usage in the treatment of alveolar cleft with iliac bone graft: A retrospective study. *J Craniomaxillofac Surg*. 2021;49(10):923-8.

51. Ellapakurthi P, Reddy GSP. The effectiveness of mineralized plasmatic matrix in the closure of alveolar clefts with volumetric assessment. *Regen Med Res.* 2021;9:1.
52. Kadry W, Eldeftar M, Nassar Y, Abou-El-Fetouh A, Hakam MM. Clinical, volumetric and densitometric evaluation of tissue engineered constructs for secondary alveolar cleft reconstruction: A randomized clinical trial. *J Craniomaxillofac Surg.* 2021;49(12):1141-50.
53. Park JJ, Rochlin DH, Parsaei Y, Shetye PR, Witek L, Leucht P, et al. Bone Tissue Engineering Strategies for Alveolar Cleft: Review of Preclinical Results and Guidelines for Future Studies. *Cleft Palate Craniofac J.* 2023;60(11):1450-61.
54. Liang F, Leland H, Jedrzejewski B, Auslander A, Maniskas S, Swanson J, et al. Alternatives to Autologous Bone Graft in Alveolar Cleft Reconstruction: The State of Alveolar Tissue Engineering. *J Craniofac Surg.* 2018;29(3):584-93.
55. Kim YK, Kim SG, Byeon JH, Lee HJ, Um IU, Lim SC, et al. Development of a novel bone grafting material using autogenous teeth. *Oral Surg Oral Med Oral Pathol Oral Radiol Endod.* 2010;109(4):496-503.
56. Kim YK, Kim SG, Yun PY, Yeo IS, Jin SC, Oh JS, et al. Autogenous teeth used for bone grafting: a comparison with traditional grafting materials. *Oral Surg Oral Med Oral Pathol Oral Radiol.* 2014;117(1):e39-45.
57. Minetti E, Taschieri S, Berardini M, Corbella S. New Classification of Autologous Tooth-Derived Grafting Materials: Fundamental Concepts. *Int J Dent.* 2025;2025:6646405.
58. Harada R, Yamashita K, Imamura K, Inagaki S, Saito A. Periodontal Regenerative Therapy with Recombinant Human Fibroblast Growth Factor-2 and Autogenous Bone Graft in Treatment of Generalized Aggressive Periodontitis (Stage III, Grade C): A Case Report with 1-year Follow-up. *Bull Tokyo Dent Coll.* 2025.
59. Hussain AA, Al-Quisi AF, Abdulkareem AA. Efficacy of Autogenous Dentin Biomaterial on Alveolar Ridge Preservation: A Randomized Controlled Clinical Trial. *Biomed Res Int.* 2023;2023:7932432.
60. Jeong K-I, Lee J, Kim K-W, Um I-W, Hara S, Mitsugi M, et al. Alveolar Cleft Reconstruction Using Chin Bone and Autogenous Tooth Bone Graft Material: Reports of 5 Cases. *Journal of Korean Dental Science.* 2013;6(1):13-21.

61. Sales PHH, Oliveira-Neto OB, Torres TS, de Lima FJC. Effectiveness of dental implants placed in bone graft area of cleft Patients. *Int J Oral Maxillofac Surg.* 2019;48(8):1109-14.
62. Krakowski PJ, J. ; Karpinski, R.; Jaworski, L. Usefulness of rapid prototyping in planning complex trauma surgeries. *Applied Computer Science.* 2019;15(3):65.-72.
63. Khalil B, Regnstrand T, Jacobs R. A novel cone beam-CT approach for quantifying maxillary changes following secondary alveolar bone grafting in unilateral cleft patients. *BMC Oral Health.* 2025;25(1):292.
64. Pálházi P, Nemes B, Swennen G, Nagy K. Three-dimensional simulation of the nasoalveolar cleft defect. *Cleft Palate Craniofac J.* 2014;51(5):593-6.
65. Fawzy HH, Hassan OMI, Elsakka D. Computer-assisted Alar Base Bone Graft Design in Unilateral Cleft Lip Reconstruction. *Plast Reconstr Surg Glob Open.* 2025;13(9):e7093.
66. Klunder LS, Merema BBJ, Matthews-Brzozowski AZ, Jansma J, Pichardo SEC, Kraeima J, et al. 3D virtual surgical planning in patients with bilateral cleft lip and palate undergoing premaxilla osteotomy combined with secondary alveolar bone grafting: a retrospective accuracy analysis. *J Craniomaxillofac Surg.* 2025;53(10):1904-10.
67. Fabian Z, Kadar K, Patonay L, K N. Application of 3D Printed Biocompatible Plastic Surgical Template for the Reconstruction of a Nasoalveolar Cleft with Preoperative Volume Analysis. *Materiale Plastice (Mater Plast).* 2019;56(2):413-5.
68. Kesztyus A, Wursching T, Nemes B, Palvolgyi L, Nagy K. Evaluation of 3D visualization, planning and printing techniques in alveolar cleft repair, and their effect on patients' burden. *J Stomatol Oral Maxillofac Surg.* 2022;123(4):484-9.
69. Wursching T, Kesztyus A, Pottel L, Swennen G, Nagy K. Comparison of two methods for segmentation of the nasoalveolar defect and design of a three-dimensional surgical template in patients with cleft lip and palate: a retrospective study. *Int J Oral Maxillofac Surg.* 2025.
70. Jahanbin A, Kamyabnezhad E, Raisolsadat MA, Farzanegan F, Bardideh E. Long-Term Stability of Alveolar Bone Graft in Cleft Lip and Palate Patients: Systematic Review and Meta-Analysis. *Journal of Craniofacial Surgery.* 2022;33(2):e194-e200.

71. Bergland O, Semb G, Abyholm FE. Elimination of the residual alveolar cleft by secondary bone grafting and subsequent orthodontic treatment. *Cleft Palate J.* 1986;23(3):175-205.
72. Hynes PJ, Earley MJ. Assessment of secondary alveolar bone grafting using a modification of the Bergland grading system. *Br J Plast Surg.* 2003;56(7):630-6.
73. Witherow H, Cox S, Jones E, Carr R, Waterhouse N. A new scale to assess radiographic success of secondary alveolar bone grafts. *Cleft Palate Craniofac J.* 2002;39(3):255-60.
74. Lemberger M, Benchimol D, Pegelow M, Jacobs R, Karsten A. Validation and comparison of 2D grading scales and 3D volumetric measurements for outcome assessment of bone-grafted alveolar clefts in children. *Eur J Orthod.* 2024;46(2).
75. Shaheen E, Danneels M, Doucet K, Dormaar T, Verdonck A, Cadenas de Llano-Perula M, et al. Validation of a 3D methodology for the evaluation and follow-up of secondary alveolar bone grafting in unilateral cleft lip and palate patients. *Orthod Craniofac Res.* 2022;25(3):377-83.
76. Suomalainen A, Aberg T, Rautio J, Hurmerinta K. Cone beam computed tomography in the assessment of alveolar bone grafting in children with unilateral cleft lip and palate. *Eur J Orthod.* 2014;36(5):603-11.
77. Oberoi S, Chigurupati R, Gill P, Hoffman WY, Vargervik K. Volumetric assessment of secondary alveolar bone grafting using cone beam computed tomography. *Cleft Palate Craniofac J.* 2009;46(5):503-11.
78. Molnar B, Wursching T, Solyom E, Palvolgyi L, Radoczy-Drajko Z, Palkovics D, et al. Alveolar cleft reconstruction utilizing a particulate autogenous tooth graft and a novel split-thickness papilla curtain flap - A retrospective study. *J Craniomaxillofac Surg.* 2024;52(1):77-84.
79. Wursching T, Meszaros B, Solyom E, Molnar B, Bogdan S, Nemeth Z, et al. Long-Term Results of Autologous Tooth Bone Grafting in Alveolar Cleft Reconstruction: A Retrospective Cohort Study. *Biomedicines.* 2025;13(7).

80. Palkovics D, Molnar B, Pinter C, Gera I, Windisch P. Utilizing a novel radiographic image segmentation method for the assessment of periodontal healing following regenerative surgical treatment. *Quintessence Int.* 2022;53(6):492-501.
81. Palkovics D, Pinter C, Bartha F, Molnar B, Windisch P. CBCT subtraction analysis of 3D changes following alveolar ridge preservation: a case series of 10 patients with 6-months follow-up. *Int J Comput Dent.* 2021;24(3):241-51.
82. Pinter C, Lasso A, Fichtinger G. Polymorph segmentation representation for medical image computing. *Comput Methods Programs Biomed.* 2019;171:19-26.
83. Segura-Castillo JL, Aguirre-Camacho H, González-Ojeda A, Michel-Perez J. Reduction of bone resorption by the application of fibrin glue in the reconstruction of the alveolar cleft. *J Craniofac Surg.* 2005;16(1):105-12.
84. Klein S, Staring M, Murphy K, Viergever MA, Pluim JP. elastix: a toolbox for intensity-based medical image registration. *IEEE Trans Med Imaging.* 2010;29(1):196-205.
85. Palkovics D, Bolya-Orosz F, Pinter C, Molnar B, Windisch P. Reconstruction of vertical alveolar ridge deficiencies utilizing a high-density polytetrafluoroethylene membrane /clinical impact of flap dehiscence on treatment outcomes: case series. *BMC Oral Health.* 2022;22(1):490.
86. Janssen NG, Schreurs R, Bittermann GKP, Borstlap WA, Koole R, Meijer GJ, et al. A novel semi-automatic segmentation protocol for volumetric assessment of alveolar cleft grafting procedures. *J Craniomaxillofac Surg.* 2017;45(5):685-9.
87. Stasiak M, Wojtaszek-Słomińska A, Racka-Pilszak B. A novel method for alveolar bone grafting assessment in cleft lip and palate patients: cone-beam computed tomography evaluation. *Clin Oral Investig.* 2021;25(4):1967-75.
88. Stasiak M, Wojtaszek-Słomińska A, Racka-Pilszak B. Current methods for secondary alveolar bone grafting assessment in cleft lip and palate patients — A systematic review. *Journal of Cranio-Maxillofacial Surgery.* 2019;47(4):578-85.
89. Stasiak M, Wojtaszek-Słomińska A, Racka-Pilszak B. Correction to: A novel method for alveolar bone grafting assessment in cleft lip and palate patients: cone-beam computed tomography evaluation. *Clin Oral Investig.* 2021;25(4):1977.

90. Hara S, Mitsugi M, Kanno T, Tatemoto Y. Bone transport and bone graft using auto-tooth bone for alveolar cleft repair. *J Craniofac Surg*. 2013;24(1):e65-8.
91. Datarkar A, Bhawalkar A. Utility of tooth as an autogenous graft material in the defects of alveolar cleft - A novel case report. *J Oral Biol Craniofac Res*. 2020;10(4):470-3.
92. Vandersluis YR, Fisher DM, Stevens K, Tompson BD, Lou W, Suri S. Comparison of dental outcomes in patients with nonsyndromic complete unilateral cleft lip and palate who receive secondary alveolar bone grafting before or after emergence of the permanent maxillary canine. *Am J Orthod Dentofacial Orthop*. 2020;157(5):668-79.
93. Ishii M, Ishii Y, Moriyama T, Gunji A, Morita K, Imaizumi F, et al. Simultaneous cortex bone plate graft with particulate marrow and cancellous bone for reliable closure of palatal fistulae associated with cleft deformities. *Cleft Palate Craniofac J*. 2002;39(3):364-9.
94. Radoczy-Drajko Z, Windisch P, Svidro E, Tajti P, Molnar B, Gerber G. Clinical, radiographical and histological evaluation of alveolar ridge preservation with an autogenous tooth derived particulate graft in EDS class 3-4 defects. *BMC Oral Health*. 2021;21(1):63.
95. Solyom E, Szalai E, Czumbel ML, Szabo B, Vancsa S, Mikulas K, et al. The use of autogenous tooth bone graft is an efficient method of alveolar ridge preservation - meta-analysis and systematic review. *BMC Oral Health*. 2023;23(1):226.
96. López-Cedrún JL, Gonzalez-Landa G, Figueroa A. Isolated keratinized gingiva incision in alveolar cleft bone grafts improves qualitative outcomes: a single surgeon's 23 year experience. *J Craniomaxillofac Surg*. 2014;42(8):1692-7.
97. Lorenzoni DC, Janson G, Bastos JC, Carvalho RM, Bastos JC, Jr., de Cassia Moura Carvalho Lauris R, et al. Evaluation of secondary alveolar bone grafting outcomes performed after canine eruption in complete unilateral cleft lip and palate. *Clin Oral Investig*. 2017;21(1):267-73.
98. Kamperos G, Theologie-Lygidakis N, Tsiklakis K, Iatrou I. A novel success scale for evaluating alveolar cleft repair using cone-beam computed tomography. *J Craniomaxillofac Surg*. 2020;48(4):391-8.
99. Kumar A, Batra P, Sharma K, Raghavan S, Talwar A, Srivastava A, et al. A Three-Dimensional Scale for the Qualitative and Quantitative Assessments of Secondary Alveolar

Bone Grafting (SABG) in Unilateral Cleft Lip and Palate Patients Using Cone-Beam Computed Tomography (CBCT). *Indian J Plast Surg.* 2023;56(2):138-46.

100. Liu L, Ma L, Lin J, Jia Q. [A new three-dimensional scale in the evaluation of the secondary alveolar bone grafting]. *Zhonghua Kou Qiang Yi Xue Za Zhi.* 2015;50(10):598-602.

10. Bibliography of the candidate's publications

Publications related to the thesis:

- Würsching, T., Mészáros, B., Sólyom, E., Molnár, B., Bogdán, S., Németh, Z., & Nagy, K. (2025). Long-Term Results of Autologous Tooth Bone Grafting in Alveolar Cleft Reconstruction: A Retrospective Cohort Study. *Biomedicines*, 13(7), 1735. <https://doi.org/10.3390/biomedicines13071735>
IF: 3.9, Q1
- Molnár, B., Würsching, T.*, Sólyom, E., Pálvölgyi, L., Radóczy-Drajkó, Z., Palkovics, D., & Nagy, K. (2024). Alveolar cleft reconstruction utilizing a particulate autogenous tooth graft and a novel split-thickness papilla curtain flap - A retrospective study. *Journal of cranio-maxillo-facial surgery*, 52(1), 77–84. <https://doi.org/10.1016/j.jcms.2023.10.006>
IF: 2.1, Q1

Publications not related to the thesis:

- Würsching, T., Kesztyűs, A., Pottel, L., Swennen, G., & Nagy, K. (2025). Comparison of two methods for segmentation of the nasoalveolar defect and design of a three-dimensional surgical template in patients with cleft lip and palate: a retrospective study. *International journal of oral and maxillofacial surgery*, 54(10), 897–903. <https://doi.org/10.1016/j.ijom.2025.05.006>
IF: 2.7, Q1
- Csókay, G., Würsching, T., Szentpéteri, S., Nolden, E., Vaszkó, M., & Bogdán, S. (2024). Páciensspecifikus implantátumok használata arckoponya-rekonstrukció során [The use of patientspecific implants in maxillofacial reconstruction]. *Orvosi Hetilap*, 165(40), 1594-1600. <https://doi.org/10.1556/650.2024.33111>
IF: 0.9, Q4

- Major, M., Mészáros, B., Würsching, T., Polyák, M., Kammerhofer, G., Németh, Z., Szabó, G., & Nagy, K. (2024). Evaluation of a Structured Light Scanner for 3D Facial Imaging: A Comparative Study with Direct Anthropometry. *Sensors (Basel, Switzerland)*, 24(16), 5286. <https://doi.org/10.3390/s24165286>
IF: 3.5, Q2
- Kesztyűs, A., Würsching, T.*, Nemes, B., Pálvölgyi, L., & Nagy, K. (2022). Evaluation of 3D visualization, planning and printing techniques in alveolar cleft repair, and their effect on patients' burden. *Journal of stomatology, oral and maxillofacial surgery*, 123(4), 484–489.
<https://doi.org/10.1016/j.jormas.2021.10.007>
IF: 2.2, Q2
- De Cuyper, B., Pottel, L., Würsching, T., Abeloos, J., De Ceulaer, J., Neyt, N., Lamoral, P., & Swennen, G. (2020). Presentation and short-term evaluation of an all-in-one patient-specific implant for cranial reconstruction: A randomized controlled trial. *International journal of oral and maxillofacial surgery*, 49(12), 1551–1558. <https://doi.org/10.1016/j.ijom.2020.04.002>
IF: 2.8, Q1

11. Acknowledgements

First and foremost, I would like to express my sincere gratitude to my supervisors, Professor Zsolt Németh and Dr. med. habil. Krisztián Nagy, PhD, associate professor, for providing me with the opportunity to work on this project, and for their constant guidance and feedback during this process.

I would also like to thank Dr. Sándor Bogdán, PhD, associate professor and the director of the Inpatient Care Section of the Department of Oro-Maxillofacial Surgery and Stomatology, for his constant guidance and reassurance.

I must thank Prof. emeritus György Szabó for his professional support.

I would like to thank colleagues of the Department of Periodontology at Semmelweis University, especially Dr. med. habil. Bálint Molnár PhD, associate professor and Dr. Eleonóra Sólyom PhD for their help and guidance during the implementation of the Bonmaker device.

I would like to thank Dr. Dániel Palkovics PhD for his tremendous help with volumetric analysis and creation of images used during publication.

I would like to thank colleagues from the Department of Paediatric Dentistry and Orthodontics at Semmelweis University, especially Dr. Lili Ács, Dr. Peggi Nghiem Lien, Dr. Réka Kulin, Dr. Anna Bosch and Dr. Bence Benedikti, for all the care they provided for the children involved in the study.

I must thank all the anesthetists, anesthetist's assistants and operating nurses at the Pediatric Centre of Semmelweis University, for providing the background for operative cleft care.

I must express my gratitude to all my colleagues at the Centre for Facial Reconstruction for their help with patient care and assistance in operations, especially Dr. Zsófia Farkas, Lea Estefán, Viktória Bartha and Dr. Bence Mészáros.

I would also like to extend my thanks to the patients and their caregivers who honored me with their trust and consented to participate in the investigations.

Finally, I would like to thank my family and friends for the support they showed during this period.



Contents lists available at ScienceDirect

Journal of Cranio-Maxillo-Facial Surgery

journal homepage: www.jcmfs.com

Alveolar cleft reconstruction utilizing a particulate autogenous tooth graft and a novel split-thickness papilla curtain flap — A retrospective study

Bálint Molnár^{a,1}, Tamás Würsching^{b,c,1,*}, Eleonóra Sólyom^a, Laura Pálvölgyi^b, Zsombor Radóczy-Drajkó^a, Dániel Palkovics^a, Krisztián Nagy^{b,d,e}

^a Department of Periodontology, Semmelweis University, Budapest, Hungary

^b Centre for Facial Reconstruction, Department of Pediatrics, Semmelweis University Budapest, Hungary

^c Department of Oro-Maxillofacial Surgery and Stomatology, Semmelweis University, Budapest, Hungary

^d Cleft and Craniofacial Centre, Division of Maxillo-Facial Surgery, General Hospital St. Jan, Bruges, Belgium

^e OMFS-IMPACT Research Group, Faculty of Medicine, Department of Imaging AndPathology, KU Leuven and Oral and Maxillofacial Surgery, University Hospitals Leuven, Leuven, Belgium

ARTICLE INFO

Handling Editor: Prof. Emeka Nkenke

Keywords:

Secondary alveolar bone grafting
Autogenous tooth bone graft
3D surgical planning
Volumetric radiographic evaluation
Unilateral cleft lip and palate

ABSTRACT

During secondary alveolar cleft grafting, the use of autogenous cancellous bone harvested from the iliac crest is still considered the gold standard. Due to the risk of donor-site morbidity and excessive graft resorption, alternative grafting materials (e.g. intraoral bone, xenografts) have been tested. Autogenous tooth bone graft (ATB) is a novel material derived from extracted teeth. ATB has successfully been used in pre-prosthetic and periodontal surgery for hard-tissue reconstruction.

Seven patients with unilateral cleft lip and palate were treated with ATB, using their own deciduous teeth for grafting. Defects were accessed utilizing a novel split-thickness papilla curtain flap. Cone-beam computed tomography scans were taken prior to and 3 months following cleft surgery to assess graft integration, graft stability, and the volume of the newly formed hard tissues. Hard-tissue gain, as measured at the 3-month follow-up, averaged $0.65 \text{ cm}^3 \pm 0.26 \text{ cm}^3$. Results showed acceptable graft integration and stability at the 3-month follow-up, with no adverse effects or excessive resorption of the graft.

The use of ATB might be a feasible alternative for alveolar cleft grafting. However, long-term studies using a large sample size are required to derive further conclusions.

1. Introduction

The comprehensive treatment of patients with cleft lip and palate is a complex and demanding task that requires the collaborative effort of different medical specialties. One of the most crucial steps in the effective treatment of these patients is alveolar bone grafting, which is necessary to reconstruct the bony defect of the alveolar process, maintain a proper arch form, support the alar base, and close the oronasal fistulae (Abyholm et al., 1981). Timing of the surgery differs across various cleft centers with secondary alveolar bone grafting (SABG) executed most commonly during the mixed dentition (Janssen et al., 2014). The most favorable outcomes have been achieved when the surgery was concluded before the eruption of the cleft-side canine (Brudnicki et al., 2017; Vandersluis et al., 2020).

In terms of local flap design for alveolar cleft closure, the most commonly utilized method is the four-flap technique, as described by Nordin and Abyholm (Eskeland et al., 1979; Larson et al., 1983), which provides an ideal soft-tissue closure above the graft. However, in cases of suture loosening due to flap tension, secondary wound healing might occur, and the consequent exposure might lead to the loss of the graft. This classic flap design does not address the scarce width and thickness of keratinized gingiva at teeth adjacent to the alveolar cleft, where consequent periodontal impairment may develop, resulting in eventual tooth loss (Huynh-Ba et al., 2009; Sahni et al., 2022).

Currently, the most common choice of material for alveolar bone grafting is autologous bone, which is considered to be the gold standard, combining all properties required in a bone graft: osteoconduction, osteoinduction, and osteogenesis. The most preferred donor site is the

* Corresponding author. Bokay Janos Street 53–54, 1083, Budapest, Hungary.
E-mail address: wursching.tamas@semmelweis.hu (T. Würsching).

¹ These authors contributed equally to the preparation of the manuscript.

<https://doi.org/10.1016/j.jcms.2023.10.006>

Received 24 January 2023; Received in revised form 20 September 2023; Accepted 15 October 2023

Available online 28 October 2023

1010-5182/© 2023 The Authors. Published by Elsevier Ltd on behalf of European Association for Cranio-Maxillo-Facial Surgery. This is an open access article under the CC BY license (<http://creativecommons.org/licenses/by/4.0/>).

iliac crest, as described by Boyne and Sands (Boyne and Sands, 1972). However, donor-site morbidity (as high as 19.37%) and excessive graft resorption need to be taken into account (Dimitriou et al., 2011; Eufinger and Leppänen, 2000).

To reduce donor-site morbidity and to possibly increase the success rate of the surgical intervention, various authors have suggested alternative grafting materials for the reconstruction of alveolar clefts (Ishii et al., 2002; Yuan et al., 2004; Alonso et al., 2010; Aly and Hammouda, 2016; Blume et al., 2019; Ellapakurthi and Reddy, 2021; Kadry et al., 2021). Aside from graft materials, the added benefits of supplementary materials, such as fibrin sealant, platelet-rich plasma, and leukocyte-/platelet-rich fibrin have also been evaluated (Wu et al., 2018; Lavagen et al., 2021).

As an alternative to autogenous bone grafts, Kim et al. introduced a method for producing autogenous tooth bone grafts (ATB) by grinding and chemically processing previously extracted teeth (Kim et al., 2017). Due to its microscopic structure, ATB has both osteoconductive and osteoinductive properties, making it a suitable material for alveolar ridge preservation, alveolar ridge augmentation, and alveolar cleft grafting, with successful outcomes (Hara et al., 2013; Jeong et al., 2015; Datarkar and Bhawalkar, 2020; Radocz-Drajko et al., 2021). Jeong et al. were able to place a 3 mm-wide implant with 45 Ncm insertion torque 3.5 months after cleft grafting (Jeong et al., 2015).

For adequate treatment planning, it is necessary to identify the extent and the shape of the alveolar cleft. In recent years, cone-beam computed tomography (CBCT) has become widespread as an imaging modality in dentistry and maxillofacial surgery (Jacobs et al., 2018). CBCT enables 3D visualization of the alveolar bone defect morphology, digital planning, and additive manufacturing of bone grafting templates. These processes aid the surgeons during the intervention, and may reduce further complications (Pálházi et al., 2014). CBCT scans can also be utilized for postoperative assessment of graft integration and volume stability (Linderup et al., 2015; Blume et al., 2019; Stasiak et al., 2019), since conventional methods lack the possibility of volumetric assessment and tend to over- or underestimate the size of the graft (Palankar et al., 2021; Kamperos et al., 2020).

To overcome the limitations of current methods utilizing advancements provided by novel treatment approaches, the aim of our pilot case series was to evaluate the efficacy of a digitally planned ATB powder block — stabilized with fibrin sealant — combined with a novel split-thickness papilla curtain flap in the treatment of unilateral alveolar cleft defects.

2. Materials and methods

2.1. Study design and patient selection

Patients exhibiting unilateral cleft lip and palate (UCLP) were recruited for this study. Enrolled patients were under treatment in the Department of Pediatrics, Semmelweis University, Budapest. The study was approved by the university's Regional and Institutional Committee of Science and Research Ethics (approval number: SE RKEB 251/2020). The study protocol was submitted and approved by the US National Library of Medicine (www.clinicaltrials.gov; trial registration number: NCT05971914). The research plan was compiled in line with current legislation and the Declaration of Helsinki of the World Medical Association (reference number: 23/2002. V.9.). Surgical interventions were undertaken with the understanding and written consent of each subject's caregiver. The exclusion criteria were: (i) major relevant general medical conditions; (ii) systemic use of steroids; (iii) current or previous intravenous bisphosphonate treatment; (iv) acute infection at the operation site; and (v) previous attempts at alveolar bone grafting. In every case the development of the cleft-side canine was considered during planning of the surgery, as was the need for orthodontic treatment. All the patients included in the study required orthodontic maxillary expansion. The development of the canine was followed using

periapical X-rays. Only once the canine's root development was between one-third and two-thirds of its expected final length, was the decision made to proceed with surgery. At this point CBCT scans were taken for surgical planning. Each patient were required to have presented at least three deciduous teeth, which were scheduled for extraction. All enrolled patients were examined by two independent dentists to assure that tooth removal was indicated according to patients' age and orthodontic planning.

2.2. Radiographic image acquisition and image processing

CBCT scans were acquired with a 12 cm × 8 cm field of view, and a 200 µm voxel size (VGI EVO®, Newtom). CBCT data were acquired at baseline and at the 3-month follow-up. At the same time points, the width of keratinized gingiva at the adjacent teeth and over the alveolar cleft was recorded using a UNC-15 periodontal probe.

Digital imaging and communications in medicine (DICOM) datasets were imported into 3D Slicer open-source image-processing software (www.slicer.org) (Pinter et al., 2019). Baseline and follow-up CBCT scans were segmented utilizing a semi-automatic segmentation method in the 'Segment Editor' module of 3D Slicer (Palkovics et al., 2021b). Separate binary label maps were generated for the bone of the maxilla. The maxilla was segmented utilizing the region-growing tool 'Grow from seeds', and thereafter the 'Watershed' tool was used to segment all the teeth separately (Pinter et al., 2019). The software automatically generated 3D models of binary label maps, with real-time rendering (Fig. 1).

2.3. The virtual surgical planning process

Based on the extent and morphology of the cleft the desired shape of the nasolabial graft was designed in 3D Slicer. Since every case was unilateral, the non-cleft side anatomy was used as a reference during graft planning. This also gave us the opportunity to determine the exact volume of the graft in cm³. This was a helpful addition in planning the surgery because the maximum amount of graft the ATB machine can produce is approximately 3 cm³. Another limiting factor is the number and condition of removable deciduous teeth.

After planning, the model was exported as a standard tessellation language (STL) file. As the final step, a grafting template was constructed using an open-source computer-aided design (CAD) software (Blender®; Blender Foundation, Amsterdam, The Netherlands), as described by Fabian et al. (2019) (Fig. 2). The designed parts were manufactured with a stereolithography (SLA) 3D printer (Phrozen Shuffle XL; Phrozen, Hsinchu City, Taiwan) using class I biocompatible, surgical-grade resin (Dental SG; NextDent BV, Soesterberg, The Netherlands).

2.4. Surgical protocol

Teeth were extracted under general anesthesia with the gentle application of forceps and elevators. Extracted teeth were prepared immediately after removal, according to the Bonmaker® protocol (Korea DentalSolution Co Ltd, Busan, Korea) (Kim et al., 2017) (Fig. 3). The outer surface of the teeth was debrided with diamond-coated burs. Following the removal of pulp tissues, carious lesions, root canal fillings, and restorations, the crowns and roots were both crushed in the Bonmaker® tooth grinder. After grinding, the tooth particles (particle size: 425–1500 µm) underwent disinfection and preparation via proprietary A, B, and C liquids inside the Bonmaker® device (Kim et al., 2017). Between patients, the equipment underwent a regular disinfection cycle, according to the manufacturer's instructions. During the preparation and disinfection procedure (which usually takes 30–35 min), flap preparation and exploration of the alveolar cleft and oronasal fistula were carried out.

Articaine hydrochloride 4% with 0.0001% epinephrine (Ultracain DS

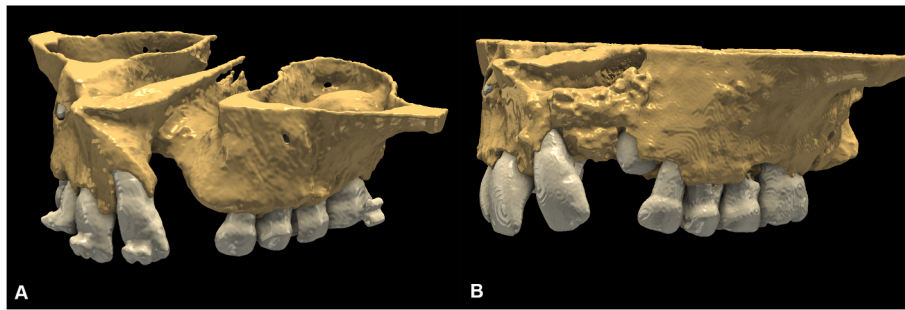


Fig. 1. Segmented 3D models of CBCT datasets: (A) virtual model of baseline hard-tissue conditions; (B) virtual model of 3-month follow-up hard-tissue conditions.

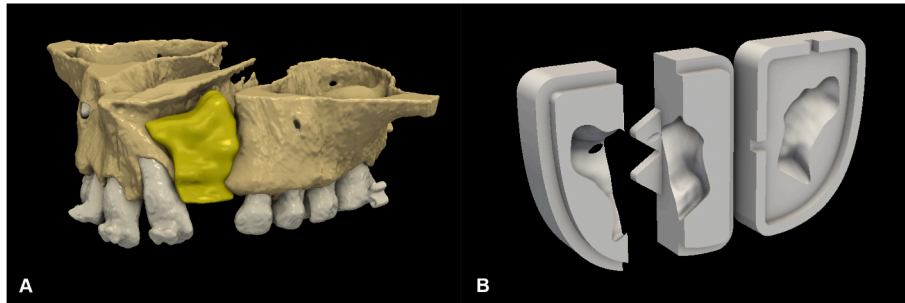


Fig. 2. Preoperative virtual planning: (A) digital 3D plan of cleft reconstruction; (B) CAD-modelled grafting template.

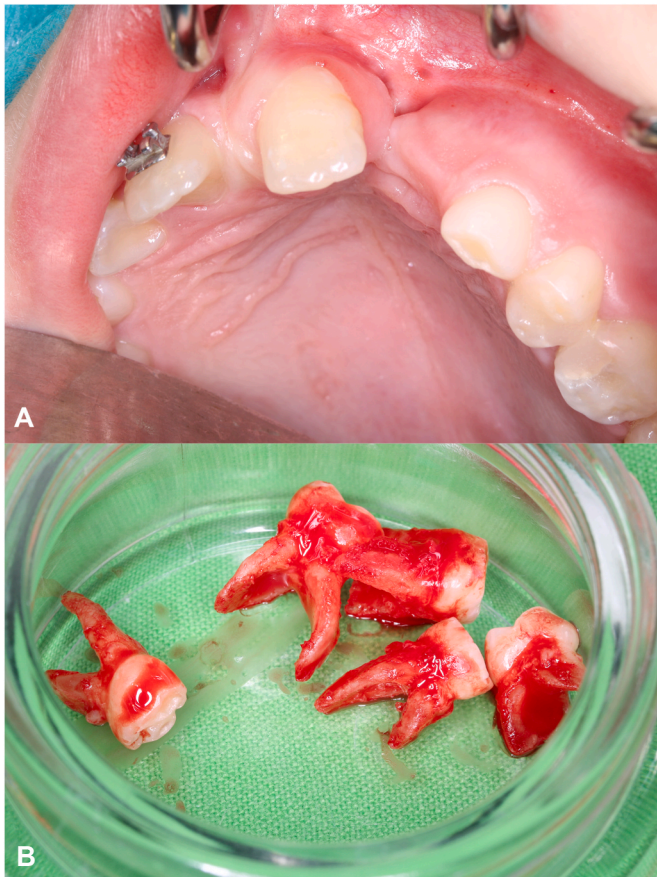


Fig. 3. Baseline clinical situation and tooth extraction: (A) baseline clinical situation; (B) extracted deciduous teeth.

Forte; Sanofi-Aventis, Paris, France) was used for local anesthesia. A full-thickness incision was made starting at the ipsilateral maxillary tuberosity, continued in a continuous intrasulcular incision along all teeth located distally from the oronasal fistula, with a no. 15 blade (Aesculap; Braun AG, Tuttlingen, Germany). At the level of the cleft and the oronasal fistula (located in the lateral incisor position), the incision was continued along the alveolar crest in full-thickness, followed by a split-thickness incision at the mucogingival junction of the adjacent central incisor, and continued vertically in the midline labial frenulum. Subsequently, the area of keratinized gingiva around teeth located distally from the cleft was elevated in full-thickness with blunt dissection. Flap elevation was continued by sharp dissection apically from the mucogingival junction of the distal teeth, as well as at the loose mucosa over the central incisor, where the keratinized gingiva was left untouched. The periosteal layer of the complete hemimaxilla was then exposed, followed by excision of the epithelial down growth in the oronasal fistula, which was closed with resorbable monofilament sutures (Chirmax Monolac 5/0) by approximating adjacent scar tissue margins. Scar tissue in the cleft area was outlined by mesial, distal, and palatal incisions to allow for nasal repositioning, exposing the bony cleft and creating a secluded space for graft insertion (Figs. 4 and 5).

Ready-to-use ATB was mixed with fibrin sealant (Segura-Castillo et al., 2005) (Tisseel®; Baxter, Glenview, Illinois, USA) in the digitally planned and 3D-printed grafting templates to obtain a sticky ATB graft that matched the shape and extent of the bony defect. The pre-shaped sticky ATB graft was then inserted in the cleft defect (Fig. 6).

Following cleft augmentation, the split-thickness papilla curtain flap was repositioned by shifting all buccal surgical papillae mesially to the adjacent or the second-adjacent interproximal space, depending on the horizontal extent of the cleft. Next, the papilla in the close vicinity of the oronasal fistula was relocated to the level of the mesial vertical incision in the midline frenulum (Fig. 7). As a result, healthy continuous keratinized gingiva was shifted over the cleft to cover the grafted area and to ensure simultaneous reconstruction of the distorted vestibulum and lacking keratinized tissues. To stabilize the tension-free split-thickness papilla curtain flap, suturing was carried out with resorbable monofilament sutures (Chirmax Monolac 5/0), utilizing circumferential double

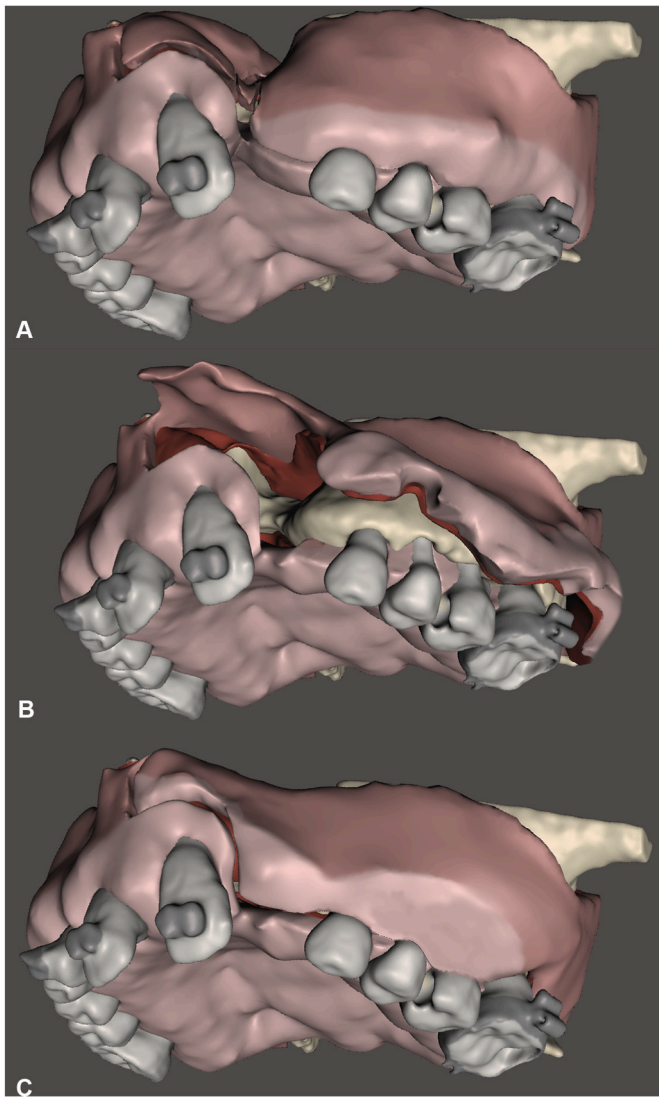


Fig. 4. Schematic presentation of the split-thickness papilla curtain flap: (A) initial incision (light pink: keratinized mucosa, dark pink: mobile mucosa); (B) flap elevation (red: periosteum); (C) mesially shifted flap closure.

slung sutures and single interrupted mucosal sutures (Fig. 8A).

Postoperative systemic antibiotic therapy (875/125 mg amoxicillin/clavulanic acid twice a day, or 300 mg clindamycin four times a day in cases of penicillin allergy) was prescribed. Patients were advised to clean the area gently with an ultra-soft toothbrush and rinse with a 0.2% chlorhexidine-diguconate mouthwash for 2 weeks after surgery. Sutures usually resorbed 3–4 weeks after surgery (Fig. 8B).

2.5. Three-dimensional radiographic evaluation

Following segmentation of both baseline and 3-month follow-up CBCT scans, spatial registration was carried out to validate volumetric and morphological hard-tissue alterations. Registration of DICOM datasets was performed using the ‘General Registration (Elastix)’ module, which is an automatic intensity-based medical image registration algorithm (Klein et al., 2010). After spatial registration, the preoperative 3D model of the maxilla was subtracted from the postoperative 3D model (Palkovics et al., 2021a, 2022a, 2022b). Subsequently, the hard-tissue difference between the two time points could be visualized and evaluated in 3D. The volumes of the newly formed hard tissues were calculated and compared with the preoperatively planned volumes.

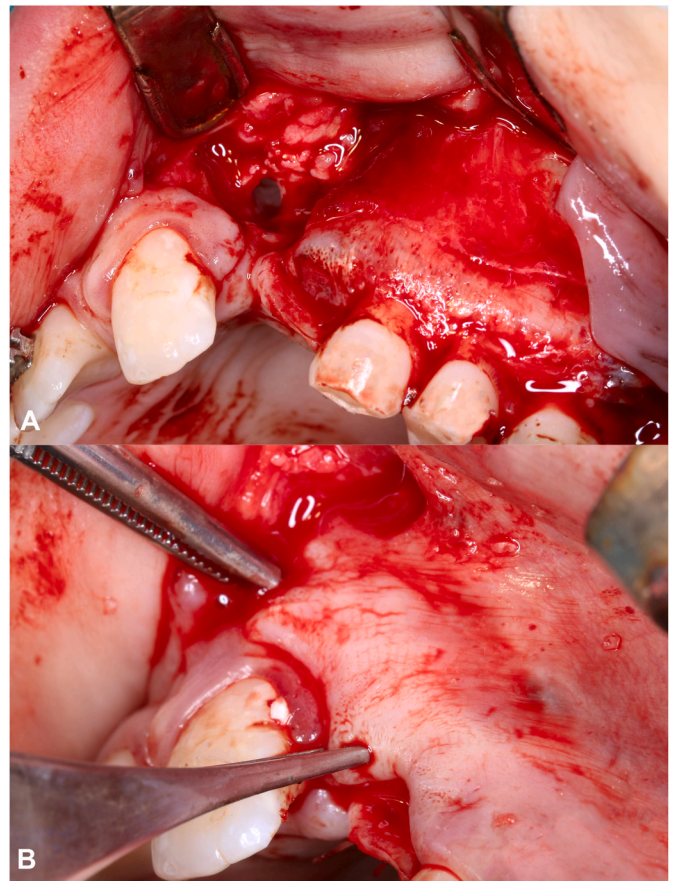


Fig. 5. Intraoperative situation: (A) surgical access of the UCLP; (B) tension-free mesial flap advancement.

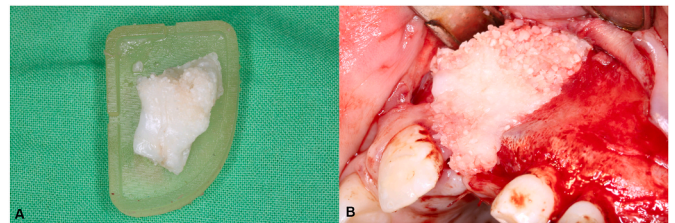


Fig. 6. Hard-tissue reconstruction of the UCLP: (A) the mixture of fibrin sealant and ATB particles was shaped by the 3D-printed grafting template to prepare the sticky ATB graft; (B) reconstruction of the UCLP with the sticky ATB graft.

2.6. Outcome measures

The primary outcome of the current investigation was the evaluation of volumetric hard-tissue gain by 3D subtraction analysis.

The secondary outcomes of the study were: (i) validation of the efficacy of the surgical procedure and volumetric stability of the graft, by calculating the ratio between the actual volumetric hard-tissue gain and the planned hard-tissue volume; and (ii) assessment of the similarity between the planned and actual hard-tissue morphologies by calculating the Dice similarity coefficient (DSC) and Hausdorff distance (HD). DSC is a spatial overlap index and a reproducibility validation metric. The value of DSC ranges from 0, indicating no spatial overlap between two sets of binary segmentation results, to 1, indicating complete overlap (Janssen et al., 2017). HD is the longest distance from a point in one of the two models to its closest point in the other model, meaning that the lower the HD value the more the two models overlap.

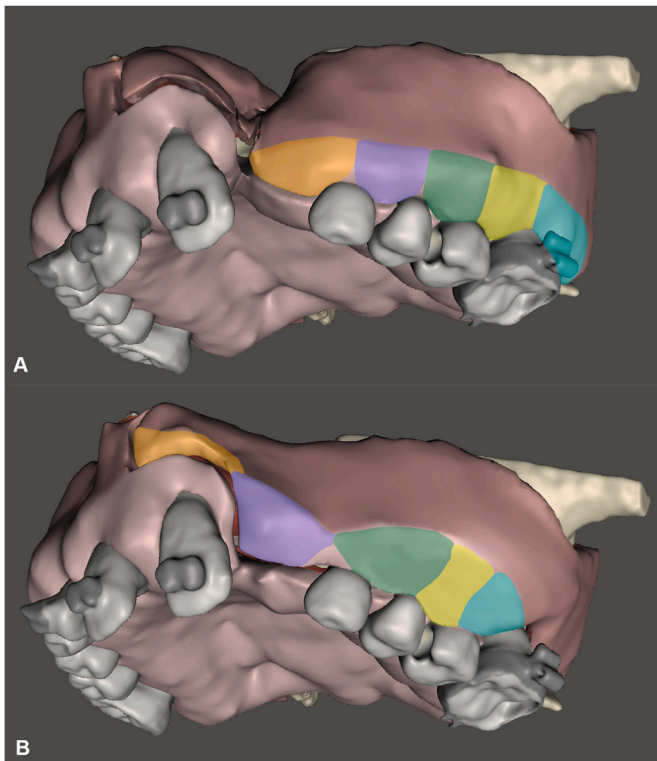


Fig. 7. Schematic demonstration of the mesial papilla shift: (A) preoperative state (the first interdental papilla is located distally to the alveolar cleft, marked in purple); (B) Postoperative state (the interdental papilla, marked in purple, was shifted mesially to cover the area of the alveolar cleft).

2.7. Statistical analysis

The primary focus of the study was to determine the amount of hard tissue change rather than determining absolute baseline and follow-up values. Therefore, only descriptive statistics were used. Data were expressed as mean value \pm standard deviation.

3. Results

3.1. Patient demographics

In total, seven participants exhibiting UCLP were enrolled in this investigation. Five patients were male, two were female. The patients were aged 9–11 years, with a mean age of 10.43 ± 0.79 years. Two defects were located on the left side and five on the right. In total, 35 deciduous teeth and two supernumerary teeth were extracted and utilized for preparation of the sticky ATB graft. In every case, the patient's own teeth provided enough material for proper reconstruction of the alveolar defect, using an average of 4.75 ± 2.49 teeth per patient. Patient demographic data are shown in [Table 1](#).

3.2. Clinical outcomes

All patients were able to be discharged from the hospital on the first postoperative day without any major complaints, and to return to normal daily activity shortly after surgery. Initial wound healing was uneventful in all seven cases, with no signs of graft exposure over the postoperative period. The quality of keratinized tissues was favorable, fully eliminating any muscle pull or vestibular distortions over the cleft. During the follow-up period, eruption of the cleft-side canine was observed in one patient.

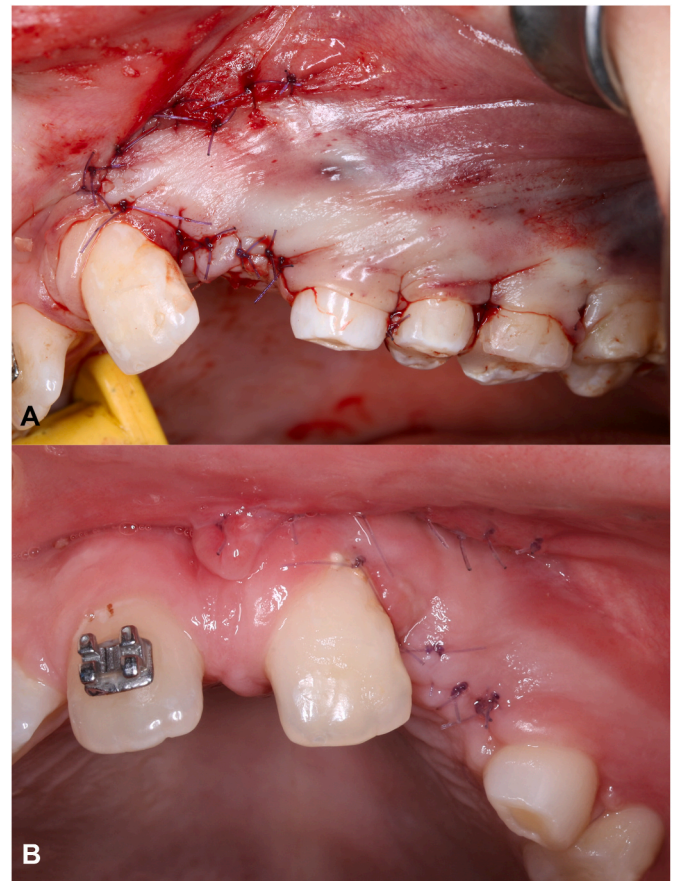


Fig. 8. Wound closure and postoperative control: (A) wound closure with primary intention; (B) 2-week postoperative control.

Table 1

Patient demographic and surgical data.

Patient	Age	Sex	No. Of extracted teeth	Surgical area location
1	11	M	4	Right side
2	10	M	5	Right side
3	11	M	10	Left side
4	11	F	4	Left side
5	10	M	4	Left side
6	9	M	5	Left side
7	11	F	5	Left side
Mean \pm standard deviation	10.43 ± 0.79	n. a.	5.29 ± 2.14	n.a.

3.3. Primary outcome measure — volumetric hard tissue alterations

Planned graft volumes averaged $1.14 \text{ cm}^3 \pm 0.36 \text{ cm}^3$, whereas hard-tissue gain, as measured on the 3-months follow-up CBCT scans, averaged $0.65 \text{ cm}^3 \pm 0.26 \text{ cm}^3$ ([Fig. 9](#)). The primary outcome data are summarized in [Table 2](#).

3.4. Secondary outcome measures

The ratio between actual and planned graft volume ranged between 34.17% and 108.21%, resulting in an average ratio of $59.92\% \pm 24.35\%$. DSC between planned and actual graft segmentation ranged between 0.14 and 0.65, with an average of 0.43 ± 0.2 for all seven cases. HD averaged $1.83 \text{ mm} \pm 0.77 \text{ mm}$ ([Fig. 10](#)). Secondary outcome data are summarized in [Table 3](#).

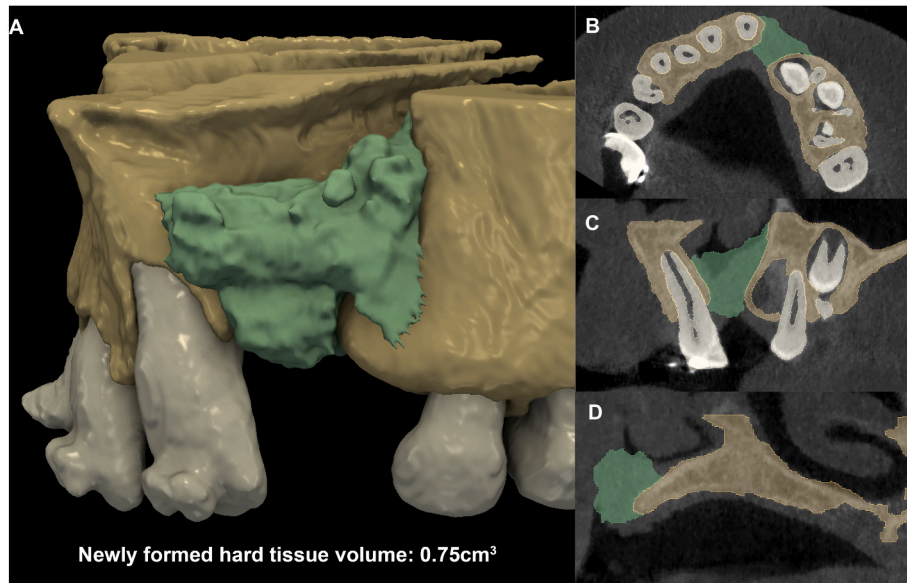


Fig. 9. Volumetric evaluation of the newly formed hard tissues: (A) 3D view; (B) axial view; (C) coronal view; (D) sagittal view.

Table 2

Planned and achieved volumetric hard-tissue gain.

Patient	Planned hard-tissue gain (cm ³)	Hard-tissue gain at 3-month follow-up (cm ³)
1	0.82	0.48
2	1.65	1.15
3	1.03	0.35
4	0.61	0.66
5	1.44	0.70
6	1.26	0.75
7	1.17	0.49
Mean ± standard deviation	1.14 ± 0.36	0.65 ± 0.26

4. Discussion

In this study the efficacy of a 3D-planned sticky ATB graft in conjunction with a split-thickness papilla curtain flap was evaluated for secondary alveolar cleft grafting. Although there have been previous case reports describing the use of ATB in secondary alveolar bone grafting (Hara et al., 2013; Jeong et al., 2015; Datarkar and Bhawalkar, 2020), these were singular case reports. To the best of our knowledge, this was the first study to report clinical and 3D-radiographic data demonstrating favorable defect fill in alveolar clefts, utilizing ATB grafting material, in a series of patients.

Although graft resorption was observed, the amount lost was in line with what can be expected from the use of iliac crest, according to the

literature (Vandersluis et al., 2020). The average volume of the remaining graft at the 3-month follow-up was well above 50% when compared with the planned graft volume. In one case, the actual graft volume even exceeded the planned volume by 8%, thereby suggesting that ATB graft could have an advantageous effect on bone regeneration.

The relatively low average DSC value (0.43 ± 0.2) and the relatively high HD (1.83 mm ± 0.77 mm) — indicated a relatively low correlation between the preoperatively planned graft shape and the actual graft shape at 3-months follow-up. This phenomenon could be observed regardless of graft volume stability, and even cases with relatively high graft stability showed a relatively low morphological similarity to the planned graft shape. According to the 3D reconstructed images, this was due to buccal displacement of the graft during healing. In most of the cases, sufficient palatal fill could not be achieved, and the sticky ATB graft did not reach the nasal base. This was most probably due to the pressure applied on the graft by the nasal and palatal flaps; which suggests a need for further modifications to the flap design on the palatal aspect, or perhaps use of a rigid barrier on the palatal/nasal aspect in conjunction with the sticky ATB graft. A similar approach was adopted by Ishii et al. (2002), who positioned a rigid cortex bone plate on the palatal aspect to compensate for the pressure applied by the nasal/palatal flaps, and to maintain a safe, secluded space.

Limitations of the current study included the relatively low sample size, due to the pilot nature of the examination, and the lack of histological information on graft integration. Although histological evaluations have been performed previously (Radoczy-Drajko et al., 2021), only tissue integration of the ATB particles could be assessed in this

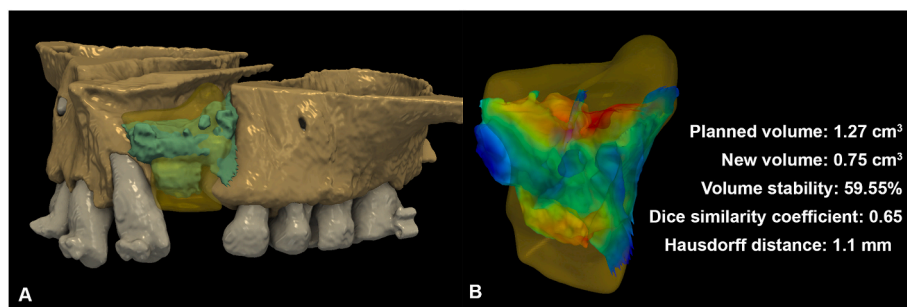


Fig. 10. Relationship between planned outcome and actual outcome: (A) 3D virtual model of planned and actual outcome; (B) colormap model visualizing the morphological differences between the newly formed hard tissues and the morphology of the planned outcome.

Table 3
Volumetric and morphological stability of the graft.

Patient	Achieved volume/ planned volume ratio (%)	Dice similarity coefficient (DSC)	Hausdorff distance (HD), average (mm)
1	58.36	0.65	0.97
2	69.27	0.57	1.56
3	34.17	0.25	2.31
4	108.21	0.41	1.91
5	48.40	0.14	3.24
6	59.55	0.65	1.10
7	41.49	0.36	1.70
Mean ± standard deviation	59.92 ± 24.35	0.43 ± 0.2	1.83 ± 0.77

current study. With the aid of 3D technology, quantitative radiographic evaluation was possible; however, the inability to perform qualitative, histological evaluation was a significant limitation.

The Bonmaker® device is suitable for preparing extracted teeth and obtaining ATB particulate grafting material. As confirmed by previous radiographic and histological studies (Radoczy-Drajko et al., 2021), ATB powder may act as a resorbable scaffold and a space-maintaining device to facilitate the healing of alveolar cleft defects. After the preparation of the ATB powder and its mixture with fibrin sealant, a sticky ATB graft was acquired with excellent intraoperative handling properties.

The time required for the harvesting of a hip graft is comparable to ATB preparation. Nevertheless, the ATB protocol has two benefits: (i) approximately half of the duration — 20 min — is fully automatic, executed by the Bonmaker device, which does not require user interaction, thus allowing medical personnel to undertake other activities during the surgery; and (ii) ATB preparation is straightforward — it does not require a highly qualified physician, with nurses fully capable of handling the graft preparation.

The estimated costs for the presented surgical approach were as follows: 3D printing 5 EUR, Bonreagent 35 EUR, fibrin glue 100 EUR. The use of these auxiliary techniques increased the costs for the operation itself, although these expenses were not considered to be exceptionally high. On the other hand, avoidance of an extraoral donor site led to reduced hospitalization time, with all patients in our study discharged from hospital on the first postoperative day. This was in contrast with the study by Brudnicki et al. (2017), who stated: ‘The mean length of hospitalization postoperatively was 2.9 days and varied from 1 to 8 days. The majority of patients were discharged on the second (66 cases) or third day (102 cases) following the procedure.’ In higher-income countries, where the cost of hospital stay is more expensive, the use of these auxiliary techniques may lower the overall costs of the treatment, but exact calculations to support this statement were beyond the scope of our study.

To ensure the compaction and tight fit of the grafting material inside the cleft, 3D preoperative planning was successfully utilized to manufacture a 3D-printed grafting template to shape the sticky ATB graft before insertion. Closure of the oronasal fistula was achieved in all cases.

Modifications of the original four-flap design, to improve certain aspects of the technique — for example, minimizing injury to the dental papillae and periodontium of the involved dentition, or increasing the amount of attached gingiva surrounding the canine — have been described previously (López-Cedrún et al., 2014). Most of these modifications continue to use a full-thickness mucoperiosteal flap, and the suture line remains directly above the graft. The novel split-thickness papilla curtain flap aims to ensure the following: (i) tension-free wound closure without compromising flap circulation, via vertical or horizontal releasing incisions; (ii) that a sufficient amount of keratinized gingiva is rotated mesially to surround the tooth on the mesial side of the cleft (usually the lateral or mesial incisor). It also has the benefit of shifting the suture line from directly above the grafted area to a more mesial position, where the sutures will rest on the well vascularized

periosteal surface of the premaxilla. The nasal and palatal mucosa on the mesial side of the cleft is still elevated in full thickness, as previously described and now widely applied.

The presented flap design resulted in primary-intention wound healing in 100% of the cases, with minimal pain and edema, as well as excellent, inflammation-free, early wound healing. These pilot results indicated the applicability of the split-thickness papilla curtain flap and, in our experience, this modification showed superior results compared with the traditional mucoperiosteal flap approach. Nevertheless, this needs to be further investigated in future comparative clinical studies.

The application of ATB as an autogenous grafting material provides a cost- and time-effective alternative for patients. Its application with the split-thickness papilla curtain flap proved to be an effective surgical approach with a low duration, while providing favorable hard- and soft-tissue conditions. This report introduces the early results of a pilot study regarding the use of ATB in alveolar cleft reconstruction, combined with a split-thickness papilla curtain flap. Although the results were favorable, the study had its limitations — namely the short follow-up period and relatively small sample size. To assess long-term outcomes of this approach each patient will need to undergo a strict follow-up protocol, with periodontal charting and follow-up intraoral scans performed on a 6-monthly basis for 5 years. CBCT scans will be performed 1 year postoperatively in order to measure long-term graft stability.

5. Conclusion

Within the limitations of the study it seems that ATB graft may be a safe and predictable grafting material in alveolar cleft reconstruction. The applied split-thickness papilla curtain flap was effectively utilized to avoid postoperative graft exposure and to improve soft-tissue conditions around the teeth adjacent to the alveolar cleft. Uneventful wound healing and favorable radiographic outcomes indicated hard- and soft-tissue stability in the grafted area. However, certain aspects of this surgical approach could be further improved, and, therefore, further research is necessary to exploit the full potential of ATB and the novel flap design in alveolar cleft grafting.

Funding

The current study received no funding.

Ethical approval

The study was approved by the university’s Regional and Institutional Committee of Science and Research Ethics (approval number: SE RKEB 251/2020). The study protocol was submitted and approved by the US National Library of Medicine (www.clinicaltrials.gov; trial registration number: NCT05971914). The research plan was compiled in line with current legislation and the Declaration of Helsinki of the World Medical Association (reference number: 23/2002. V.9.).

Patient consent

Surgical interventions were undertaken with the understanding and written consent of each subject’s caregiver.

Declaration of competing interests

The authors declare no competing interests.

Acknowledgements

Not applicable.

References

- Abyholm, F.E., Bergland, O., Semb, G., 1981. Secondary bone grafting of alveolar clefts. A surgical/orthodontic treatment enabling a non-prosthetic rehabilitation in cleft lip and palate patients. *Scand. J. Plast. Reconstr. Surg.* 15, 127–140.
- Alonso, N., Tanikawa, D.Y., Freitas Rda, S., Canan Jr., L., Ozawa, T.O., Rocha, D.L., 2010. Evaluation of maxillary alveolar reconstruction using a resorbable collagen sponge with recombinant human bone morphogenetic protein-2 in cleft lip and palate patients. *Tissue Eng. C Methods* 16, 1183–1189.
- Aly, L.A., Hammouda, N., 2016. Secondary closure of alveolar cleft with resorbable collagen membrane and a combination of intraoral autogenous bone graft and deproteinized anorganic bovine bone. *Ann Maxillofac Surg* 6, 165–171.
- Blume, O., Back, M., Born, T., Donkiewicz, P., 2019. Reconstruction of a unilateral alveolar cleft using a customized allogenic bone block and subsequent dental implant placement in an adult patient. *J. Oral Maxillofac. Surg.* 77, 2127 e2121–2127.e2111.
- Boyne, P.J., Sands, N.R., 1972. Secondary bone grafting of residual alveolar and palatal clefts. *J. Oral Surg.* 30, 87–92.
- Brudnicki, A., Sawicka, E., Brudnicka, R., Fudalej, P.S., 2017. Cephalometric comparison of early and late secondary bone grafting in the treatment of patients suffering from unilateral cleft lip and palate. *J. Cranio-Maxillo-Fac. Surg.* 45 (4), 479–484.
- Datarak, A., Bhawalkar, A., 2020. Utility of tooth as an autogenous graft material in the defects of alveolar cleft — a novel case report. *J Oral Biol Craniofac Res* 10, 470–473.
- Dimitriou, R., Mataliotakis, G.I., Angoules, A.G., Kanakaris, N.K., Giannoudis, P.V., 2011. Complications following autologous bone graft harvesting from the iliac crest and using the RIA: a systematic review. *Injury* 42 (Suppl. 2), S3–15.
- Ellapakurthi, P., Reddy, G.S.P., 2021. The effectiveness of mineralized plasmatic matrix in the closure of alveolar clefts with volumetric assessment. *Regen Med Res* 9, 1.
- Eskeland, G., Borchgrevink, H., Abyholm, F.E., 1979. Columella lengthening in bilateral cleft lip patients. Experience with the forked flap procedure. *Scand. J. Plast. Reconstr. Surg.* 13, 429–436.
- Eufinger, H., Leppänen, H., 2000. Iliac crest donor site morbidity following open and closed methods of bone harvest for alveolar cleft osteoplasty. *J. Cranio-Maxillo-Fac. Surg.* 28 (1), 31–38.
- Fabian, Z., Kádár, K., Patonay, L., Nagy, K., 2019. Application of 3D printed biocompatible plastic surgical template for the reconstruction of a nasoalveolar cleft with preoperative volume analysis. *Mater. Plast.* 56, 413–415.
- Hara, S., Mitsugi, M., Kanno, T., Tatemoto, Y., 2013. Bone transport and bone graft using auto-tooth bone for alveolar cleft repair. *J. Craniofac. Surg.* 24, e65–e68.
- Huynh-Ba, G., Brägger, U., Zwahlen, M., Lang, N.P., Salvi, G.E., 2009. Periodontal disease progression in subjects with orofacial clefts over a 25-year follow-up period. *J. Clin. Periodontol.* 36, 836–842.
- Ishii, M., Ishii, Y., Moriyama, T., Gunji, A., Morita, K., Imaizumi, F., Enomoto, S., 2002. Simultaneous cortex bone plate graft with particulate marrow and cancellous bone for reliable closure of palatal fistulae associated with cleft deformities. *Cleft Palate Craniofac J* 39, 364–369.
- Jacobs, R., Salmon, B., Codari, M., Hassan, B., Bornstein, M.M., 2018. Cone beam computed tomography in implant dentistry: recommendations for clinical use. *BMC Oral Health* 18, 88.
- Janssen, N.G., Weijts, W.L., Koole, R., Rosenberg, A.J., Meijer, G.J., 2014. Tissue engineering strategies for alveolar cleft reconstruction: a systematic review of the literature. *Clin. Oral Invest.* 18, 219–226.
- Janssen, N.G., Schreurs, R., Gkp, Bittermann, Borstlap, W.A., Koole, R., Meijer, G.J., Tjj, Maal, 2017. A novel semi-automatic segmentation protocol for volumetric assessment of alveolar cleft grafting procedures. *J. Cranio-Maxillo-Fac. Surg.* 45 (5), 685–689.
- Jeong, K.I., Lee, J., Um, I.W., Kim, Y.K., 2015. Alveolar cleft restoration using autogenous tooth bone graft material for implant placement: a case report. *J. Oral Implantol.* 41, 487–490.
- Kadry, W., Eldefar, M., Nassar, Y., Abou-El-Fetouh, A., Hakam, M.M., 2021. Clinical, volumetric and densitometric evaluation of tissue engineered constructs for secondary alveolar cleft reconstruction: a randomized clinical trial. *J. Cranio-Maxillo-Fac. Surg.* 49 (12), 1141–1150.
- Kamperos, G., Theologie-Lygidakis, N., Tsiklakis, K., Iatrou, I., 2020. A novel success scale for evaluating alveolar cleft repair using cone-beam computed tomography. *J. Cranio-Maxillo-Fac. Surg.* 48 (4), 391–398.
- Kim, S.Y., Kim, Y.K., Kim, H.S., Yun, P.Y., Kim, S.G., Choi, Y.H., 2017. Extraction socket sealing using palatal gingival grafts and resorbable collagen membranes. *Maxillofac. Plast Reconstr Surg* 39, 39.
- Klein, S., Staring, M., Murphy, K., Vieregger, M.A., Pluim, J.P., 2010. Elastix: a toolbox for intensity-based medical image registration. *IEEE Trans. Med. Imag.* 29, 196–205.
- Larson, O., Nordin, K.E., Nylén, B., Eklund, G., 1983. Early bone grafting in complete cleft lip and palate cases following maxillofacial orthopedics. II. The soft tissue development from seven to thirteen years of age. *Scand. J. Plast. Reconstr. Surg.* 17, 51–62.
- Lavagen, N., Nokovitch, L., Algrin, A., Dakpe, S., Testelin, S., Devauchelle, B., Gbaguidi, C., 2021. Efficiency of advanced-PRF usage in the treatment of alveolar cleft with iliac bone graft: a retrospective study. *J. Cranio-Maxillo-Fac. Surg.* 49 (10), 923–928.
- Linderup, B.W., Küsel, A., Jensen, J., Cattaneo, P.M., 2015. A novel semiautomatic technique for volumetric assessment of the alveolar bone defect using cone beam computed tomography. *Cleft Palate Craniofac J* 52, e47–e55.
- López-Cedrón, J.L., Gonzalez-Landa, G., Figueroa, A., 2014. Isolated keratinized gingiva incision in alveolar cleft bone grafts improves qualitative outcomes: a single surgeon's 23 year experience. *J. Cranio-Maxillo-Fac. Surg.* 42 (8), 1692–1697.
- Palankar, V., Sattur, A., Palankar, A., Rajeswari, S.R., Thakur, S., Desai, A.K., 2021. Evaluation of long-term stability of secondary alveolar bone grafts in cleft palate patients using multislice computed tomography and three-dimensional printed models: a prospective study. *J. Pharm. BioAllied Sci.* 13, S1496–S1500.
- Pálházi, P., Nemes, B., Swennen, G., Nagy, K., 2014. Three-dimensional simulation of the nasoalveolar cleft defect. *Cleft Palate Craniofac J* 51, 593–596.
- Palkovics, D., Bolya-Orosz, F., Pinter, C., Molnar, B., Windisch, P., 2022a. Reconstruction of vertical alveolar ridge deficiencies utilizing a high-density polytetrafluoroethylene membrane/clinical impact of flap dehiscence on treatment outcomes: case series. *BMC Oral Health* 22, 490.
- Palkovics, D., Molnar, B., Pinter, C., Gera, I., Windisch, P., 2022b. Utilizing a novel radiographic image segmentation method for the assessment of periodontal healing following regenerative surgical treatment. *Quintessence Int.* 53, 492–501.
- Palkovics, D., Pinter, C., Bartha, F., Molnar, B., Windisch, P., 2021a. CBCT subtraction analysis of 3D changes following alveolar ridge preservation: a case series of 10 patients with 6-months follow-up. *Int. J. Comput. Dent.* 24, 241–251.
- Palkovics, D., Solyom, E., Molnar, B., Pinter, C., Windisch, P., 2021b. Digital hybrid model preparation for virtual planning of reconstructive dentoalveolar surgical procedures. *J. Vis. Exp.* (174).
- Pinter, C., Lasso, A., Fichtinger, G., 2019. Polymorph segmentation representation for medical image computing. *Comput. Methods Progr. Biomed.* 171, 19–26.
- Radoczy-Drajok, Z., Windisch, P., Svidro, E., Tajti, P., Molnar, B., Gerber, G., 2021. Clinical, radiographical and histological evaluation of alveolar ridge preservation with an autogenous tooth derived particulate graft in EDS class 3-4 defects. *BMC Oral Health* 21, 63.
- Sahni, V., Grover, V., Sood, S., Jain, A., 2022. The periodontal status of orofacial cleft patients: a systematic review and meta-analysis. *Cleft Palate Craniofac J*, 10556656221127549.
- Segura-Castillo, J.L., Aguirre-Camacho, H., González-Ojeda, A., Michel-Perez, J., 2005. Reduction of bone resorption by the application of fibrin glue in the reconstruction of the alveolar cleft. *J. Craniofac. Surg.* 16, 105–112.
- Stasiak, M., Wojtaszek-Słomińska, A., Racka-Pilszak, B., 2019. Current methods for secondary alveolar bone grafting assessment in cleft lip and palate patients — a systematic review. *J. Cranio-Maxillo-Fac. Surg.* 47 (4), 578–585.
- Vandersluis, Y.R., Fisher, D.M., Stevens, K., Tompson, B.D., Lou, W., Suri, S., 2020. Comparison of dental outcomes in patients with nonsyndromic complete unilateral cleft lip and palate who receive secondary alveolar bone grafting before or after emergence of the permanent maxillary canine. *Am. J. Orthod. Dentofacial Orthop.* 157, 668–679.
- Wu, C., Pan, W., Feng, C., Su, Z., Duan, Z., Zheng, Q., Hua, C., Li, C., 2018. Grafting materials for alveolar cleft reconstruction: a systematic review and best-evidence synthesis. *Int. J. Oral Maxillofac. Surg.* 47, 345–356.
- Yuan, K.F., Lai, Q.G., Qi, C., Guo, X.H., Shi, R.J., Xu, X., Wei, F.C., 2004. [Clinical study of bioglass for repairing alveolar cleft. *Shang Hai Kou Qiang Yi Xue* 13, 465–468.



Article

Long-Term Results of Autologous Tooth Bone Grafting in Alveolar Cleft Reconstruction: A Retrospective Cohort Study

Tamás Würsching^{1,2,*}, Bence Mészáros², Eleonóra Sólyom³, Bálint Molnár³, Sándor Bogdán¹ , Zsolt Németh^{1,†} and Krisztián Nagy^{2,†}

¹ Department of Oro-Maxillofacial Surgery and Stomatology, Semmelweis University, 1085 Budapest, Hungary; bogdan.sandor@semmelweis.hu (S.B.); nemeth.zsolt@semmelweis.hu (Z.N.)

² Pediatric Center, Semmelweis University, 1083 Budapest, Hungary; meszaros.bence@semmelweis.hu (B.M.); nagy.krisztian@semmelweis.hu (K.N.)

³ Department Periodontology, Semmelweis University, 1088 Budapest, Hungary; solyom.eleonora@semmelweis.hu (E.S.); molnar.balint@semmelweis.hu (B.M.)

* Correspondence: wursching.tamas@semmelweis.hu; Tel.: +36-12427226

† These authors contributed equally to this work.

Abstract

Background/Objectives: During alveolar cleft grafting, the use of autogenous cancellous bone harvested from the iliac crest is still considered the gold standard. Due to the risk of donor-site morbidity and excessive graft resorption, alternative grafting materials (e.g., intraoral bone, xenografts) are being tested. The aim of this study was to compare the efficacy of using an autologous tooth-derived graft material and iliac crest cancellous bone in the reconstruction of the alveolar cleft in patients with a unilateral cleft lip and palate. **Methods:** A total of 21 patients with a unilateral cleft lip and palate, who underwent alveolar bone grafting between 2020 and 2023 were included in the study. In 11 cases, the donor site was the iliac crest; in the rest of the cases, deciduous teeth were harvested, processed, and used as an autologous particulate graft material for alveolar reconstruction. The mean follow-up time was 30.0 months, CBCT scans were taken, and the results were compared based on the ranking system published by Stasiak et al. **Results:** The Wilcoxon signed-rank test showed that the amount of bone on the cleft side was significantly less than that on the contralateral non-cleft side (ATB: $p = 0.002$, iliac crest: $p = 0.005$). The Mann–Whitney U test showed that there were no significant differences in bone quantity on the cleft side between the two groups ($U = 47.5$, $p = 0.617$). **Conclusions:** The use of ATB might be a feasible alternative to autologous bone during alveolar cleft reconstruction. This type of graft shows long-term stability, which is comparable to the bone harvested from the iliac crest.

Keywords: alveolar bone grafting; autogenous tooth bone graft; 3D surgical planning; volumetric radiographic evaluation; unilateral cleft lip and palate



Academic Editor: Antonio Apicella

Received: 28 May 2025

Revised: 11 July 2025

Accepted: 12 July 2025

Published: 16 July 2025

Citation: Würsching, T.; Mészáros, B.; Sólyom, E.; Molnár, B.; Bogdán, S.; Németh, Z.; Nagy, K. Long-Term Results of Autologous Tooth Bone Grafting in Alveolar Cleft Reconstruction: A Retrospective Cohort Study. *Biomedicines* **2025**, *13*, 1735. <https://doi.org/10.3390/biomedicines13071735>

Copyright: © 2025 by the authors. Licensee MDPI, Basel, Switzerland. This article is an open access article distributed under the terms and conditions of the Creative Commons Attribution (CC BY) license (<https://creativecommons.org/licenses/by/4.0/>).

1. Introduction

Cleft lip and palate (CLP) are the most common congenital anomalies affecting the craniofacial region, characterized by the discontinuity of anatomical structures and varying degrees of tissue hypoplasia, affecting approximately 1 in every 700 children worldwide. The etiology is multifactorial, involving both genetic predispositions and environmental influences [1]. The comprehensive management of these patients presents significant clinical

challenges and requires a coordinated, interdisciplinary approach, involving multiple medical and dental specialties. A critical component of this treatment protocol is alveolar bone grafting (ABG), which, usually combined with orthodontic treatment, plays a pivotal role in the anatomical and functional rehabilitation of the maxillary arch. The main objectives of ABG include reconstruction of the alveolar bony defect, restoration of arch continuity, support of the alar base, and closure of oronasal fistulae. The success of ABG is a crucial determinant in continuing orthodontic treatment and achieving favorable functional and aesthetic outcomes.

ABG is mostly performed during the mixed dentition phase, with the best outcomes observed when grafting is completed prior to the eruption of the cleft-side canine, usually between the ages of 9–12 years [2]. Early grafting allows the erupting tooth to stimulate and maintain the grafted bone, enhancing its integration and long-term stability. In cases where the lateral incisor is congenitally missing, an occurrence frequently seen in CLP patients, the success of the graft directly influences subsequent orthodontic decisions regarding space closure versus prosthetic replacement [3].

In terms of soft tissue management, the 4-flap technique described by Nordin and Abyholm is widely employed due to its effectiveness in achieving tension-free closure over the graft site. However, this method may not adequately address the limited width and thickness of keratinized gingiva adjacent to the cleft, potentially resulting in periodontal compromise and, in severe cases, eventual tooth loss. Moreover, if flap tension leads to wound dehiscence or suture failure, secondary healing and graft exposure can occur, increasing the risk of graft failure [4].

The preferred graft material for this procedure remains autologous bone, particularly from the iliac crest, as originally described by Boyne and Sands [5]. This donor site is favored because it provides ample cancellous bone and exhibits all three key osteogenic properties: osteoconduction, osteoinduction, and osteogenesis. Nevertheless, iliac crest harvesting is associated with notable donor-site morbidity, in addition to the risk of excessive graft resorption over time [6].

To address these limitations, recent research has focused on alternative grafting materials, such as allografts and synthetic substitutes, as well as biologically active adjuncts, including fibrin sealants, platelet-rich plasma (PRP), and leukocyte–platelet rich fibrin (L-PRF) [7–10]. These materials aim to reduce post-operative complications, enhance healing, and potentially improve the success rate of the grafting procedure [8,11]. One such material is auto-tooth bone, or ATB.

Auto-tooth bone is a bio-recycled material, originally developed in Korea, which is derived from extracted teeth and used as an autogenous bone graft after chemical and mechanical preparation. Unlike synthetic grafting materials, it possesses both osteoconductive and osteoinductive properties, promoting rapid new bone formation and remodeling. This graft material is composed of an incompletely demineralized dentin matrix, which contains type I collagen, similarly to alveolar bone, as well as bone morphogenetic proteins (BMPs) and calcium phosphate, all of which are key components of bone regeneration [12]. The mineral components of ATB graft materials consist of four stages (types) of calcium phosphate: hydroxyapatite, tricalcium phosphate, octacalcium phosphate, and amorphous calcium phosphate [13]. When using ABG for guided bone regeneration, Kim et al. found that after 3 months, most ATB underwent resorption, and excellent bone healing and bone remodeling were observed, which occurred as a result of osteoinduction and osteoconduction. In regard to the histomorphometric analysis of the samples collected during the 3–6-month healing period, new bone formation was detected in 46–87% of the area of interest, and excellent bony remodeling was achieved [14]. The aim of the present study was to assess the long-term results of ABG using ATB derived from deciduous or supernumerary

teeth. The hypothesis was that ATB might be a feasible alternative to autologous cancellous bone graft harvested from the iliac crest.

Although there is a general consensus regarding the necessity of the reconstruction of the alveolar cleft, the proper assessment of surgical outcomes remains challenging. A post-operative evaluation is crucial not only to measure the success of the procedure, but also to enable the early detection of graft resorption or displacement, which are among the most frequent complications of alveolar bone grafting.

The earliest assessment methods, such as the use of Bergland and Chelsea scales, relied on a two-dimensional approach, using intraoral X-rays [15]. Over time, with the emergence of computed tomography (CT) and especially cone-beam computed tomography (CBCT) technologies, several 3D evaluation methods have been developed to assess the outcomes of ABG. While 2D methods are limited by structural overlaps and cannot provide volumetric data, 3D techniques using CT overcome these limitations. Moreover, CBCT is often preferred over conventional CT for evaluating bone grafts due to its lower radiation exposure and its ability to accurately estimate the graft volume [16].

A preoperative CBCT scan also enables the 3D visualization of the alveolar bone defect morphology. The use of intraoral and extraoral scanners can also provide valuable information on the relevant soft tissues. Combining this data with specific software provides the opportunity for virtual surgical planning of both soft and hard tissue changes [17]. With the constant evolution and decreasing price of 3D printing, surgical templates and guides have become commonly used aids during maxillofacial surgery. Employing a 3D model for ABG to assess the complex anatomy of the defect can be beneficial during graft harvesting and can lead to a more accurate reconstruction. Auxiliary processes, such as rapid prototyping, augmented reality, and virtual reality, can also aid surgeons during the intervention and may reduce further complications.

2. Materials and Methods

2.1. Study Design and Patient Selection

Patients exhibiting a unilateral cleft lip and palate (UCLP), who had undergone alveolar bone grafting between 2020 and 2023, were recruited for this study. The enrolled patients were being treated at the Pediatric Center at Semmelweis University, Budapest. The study was approved by the university's Regional and Institutional Committee of Science and Research Ethics (Approval Number: SE RKEB 251/2020). The study protocol was submitted and approved by the U.S. National Library of Medicine (www.clinicaltrials.gov; trial registration number: NCT05971914). The research plan was compiled following the legislation in force and the Declaration of Helsinki from the World Medical Association (reference number: 23/2002. V.9.). Surgical interventions were undertaken with the understanding and written consent of each subject's caregiver. The eligibility criteria were complete UCLP without other congenital deformities, ABG surgery using either a iliac crest cancellous bone graft or ATB from deciduous or supernumerary teeth, and CBCT imaging at least one year after grafting. The exclusion criteria were bilateral clefts, any previous attempt at bone grafting, the use of any other type of grafting material (e.g., xenografts, other donor site), and a lack of long-term follow-up CBCT. The STROBE checklist was used during the preparation of this manuscript.

2.2. Surgical Protocol

Every patient underwent the same preoperative preparation. In every case, the development of the cleft-side canines was considered during the planning of the surgery, as was the need for orthodontic treatment. All the patients included in the study required orthodontic maxillary expansion. The development of the canines was monitored using

periapical X-rays. Only once the canine's root development was between one-third and two-thirds of its expected final length was the decision made to proceed with surgery. At this point, CBCT scans were taken for surgical planning. All the enrolled patients were examined by two orthodontists to provide assurance that tooth removal was indicated, according to the patient's age and orthodontic planning.

Based on the extent and morphology of the cleft, the desired shape of the nasopalveolar graft was designed using the freeware software 3D Slicer (www.slicer.org). Since every case was unilateral, the non-cleft side anatomy was used as a reference during graft planning. The upper border of the defect was taken as the lowest part of the piriform aperture on the non-affected side, while the lower border was taken as the cemento-enamel junction of the neighboring teeth. The buccal and palatal borders were determined by a line connecting the most buccal and palatal points of the alveolar process, next to the defect [18]. This also provided the opportunity to determine the exact volume of the graft in cm^3 . This was a helpful addition in regard to planning the surgery because the maximum amount of material the ATB machine can produce is approximately 3 cm^3 , and the achievable volume of the ATB could be predicted based on the volume of the deciduous teeth.

After planning, the model was exported as a standard tessellation language (STL) file. As the final step, a grafting template was constructed using an open-source computer-aided design (CAD) software, Blender (Blender Foundation, Amsterdam, The Netherlands), as described by Fabian et al. [19]. The designed parts were manufactured with a stereolithography (SLA) 3D printer (Phrozen Shuffle XL; Phrozen, Hsinchu City, Taiwan), using class I biocompatible, surgical-grade resin (Dental SG; NextDent BV, Soesterberg, The Netherlands) (Figure 1).

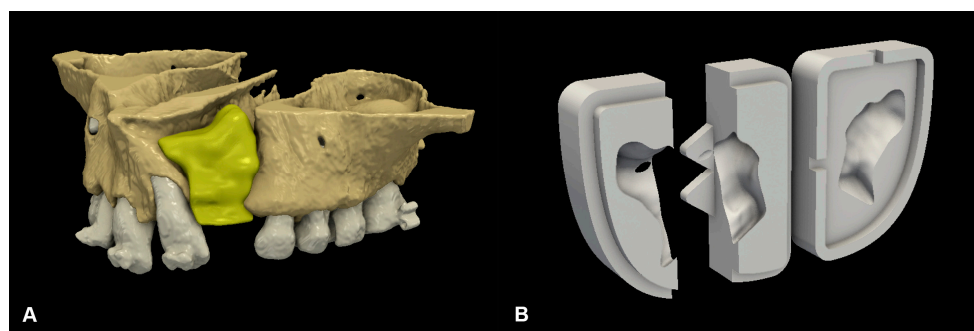


Figure 1. Preoperative virtual planning: (A) digital 3D plan of cleft reconstruction; and (B) CAD-modelled grafting template.

In cases where the teeth were used for ATB, they were extracted under general anesthesia during the same surgery as when the ABG was performed. The extracted teeth were prepared immediately after removal, according to the Bonmaker[®] protocol (Korea Dental Solution Co., Ltd., Busan, Republic of Korea). Ready-to-use ATB was mixed with a fibrin sealant (Tisseel[®]; Baxter, Glenview, IL, USA) in the digitally planned and 3D-printed grafting templates to obtain a sticky ATB graft that matched the shape and extent of the bony defect. The pre-shaped ATB graft was then inserted into the cleft defect. The detailed surgical protocol is described in the authors' previous article [20] (Figure 2). In cases where the number of extractable teeth was not enough for the preparation of a sufficient amount of ATB, cancellous bone from the iliac crest was used instead.

In these cases, a two-team approach was chosen to reduce the operation time. The skin was draped and prepared, leaving the anterior superior iliac spine (ASIS) and the anterior iliac crest exposed. Before incision, local anesthetic was administered (Lidocaine with 0.2% Adrenaline). The skin incision was usually about 2 cm long and respected the patient's relaxed skin tension lines. During the early adolescent age, when alveolar bone grafting is

performed, the iliac crest is usually still covered by a layer of cartilage, which is incised in a rectangular shape. This piece was elevated medially, hinged on the inner edge of the iliac crest. Curettes were used to harvest cancellous bone chips. These were inserted into the 3D-printed mold and were mixed with Tisseel fibrin glue, as described above, to give the graft better formal stability. After the setting of the fibrin glue, the graft was removed from the mold, preserving the shape designed preoperatively, and was ready to be transferred to the cleft site. A collagen sponge was inserted into the donor area to promote hemostasis. The retracted cartilage was repositioned, and the wound was closed in layers. No drains were used [21].

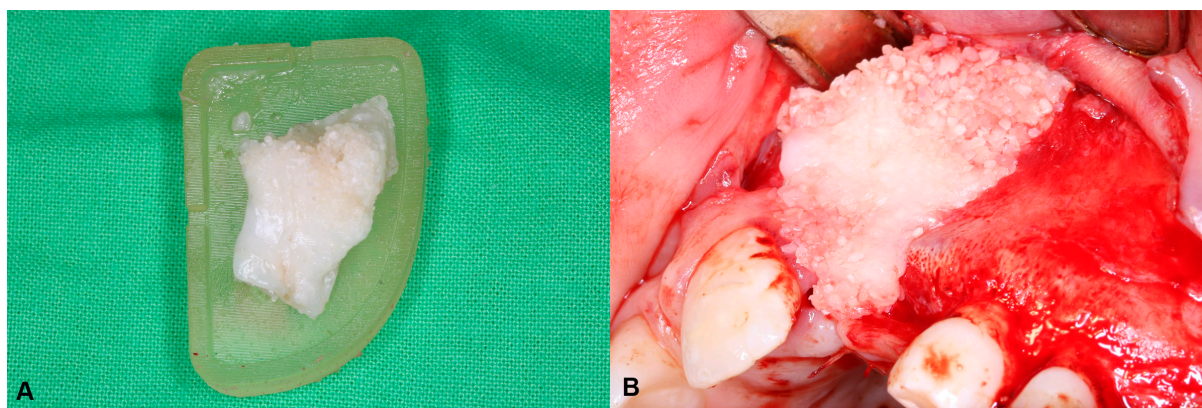


Figure 2. Hard-tissue reconstruction of the alveolar cleft: (A) the mixture of fibrin sealant and ATB particles was shaped by the 3D-printed grafting template; and (B) reconstruction of the alveolar defect using the ATB graft.

2.3. Radiographic Image Acquisition and Assessment of Surgical Outcomes

CBCT scans were acquired, with a 10×8 cm field of view and a $200 \mu\text{m}$ voxel size, 110 kV, 5 mAs, using a Newtom VGI EVO[®] device (Cefla S.C., Imola, Italy). The Digital Imaging and Communications in Medicine (DICOM) datasets were imported into the image processing software, Radiant (Medixant, Poznan, Poland, <https://www.radiantviewer.com>).

Assessment of the surgical outcomes was performed following the protocol described by Stasiak et al. [22], namely using a CBCT-based qualitative scoring system that is based on the presence and the relative dimensions of the bony bridge between the medial and lateral side of the alveolar cleft in four different vertical positions along the central incisor.

The evaluation began by reorienting the images along the long axes of the central incisors on each respective side. The cemento-enamel junction (CEJ) served as the reference point for determining four measurement levels: 3 mm, 5 mm, 7 mm, and 9 mm. The CEJ was defined as the most apical point of the enamel in the midsagittal section of the incisor.

The next step involved examining the presence or absence of a bone bridge through the continuous analysis of the region. Next, the alveolar bone was ranked at the designated levels by identifying the narrowest points between the central incisors and canines, using a horizontal scale, as follows:

- 0 = No alveolar bone bridge;
- 1 = The thickness of the alveolar bone bridge $< \frac{1}{2}$ of the labiolingual width of the central incisor's root;
- 2 = The thickness of the alveolar bone bridge $\geq \frac{1}{2}$ of the labiolingual width of the central incisor's root and less than the labiolingual width of the central incisor's root;
- 3 = The thickness of the alveolar bone bridge is at least the labiolingual width of the central incisor's root (Figure 3).


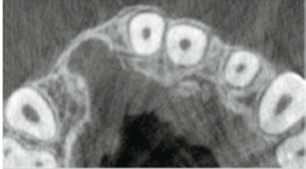
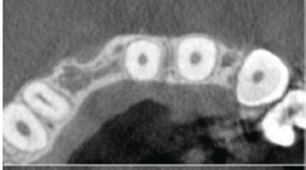
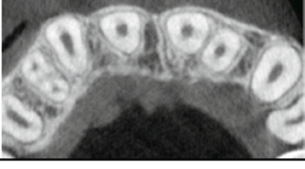
Score	CBCT cross-sectional image (left side is on the left side)	Description
0		No alveolar bone bridge.
1		Thickness of the alveolar bone bridge < ½ of the labiolingual width of central incisor's root.
2		Thickness of the alveolar bone bridge ≥ ½ of the labiolingual width of central incisor's root and less than the labiolingual width of central incisor's root.
3		Thickness of the alveolar bone bridge is more than the labiolingual width of central incisor's root.

Figure 3. Horizontal scale for bone fill assessment, as described by Stasiak et al. [22].

To assess the overall bone quality, the rank scores for each level were summed up for each side. The total score was interpreted using an interval scale, as follows:

- 0 = Failure;
- 1–4 = Poor outcome;
- 5–8 = Moderate outcome;
- 9–12 = Good outcome.

A score of 0 was assigned when no bone bridge was present. In cases where a narrow bone bridge existed but fell between or above the designated measurement levels (3, 5, 7, or 9 mm), a modified evaluation was applied. This involved conducting scoring at the actual bone bridge level and attributing the score to the nearest standard level.

Additionally, for cases with severe root resorption of the central incisors, classification using the horizontal scale was still performed at the 9 mm level. However, the assessment was adjusted by comparing the root width, measured 0.5 mm below the apex, to provide a more accurate evaluation.

2.4. Statistical Analysis

The data was collected in Microsoft Excel (Microsoft, Washington, CA, USA). Statistical analyses were performed using SPSS version 30.0. (IBM Corporation, Redmond, WA, USA). The Kappa correlation coefficient with linear weights was used for the intra-rater and inter-rater reproducibility measurements. To test the normality of the acquired data, the Shapiro–Wilk test was used. The non-parametric Wilcoxon signed-rank test was used for a comparison of the cleft-side and non-cleft-side bone volume. The non-parametric Mann–Whitney U test was used to compare the Stasiak score and the patient's age at the time of surgery of the iliac crest group and the ATB group. Student's t-test was used to compare the initial defect volume of the two groups. The correlation between the bone

defect volume and the outcome score was analyzed separately for the iliac crest and ATB groups, using Spearman's rank correlation.

3. Results

3.1. Patient Demographics and Descriptive Statistics

During the period examined, a total of 42 ABG surgeries were performed in our department. In 12 cases, the defect was bilateral; in 30 cases, the defect was unilateral. In 14 cases, an ATB graft was used; in 25 cases, the donor site was the iliac crest; in three cases, the donor site was the chin. Long-term CBCT data was available for 39 patients; three patients were lost to follow-up. Twenty-one participants exhibiting UCLP were found to be eligible and were enrolled in the current study (Figure 4.). Thirteen patients were male, eight were female. Their age at the time of surgery was between 8 and 14 years; the mean age was 10.4 ± 1.7 years. Sixteen defects were located on the left side and five on the right side. In eleven cases, the donor site for the graft was the iliac crest. In the other 10 cases, a total of 53 deciduous teeth and 4 supernumerary teeth were extracted and utilized for the preparation of the ATB graft. In these cases, the patient's own teeth provided enough material for the proper reconstruction of the alveolar defect, using an average of 5.3 ± 2.26 teeth per patient. The mean follow-up time was 30 ± 13.1 months.

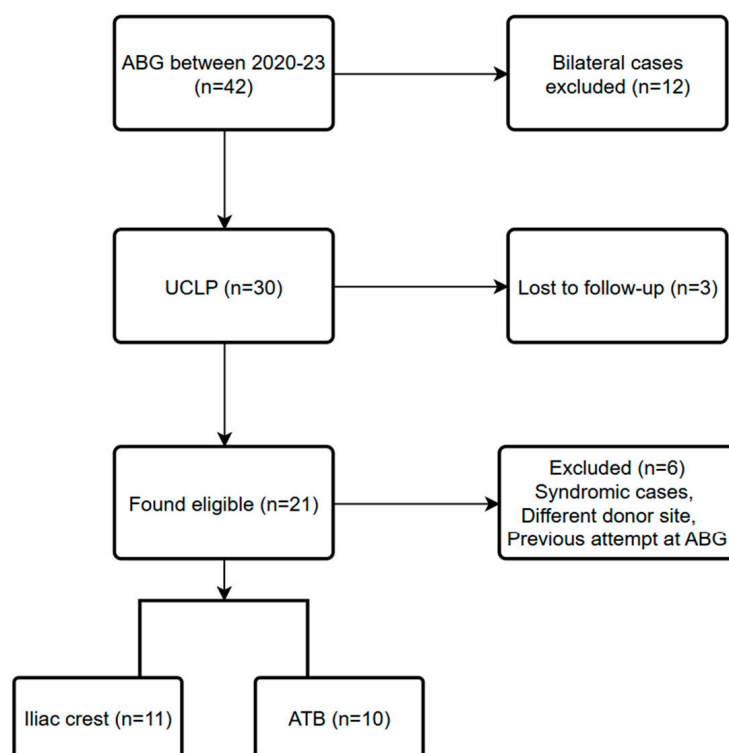


Figure 4. STROBE flowchart.

The mean volume of the initial defect in the iliac crest group was 0.927 cm^3 ($\text{SD} = 0.316 \text{ cm}^3$) and, in the ATB group, it was 1.176 cm^3 ($\text{SD} = 0.449 \text{ cm}^3$). The mean age during the time of surgery in the iliac crest group was 10.9 years ($\text{SD} = 2.1$ years) and, in the ATB group, it was 9.9 years ($\text{SD} = 1.2$ years). There was no obvious difference between the occurrence of early (dehiscence) or late (fistula) complications. In one patient, a severe periodontal defect also developed on the distal surface of tooth 21, which led to extraction. In the ATB group, canine eruption did not happen in two cases during the observed period, whereas no such problems were observed in the other group (Tables 1 and 2).

Table 1. Descriptive statistics of the iliac crest group.

Iliac Crest	Vdefect (cm ³)	Dehiscence	Fistula	Canine	Stasiak Score	Age at Surgery (years)	Follow-Up (months)
Patient 1	1.085	no	no	erupted	11	9	58
Patient 2	1.492	yes	fistula	erupted	9	14	24
Patient 3	0.973	no	no	erupted	0	14	41
Patient 4	0.578	no	no	erupted	9	12	36
Patient 5	0.504	yes	no	erupted	11	13	14
Patient 6	0.916	no	no	erupted	0	10	49
Patient 7	0.973	no	no	erupted	9	8	18
Patient 8	0.788	no	fistula	erupted	6	10	24
Patient 9	0.512	no	no	erupted	8	9	52
Patient 10	1.295	no	no	erupted	0	10	12
Patient 11	1.079	yes	no	erupted	1	11	56

Table 2. Descriptive statistics of the ATB group.

ATB	Vdefect (cm ³)	Dehiscence	Fistula	Canine	Stasiak Score	Age at Surgery (years)	Follow-Up (months)
Patient 12	1.994	no	no	not erupted	0	10	28
Patient 13	0.819	no	no	erupted	9	9	25
Patient 14	1.653	yes	no	erupted	10	8	20
Patient 15	1.03	no	no	erupted	7	11	20
Patient 16	1.226	yes	21 perio	erupted	2	11	26
Patient 17	0.609	no	no	erupted	11	11	28
Patient 18	1.438	no	no	not erupted	3	8	29
Patient 19	1.256	no	no	erupted	11	10	25
Patient 20	1.169	no	fistula	erupted	2	11	25
Patient 21	0.565	no	no	erupted	9	10	23

3.2. Radiographical Assessment

The measurements on both the cleft and non-cleft sides were performed three times in all the patients and, during each instance, all the 168 sites were measured. The first author performed the measurements twice during a 4-week period, and the second author performed the measurements only once. Finally, a consensus reading was performed by both authors.

On the cleft side of the iliac crest group, fifteen sites were classified as 0, four sites as 1, ten sites as 2, and thirteen sites as 3. On the cleft side of the ATB group, twelve sites were classified as 0, five sites as 1, ten sites as 2, and thirteen sites as 3.

On the control side, no 0 or 1 scores were obtained. There were six sites classified as 2 and seventy-eight sites as 3.

The surgical outcome showed a high level of variability. The mean total score on the cleft side in the iliac crest group was 5.8 (SD: ±4.6); in the ATB group, the mean total score on the cleft side was 6.4 (SD: ±4.2). (Figure 5). On the non-cleft side, the mean total score was 11.7 (SD: ±0.5). In the iliac crest group, the results showed 27% failure, 9% poor, 18% moderate, and 46% good results of the surgical procedure. In the ATB group, the results

were 10% failure, 30% poor, 10% moderate, and 50% good. The alveolar bone was classified as good in all the patients on the non-cleft side (Figure 6).

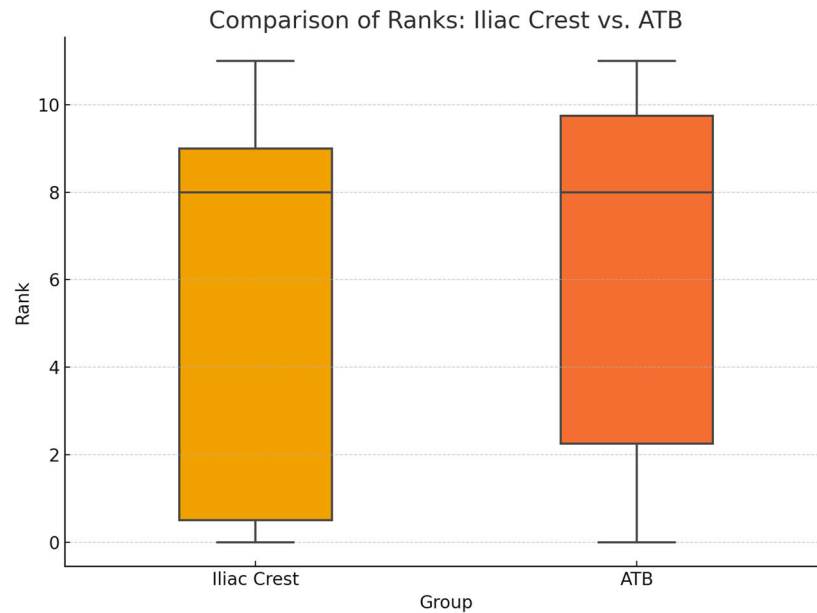


Figure 5. Comparison of the mean of the rank scores on the cleft side.

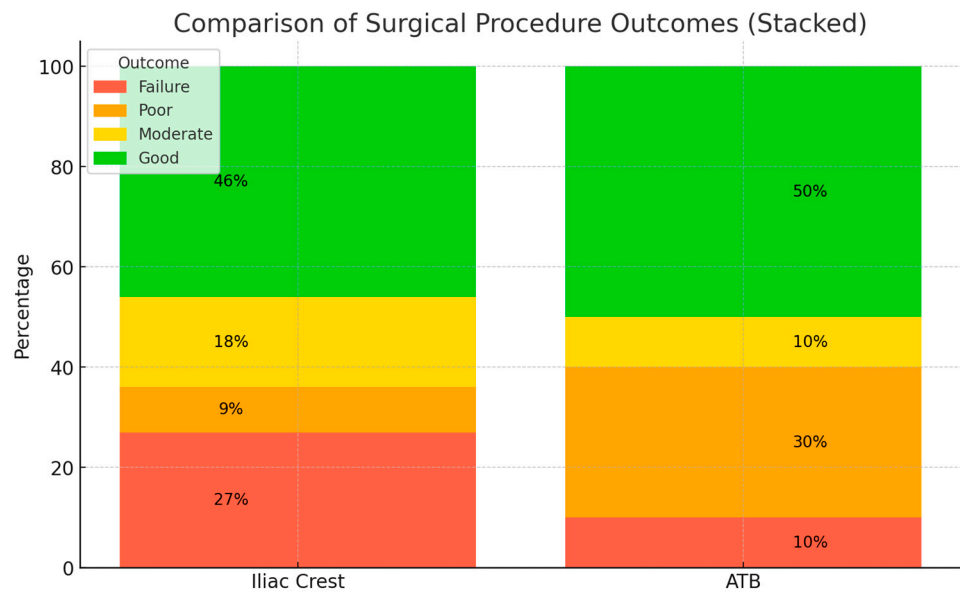


Figure 6. Comparison of surgical procedure outcomes.

3.3. Statistical Analysis

In regard to all the statistical measurements, a 95% confidence interval was adopted. The Wilcoxon signed-rank test showed statistically significant (ATB: $p = 0.002$, iliac crest: $p = 0.005$) differences between the cleft- and non-cleft-side measurements, which did not depend on the type of graft being used. The linearly weighted Kappa coefficient result was 0.85 for intra-rater and 0.82 for inter-rater reproducibility. These results showed the excellent reproducibility of the method presented. The Mann–Whitney U test showed no significant differences between either the Stasiak scores ($U = 47.5, p = 0.617$) or the age at the time of surgery ($U = 67.5, p = 0.388$) of the two groups.

A comparison of the defect volumes between the two groups was performed using an independent sample Student’s t -test. Prior to the analysis, the assumptions for parametric

testing were evaluated: Shapiro–Wilk tests confirmed that the volume data were normally distributed in both the iliac crest ($p = 0.61$) and ATB ($p = 0.86$) groups, and Levene’s test indicated the homogeneity of the variances ($p = 0.36$). The t-test revealed no statistically significant difference in the mean defect volume between the iliac crest group and the ATB group ($t(df) = -1.48, p = 0.155$).

The correlation between the bone defect volume and the outcome score was analyzed separately for the iliac crest and ATB groups, using Spearman’s rank correlation. In the iliac crest group, a weak negative correlation was observed ($\rho = -0.19, p = 0.58$), while the ATB group showed a moderate negative correlation ($\rho = -0.36, p = 0.31$). However, neither correlation reached statistical significance ($p > 0.05$). Scatter plots with trendlines are used to illustrate the inverse relationship between the defect volume and outcome score in both groups (Figure 7).

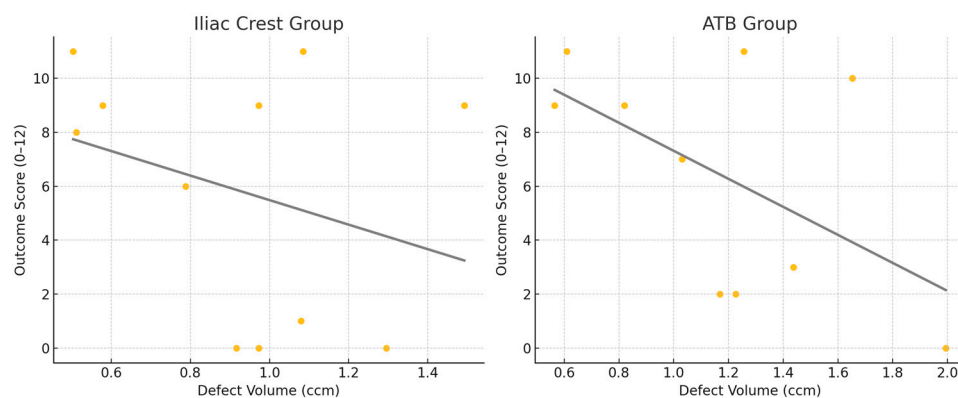


Figure 7. Correlation between initial defect size and outcome score.

4. Discussion

In the present study, the long-term outcomes of using ATB for alveolar bone grafting in patients with a cleft lip and palate were compared to the results achieved by using the iliac crest as a donor site.

Auto-tooth bone grafts can effectively restore damaged alveolar bone using natural bone tissue and offer solutions to several challenges associated with other grafting materials, such as insufficient osteoinduction, a lack of osteoconduction, sterilization concerns, and the risk of disease transmission. This type of graft is commonly used in preprosthetic and periodontal regenerative surgery [23,24].

Although there are articles describing the use of ATB in cleft alveolar bone grafting that have been published previously, they are singular case reports [25–27]. The authors have previously published the short-term results of a case series involving ATB, which showed that although after three months graft resorption could be observed, the amount that was lost was on a par with what could be expected from the use of bone from the iliac crest, according to the literature [20]. Long-term results on the use of ATB in alveolar bone grafting have not yet been published.

Nowadays, there are several similar devices available that are based on the same principle, namely preparing an autologous graft from the patient’s tooth. In the present study, the Bonmaker[®] device (Korea Dental Solution Co., Ltd., Busan, Korea) was used, in the cases where the number of deciduous teeth was adequate. For the rest of the patients, the donor site was the iliac crest, in which a two-team approach was adopted to optimize the surgical time. To achieve the proper amount of graft material according to the preoperative planning, an average of 5.3 ± 2.26 teeth per patient were used. As the early loss of deciduous teeth can lead to complications during eruption of the patient’s permanent teeth, our aim was to avoid unnecessary extractions. This means, however,

that the roots of these teeth were usually partially or completely resorbed, meaning less graft volume per tooth was extracted. This also means that the amount of graft that can be prepared through the use of this method is usually only sufficient for unilateral clefts, so no bilateral cases were treated this way, and they were excluded from this study.

Apart from the lack of an extraoral donor site, the ATB protocol offers two other notable advantages: (i) Approximately half of the process, around 20 min, is fully automated and is carried out by the Bonmaker device without requiring any user input. This automation allows medical staff to focus on other tasks during surgery. (ii) The preparation of the ATB graft is simple and does not require a highly specialized physician. Nurses are fully capable of managing the graft preparation process independently.

The estimated costs associated with the use of ATB are approximately EUR 35–40, depending on the type of device and differences in local prices, and the price of the device itself is also a one-time additional cost. While this contributes to the overall surgical expenses, the costs are not considered extremely high. Moreover, the use of this approach eliminates the need for an extraoral donor site, leading to shorter hospital stays.

After using the iliac crest as a donor site, Brudnicki et al. [28] reported an average hospital stay of 2.9 days, ranging from 1 to 8 days, with most patients being discharged on the second or third day after surgery. In higher-income countries, where hospital stays are more costly, the reduced length of hospitalization associated with the ATB protocol could potentially lower the overall treatment costs. However, a detailed cost-effectiveness analysis was beyond the scope of this study.

Alveolar bone grafting is considered successful when it achieves sufficient bone filling in the alveolar cleft. The eruption of adjacent teeth, particularly the canine, through the grafted bone is also a critical indicator of treatment success. Additionally, the lack of oronasal fistulae, healthy periodontal tissues around teeth adjacent to the graft site, and the maintenance of alveolar bone stability and continuity over time are also essential criteria [29]. A recent meta-analysis by Jahanbin et al. showed that the total percentage of bone filling after 1 year, according to CBCT, was about 63.38% [30].

Due to the limited sample size in this study, it is not possible to conclude whether there is a significant difference between the rate of early or late complications between the two groups. However, the fact that canine eruption in the iliac crest group happened in every case and, in the ATB group, there were two cases out of ten where it did not, needs to be addressed. This must be followed on a longer-term basis and in regard to a larger sample size, as the failure of the canines to spontaneously erupt leads to further surgical interventions, which is a factor that must be considered when choosing ATB as a potential graft material.

CBCT is increasingly used to evaluate the results of ABG, due to its ability to provide detailed 3D imaging with lower radiation than conventional CT, replacing conventional methods based on 2D X-rays. While several CBCT-based methods exist, none have achieved universal recognition [31,32]. Volumetric assessments quantify bone fill (BF), but lack spatial specificity, limiting their value in regard to clinical decision making. Grading scales using 2D measurements at vertical levels, such as those by Soumalainen and Liu [33], offer partial localization, but are affected by the dental eruption status and have limited generalizability.

Assessment approaches are generally classified as continuous (e.g., bone volume or resorption rates) or categorical (e.g., bone height/width). Continuous methods, while quantitative, lack standardized clinical thresholds and fail to identify critical bone deficits impacting orthodontic outcomes.

Stasiak et al. introduced a more advanced, clinically applicable method that divides the cleft into defined zones, enabling the precise localization of bone presence and resorption. It uniquely considers the impact of bone loss on adjacent teeth and also considers root

resorption. This spatially detailed approach supports more informed decisions about regrafting and orthodontic planning, representing a major improvement to CBCT-based ABG evaluations. This method was implemented in the current study, and proved to be reliable and reproducible, with excellent rates of intra- and inter-rater reliability.

The results show that there are no significant differences between the outcomes of the two groups based on the Stasiak scale and, in both groups, at least 60% of the cases fell into the moderate or good category, meaning no regrafting was deemed necessary. In terms of the other cases, approximately 40% of the cases where the outcome fell into the poor or the failure category, regrafting or prosthetic rehabilitation needed to be considered on an individual basis.

5. Conclusions

Alveolar bone grafting in patients with a cleft lip and palate remains a challenging task, with no currently known method or type of graft material providing a substantially higher rate of success than the others. The results of this study indicate that an ATB graft is a safe and predictable graft material with long-term volumetric stability, which may be utilized in alveolar cleft reconstruction. The main limitation of this study is the relatively small sample size, which causes us to be cautious about generalizing the results in regard to cleft surgery. The use of ATB, however, is well-documented, and is already deemed a reliable material in preprosthetic and periodontal surgery. Another limiting factor is that the long-term results were not compared to the initial defect size in a volume-based manner, but instead the categorical scaling system developed by Stasiak et al. was used. This system, however, is straightforward, reliable, and aids the user in regard to clinical decision making.

Although the sample size was small, no significant differences were observed compared to the current gold standard of grafts, the iliac crest; however, the bone volume at the reconstructed site was still significantly less than on the healthy contralateral side, regardless of the type of graft used. The application of an ATB graft requires additional training and equipment, but the good clinical results and the lack of an extraoral donor site may compensate for this and lead to this method being recommended for the alveolar reconstruction of patients with a cleft lip and palate. However, due to the limited amount of graft that can be prepared from deciduous or supernumerary teeth in this patient population, the method presented is recommended by the authors for use in small-to-medium size unilateral alveolar defects. Further studies with larger sample sizes are of course necessary to support the findings in the present study.

Author Contributions: Conceptualization, T.W. and K.N.; methodology, T.W.; software, B.M. (Bence Mészáros); validation, T.W. and B.M. (Bence Mészáros); formal analysis, S.B.; investigation, E.S.; resources, B.M. (Bálint Molnár); data curation, B.M. (Bálint Molnár); writing—original draft preparation, T.W.; writing—review and editing, K.N., Z.N. and S.B.; visualization, E.S.; supervision, B.M. (Bálint Molnár); project administration, Z.N. All authors have read and agreed to the published version of the manuscript.

Funding: This research received no external funding.

Institutional Review Board Statement: The study was approved by the university's Regional and Institutional Committee of Science and Research Ethics (Approval Number: SE RKEB 251/2020, 17 December 2020). The study protocol was submitted and approved by the U.S. National Library of Medicine (www.clinicaltrials.gov; trial registration number: NCT05971914). The research plan was compiled following the legislation in force and the Declaration of Helsinki from the World Medical Association (reference number: 23/2002. V.9).

Informed Consent Statement: Surgical interventions were undertaken with the understanding and written consent of each subject's caregiver.

Data Availability Statement: The data presented in this study is available on request from the corresponding author. Measurements based on CBCT can be presented after patient anonymization, the raw CBCT data is not available due to patient privacy.

Conflicts of Interest: The authors declare that there are no conflicts of interest.

Abbreviations

The following abbreviations are used in this manuscript:

CLP	Cleft lip and palate
ABG	Alveolar bone grafting
ATB	Auto-tooth bone
PRP	Platelet-rich plasma
L-PRF	Leukocyte-platelet rich fibrin
BMP	Bone morphogenic protein
HA	Hydroxyapatite
CT	Computed tomography
CBCT	Cone-beam computed tomography
UCLP	Unilateral cleft lip and palate
STL	Standard tessellation language
CAD	Computer-aided design
SLA	Stereolithography
CEJ	Cemento-enamel junction

References

1. Acs, L.; Nemes, B.; Nagy, K.; Acs, M.; Banhid, F.; Rozsa, N. Maternal factors in the origin of cleft lip/cleft palate: A population-based case-control study. *Orthod. Craniofacial Res.* **2024**, *27* (Suppl. S1), 6–13. [[CrossRef](#)] [[PubMed](#)]
2. Vandersluis, Y.R.; Fisher, D.M.; Stevens, K.; Tompson, B.D.; Lou, W.; Suri, S. Comparison of dental outcomes in patients with nonsyndromic complete unilateral cleft lip and palate who receive secondary alveolar bone grafting before or after emergence of the permanent maxillary canine. *Am. J. Orthod. Dentofac. Orthop.* **2020**, *157*, 668–679. [[CrossRef](#)] [[PubMed](#)]
3. Fahradyan, A.; Tsuha, M.; Wolfswinkel, E.M.; Mitchell, K.S.; Hammoudeh, J.A.; Magee, W., 3rd. Optimal Timing of Secondary Alveolar Bone Grafting: A Literature Review. *J. Oral. Maxillofac. Surg.* **2019**, *77*, 843–849. [[CrossRef](#)] [[PubMed](#)]
4. Åbyholm, F.E.; Olav, B.; Semb, G. Secondary Bone Grafting of Alveolar Clefts: A Surgical/Orthodontic Treatment Enabling a Non-prosthetic Rehabilitation in Cleft Lip and Palate Patients. *Scand. J. Plast. Reconstr. Surg.* **1981**, *15*, 127–140. [[CrossRef](#)] [[PubMed](#)]
5. Boyne, P.J.; Sands, N.R. Secondary bone grafting of residual alveolar and palatal clefts. *J. Oral Surg.* **1972**, *30*, 87–92. [[PubMed](#)]
6. Dimitriou, R.; Mataliotakis, G.I.; Angoules, A.G.; Kanakaris, N.K.; Giannoudis, P.V. Complications following autologous bone graft harvesting from the iliac crest and using the RIA: A systematic review. *Injury* **2011**, *42* (Suppl. S2), S3–S15. [[CrossRef](#)] [[PubMed](#)]
7. Brezulier, D.; Chaigneau, L.; Jeanne, S.; Lebullenger, R. The Challenge of 3D Bioprinting of Composite Natural Polymers PLA/Bioglass: Trends and Benefits in Cleft Palate Surgery. *Biomedicines* **2021**, *9*, 1553. [[CrossRef](#)] [[PubMed](#)]
8. Ellapakurthi, P.; Reddy, G.S.P. The effectiveness of mineralized plasmatic matrix in the closure of alveolar clefts with volumetric assessment. *Regen. Med. Res.* **2021**, *9*, 1. [[CrossRef](#)] [[PubMed](#)]
9. Janssen, N.G.; Weijjs, W.L.; Koole, R.; Rosenberg, A.J.; Meijer, G.J. Tissue engineering strategies for alveolar cleft reconstruction: A systematic review of the literature. *Clin. Oral. Investig.* **2014**, *18*, 219–226. [[CrossRef](#)] [[PubMed](#)]
10. Wu, C.; Pan, W.; Feng, C.; Su, Z.; Duan, Z.; Zheng, Q.; Hua, C.; Li, C. Grafting materials for alveolar cleft reconstruction: A systematic review and best-evidence synthesis. *Int. J. Oral. Maxillofac. Surg.* **2018**, *47*, 345–356. [[CrossRef](#)] [[PubMed](#)]
11. Leal, C.R.; de Carvalho, R.M.; Ozawa, T.O.; de Almeida, A.M.; da Silva Dalben, G.; da Cunha Bastos, J.C., Jr.; Garib, D.G. Outcomes of Alveolar Graft With Rhbmp-2 in CLP: Influence of Cleft Type and Width, Canine Eruption, and Surgeon. *Cleft Palate Craniofacial J.* **2019**, *56*, 383–389. [[CrossRef](#)] [[PubMed](#)]
12. Hussain, A.A.; Al-Quisi, A.F.; Abdulkareem, A.A. Efficacy of Autogenous Dentin Biomaterial on Alveolar Ridge Preservation: A Randomized Controlled Clinical Trial. *Biomed Res. Int.* **2023**, *2023*, 7932432. [[CrossRef](#)] [[PubMed](#)]
13. Kim, Y.K.; Kim, S.G.; Yun, P.Y.; Yeo, I.S.; Jin, S.C.; Oh, J.S.; Kim, H.J.; Yu, S.K.; Lee, S.Y.; Kim, J.S.; et al. Autogenous teeth used for bone grafting: A comparison with traditional grafting materials. *Oral Surg. Oral Med. Oral Pathol. Oral Radiol.* **2014**, *117*, e39–e45. [[CrossRef](#)] [[PubMed](#)]

14. Kim, Y.K.; Kim, S.G.; Byeon, J.H.; Lee, H.J.; Um, I.U.; Lim, S.C.; Kim, S.Y. Development of a novel bone grafting material using autogenous teeth. *Oral Surg. Oral Med. Oral Pathol. Oral Radiol. Endodontology* **2010**, *109*, 496–503. [[CrossRef](#)] [[PubMed](#)]
15. Lorenzoni, D.C.; Janson, G.; Bastos, J.C.; Carvalho, R.M.; Bastos, J.C., Jr.; de Cassia Moura Carvalho Lauris, R.; Henriques, J.F.; Ozawa, T.O. Evaluation of secondary alveolar bone grafting outcomes performed after canine eruption in complete unilateral cleft lip and palate. *Clin. Oral Investig.* **2017**, *21*, 267–273. [[CrossRef](#)] [[PubMed](#)]
16. Lemberger, M.; Benchimol, D.; Pegelow, M.; Jacobs, R.; Karsten, A. Validation and comparison of 2D grading scales and 3D volumetric measurements for outcome assessment of bone-grafted alveolar clefts in children. *Eur. J. Orthod.* **2024**, *46*, cjae002. [[CrossRef](#)] [[PubMed](#)]
17. Major, M.; Meszaros, B.; Wursching, T.; Polyak, M.; Kammerhofer, G.; Nemeth, Z.; Szabo, G.; Nagy, K. Evaluation of a Structured Light Scanner for 3D Facial Imaging: A Comparative Study with Direct Anthropometry. *Sensors* **2024**, *24*, 5286. [[CrossRef](#)] [[PubMed](#)]
18. Wursching, T.; Kesztyus, A.; Pottel, L.; Swennen, G.; Nagy, K. Comparison of two methods for segmentation of the nasoalveolar defect and design of a three-dimensional surgical template in patients with cleft lip and palate: A retrospective study. *Int. J. Oral Maxillofac. Surg.* **2025**. [[CrossRef](#)] [[PubMed](#)]
19. Fabian, Z.; Kadar, K.; Patonay, L.; Nagy, K. Application of 3D Printed Biocompatible Plastic Surgical Template for the Reconstruction of a Nasoalveolar Cleft with Preoperative Volume Analysis. *Mater. Plast.* **2019**, *56*, 413–415. [[CrossRef](#)]
20. Molnar, B.; Wursching, T.; Solyom, E.; Palvolgyi, L.; Radoczy-Drajko, Z.; Palkovics, D.; Nagy, K. Alveolar cleft reconstruction utilizing a particulate autogenous tooth graft and a novel split-thickness papilla curtain flap—A retrospective study. *J. Cranio-Maxillofac. Surg.* **2024**, *52*, 77–84. [[CrossRef](#)] [[PubMed](#)]
21. Kesztyus, A.; Wursching, T.; Nemes, B.; Palvolgyi, L.; Nagy, K. Evaluation of 3D visualization, planning and printing techniques in alveolar cleft repair, and their effect on patients' burden. *J. Stomatol. Oral Maxillofac. Surg.* **2022**, *123*, 484–489. [[CrossRef](#)] [[PubMed](#)]
22. Stasiak, M.; Wojtaszek-Slominska, A.; Racka-Pilszak, B. A novel method for alveolar bone grafting assessment in cleft lip and palate patients: Cone-beam computed tomography evaluation. *Clin. Oral Investig.* **2021**, *25*, 1967–1975. [[CrossRef](#)] [[PubMed](#)]
23. Radoczy-Drajko, Z.; Windisch, P.; Svidro, E.; Tajti, P.; Molnar, B.; Gerber, G. Clinical, radiographical and histological evaluation of alveolar ridge preservation with an autogenous tooth derived particulate graft in EDS class 3–4 defects. *BMC Oral Health* **2021**, *21*, 63. [[CrossRef](#)] [[PubMed](#)]
24. Solyom, E.; Szalai, E.; Czumbel, M.L.; Szabo, B.; Vancsa, S.; Mikulas, K.; Radoczy-Drajko, Z.; Varga, G.; Hegyi, P.; Molnar, B.; et al. The use of autogenous tooth bone graft is an efficient method of alveolar ridge preservation—Meta-analysis and systematic review. *BMC Oral Health* **2023**, *23*, 226. [[CrossRef](#)] [[PubMed](#)]
25. Jeong, K.-I.; Lee, J.; Kim, K.-W.; Um, I.-W.; Hara, S.; Mitsugi, M.; Kim, Y.-K. Alveolar Cleft Reconstruction Using Chin Bone and Autogenous Tooth Bone Graft Material: Reports of 5 Cases. *J. Korean Dent. Sci.* **2013**, *6*, 13–21. [[CrossRef](#)]
26. Datarkar, A.; Bhawalkar, A. Utility of tooth as an autogenous graft material in the defects of alveolar cleft—A novel case report. *J. Oral Biol. Craniofacial Res.* **2020**, *10*, 470–473. [[CrossRef](#)] [[PubMed](#)]
27. Hara, S.; Mitsugi, M.; Kanno, T.; Tatemoto, Y. Bone transport and bone graft using auto-tooth bone for alveolar cleft repair. *J. Craniofacial Surg.* **2013**, *24*, e65–e68. [[CrossRef](#)] [[PubMed](#)]
28. Brudnicki, A.; Regulski, P.A.; Sawicka, E.; Fudalej, P.S. Alveolar Volume Following Different Timings of Secondary Bone Grafting in Patients with Unilateral Cleft Lip and Palate. A Pilot Study. *J. Clin. Med.* **2021**, *10*, 3524. [[CrossRef](#)] [[PubMed](#)]
29. Yu, X.; Huang, Y.; Li, W. Correlation between alveolar cleft morphology and the outcome of secondary alveolar bone grafting for unilateral cleft lip and palate. *BMC Oral Health* **2022**, *22*, 251. [[CrossRef](#)] [[PubMed](#)]
30. Jahanbin, A.; Kamyabnezhad, E.; Raisolsadat, M.A.; Farzanegan, F.; Bardideh, E. Long-Term Stability of Alveolar Bone Graft in Cleft Lip and Palate Patients: Systematic Review and Meta-Analysis. *J. Craniofacial Surg.* **2022**, *33*, e194–e200. [[CrossRef](#)] [[PubMed](#)]
31. Kumar, A.; Batra, P.; Sharma, K.; Raghavan, S.; Talwar, A.; Srivastava, A.; Sood, S.C. A Three-Dimensional Scale for the Qualitative and Quantitative Assessments of Secondary Alveolar Bone Grafting (SABG) in Unilateral Cleft Lip and Palate Patients Using Cone-Beam Computed Tomography (CBCT). *Indian. J. Plast. Surg.* **2022**, *56*, 138–146. [[CrossRef](#)] [[PubMed](#)]
32. Shaheen, E.; Danneels, M.; Doucet, K.; Dormaar, T.; Verdonck, A.; Cadenas de Llano-Perula, M.; Willems, G.; Politis, C.; Jacobs, R. Validation of a 3D methodology for the evaluation and follow-up of secondary alveolar bone grafting in unilateral cleft lip and palate patients. *Orthod. Craniofacial Res.* **2022**, *25*, 377–383. [[CrossRef](#)] [[PubMed](#)]
33. Suomalainen, A.; Aberg, T.; Rautio, J.; Hurmerinta, K. Cone beam computed tomography in the assessment of alveolar bone grafting in children with unilateral cleft lip and palate. *Eur. J. Orthod.* **2014**, *36*, 603–611. [[CrossRef](#)] [[PubMed](#)]

Disclaimer/Publisher's Note: The statements, opinions and data contained in all publications are solely those of the individual author(s) and contributor(s) and not of MDPI and/or the editor(s). MDPI and/or the editor(s) disclaim responsibility for any injury to people or property resulting from any ideas, methods, instructions or products referred to in the content.